UNIVERSITY OF CALIFORNIA, SAN DIEGO

Mechanisms underlying spontaneous activity in the developing retina

A Dissertation submitted in partial satisfaction of the requirements for the degree

Doctor of Philosophy

in

Neurosciences

by

Aaron Gregory Blankenship

Committee in charge:

Professor Jeffry Isaacson, Chair
Professor Sascha du Lac
Professor Marla B. Feller
Professor David Rapaport
Professor Nicholas Spitzer

2009

The Dissertation of Aaron Gregory Blankenship is approved, and it is acceptable in quality and form for publication on microfilm and electronically:

_____

_____

_____

_____

_____

Chair

University of California, San Diego

2009

DEDICATION

In memory of

Lyle Albert Mahnke

TABLE OF CONTENTS

LIST OF FIGURES AND TABLES

ACKNOWLEDGEMENTS

I thank Marla, whose commitment to her students is unsurpassed. She is truly always willing to help, is unfailingly supportive, and has taught me more about being a scientist than anyone else, many times over. She is the definition of a role model: when I am a mentor, it is her example I will follow.

I thank my committee, for their help and encouragement. Jeff Isaacson deserves special thanks, for his assistance in designing many experiments.

I thank my collaborators: Juliette Johnson, David Copenhagen, Rebecca Seal and Robert Edwards for providing us with the VGLUT1 and VGLUT3 knockout mice; Stephan Maxeiner and Klaus Willecke for providing us with the connexin 45 knockout mouse.

I thank W. Robert Batsell, Jr. His support, encouragement and guidance are what led me into graduate school.

I thank all of the other inspiring teachers I have been lucky enough to study with. They taught me to love learning, a gift I will enjoy for the rest of my life.

I thank the Feller lab. They are a wonderful group of colleagues—helpful, knowledgeable, patient and generous. In particular I thank Michael Fikhman, for help with immunohistochemistry; Aaron Hamby, for our ongoing collaboration; Kevin Ford, for his collaboration on Chapter II of this dissertation; Will Barkis, for establishing the multicell bolus loading technique, and Justin Elstrott, for being extraordinarily helpful and fun, and for being a friend since the very beginning of graduate school.

I thank all of my friends. It is because of them that UCSD was a great place to be a graduate student. I thank Norma, for being truly amazing and a source of years of joy. I thank Will Barkis, for years of fun and talks about science and life. Some friends are so special that they define an era of one's life. Will is one of those friends. I thank Sabine, for being patient, open, giving, brave, and the best part of my life.

I thank my family. There is no family more supportive. My mom and dad were given a child who ceaselessly asked why. Incredibly, they responded with never-ending love and encouragement, thereby guiding me into a life of inquisitiveness. For their support, love, patience, wisdom, and friendship I am not merely grateful; for these things I am.

Chapter 1 is original work submitted as: Blankenship, AG; Feller, MB. Mechanisms underlying spontaneous patterned activity in developing neural circuits. Nature Reviews Neuroscience., and is included with permission from all authors. The dissertation author was the primary author of this paper.

Chapter 2, in full, is a reprint of the material as it appears in: Blankenship, AG; Ford, KJ; Johnson, J; Seal, RP; Edwards, RH; Copenhagen, DR; Feller, MB. Synaptic and Extrasynaptic Factors Governing Glutamatergic Retinal Waves. Neuron, vol. 62, 2009, and is included with permission from all authors. The dissertation author was the primary author of this paper.

Chapter 3 is original work in preparation as: Blankenship, AG; Maxeiner, S; Willecke, K; Feller, MB. Neuronal connexin 45 does not contribute to retinal wave function and is included with permission from all the manuscript's authors. The dissertation author was the primary author of this paper.

VITA

2001-2002	Research Assistant, Kalamazoo College
2002	B.A., Psychology, *magna cum laude*, Kalamazoo College
2002-2003	Research Technician, Max Delbrück Center for Molecular Medicine, Berlin, Germany
2009	Ph.D., Neurosciences, University of California, San Diego

PUBLICATIONS

Blankenship A.G., Ford K.J., Johnson J., Seal R.P., Edwards R.H., Copenhagen D.R., Feller M.B. (2009). Synaptic and extrasynaptic factors governing glutamatergic retinal waves. Neuron, 62, pp. 230-241.

Feller, M.F. and Blankenship, A.G. (2008) The function of the retina prior to vision – the phenomenon of retinal waves and retinotopic refinement. Eye, Retina, and Visual System of the Mouse, Leo M. Chalupa and Robert W. Williams, Editors, MIT Press.

Wang C.T., Blankenship A.G., Anishchenko A., Elstrott J., Fikhman M., Nakanishi S., Feller M.B. (2007). GABA(A) receptor-mediated signaling alters the structure of spontaneous activity in the developing retina. J Neurosci, 27, pp. 9130-40.

Wolf S.A., Kronenberg G., Lehmann K., Blankenship A., Overall R., Staufenbiel M., Kempermann G. (2006). Cognitive and physical activity differently modulate disease progression in the APP23 model of Alzheimer's disease. Biological Psychiatry, 60, pp. 1314-23.

Batsell, W.R., Jr., Trost, C., Cochran, S., Blankenship, A.G., & Batson, J.D. (2003). Postconditioning inflation in taste-odor aversion learning. Learning & Behavior, 31, pp. 173-184.

Batsell, W.R., Jr., & Blankenship, A.G. (2002). Beyond potentiation: Synergistic conditioning in flavor-aversion learning. Brain and Mind, 3, pp. 383-408.

AWARDS

2006-2009	NIH National Research Service Award
2008	Anuradha Rao Memorial Travel Award from Neuron
2004,2005	Honorable Mention, NSF Graduate Research Fellowship
2004	Ray Thomas Edwards Graduate Student Travel Award
2003	Merck Fellowship
2002-2003	Hanns Seidel Graduate Fellowship
2002	Departmental honors, Kalamazoo College
2002	Donald Van Liere Prize for Excellence in Research
2002	Van Liere Senior Prize for Excellence in Psych. Coursework
1998-2002	Kalamazoo College Dean's List
1999	William Beaumont Hospital Scholarship
1998	Kalamazoo College Science/Math Competitive Scholarship
1998	Kalamazoo College Honors Scholarship

ABSTRACT OF THE DISSERTATION

Mechanisms underlying spontaneous activity in the developing retina

by

Aaron Gregory Blankenship

Doctor of Philosophy in Neurosciences

University of California, San Diego, 2009

Professor Jeffry Isaacson, Chair

Many circuits in the developing nervous system generate spontaneous activity. This phenomenon has been studied extensively in the developing retina. Before vision is possible in the retina, neighboring retinal ganglion cells, the retina's projection neurons, spontaneously fire correlated bursts of action potentials separated by long periods of silence. This bursting activity propagates across the retina in the form of "retinal waves".

My overall goal was to elucidate the transient features of the developing retina that are the synaptic basis of retinal waves. In the adult retina, circuitry is organized vertically, such that signals travel from the light-sensitive photoreceptors, through a class of excitatory interneuron known as bipolar cells, to retinal ganglion cells, whence the signal is transmitted to the brain. Hence, in the adult retina, each point in

visual space is represented by excitation in a small group of cells, with minimal lateral communication among neighboring groups of cells. In contrast, during development, retinal waves propagate laterally across many degrees of visual space.

Using a combination of transgenic mice and physiological recordings from acutely isolated mouse retinas, I tested two hypotheses regarding how activity propagates laterally across the retina during development. First, I tested whether extrasynaptic glutamate provides a source of coupling among neighboring bipolar cells. Second, I tested whether specific neuronal connexins, which are the proteins that form electrical synapses, are involved in wave generation.

These experiments will help us to better understand the mechanisms by which cells in the brain form the correct connections during development. The knowledge gained from these experiments may help to explain congenital defects of the visual system and could be used to help reestablish connections in the injured brain.

I. Mechanisms underlying spontaneous patterned activity in developing neural circuits.

Abstract

Patterned, spontaneous activity occurs in many developing neural circuits, including retina, cochlea, spinal cord, cerebellum and hippocampus, where it provides signals that are important for the development of neurons and their connections. Despite differences in adult architecture and output across these various circuits, the patterns of spontaneous network activity and the mechanisms that generate it are remarkably similar. Interestingly, spontaneous activity is robust; if one element of a circuit is disrupted another will generate similar activity. This research indicates that developing neural circuits exhibit transient and tunable features that maintain a robust source of correlated activity during critical stages of development.

Introduction

One way to understand the complexity of neural circuits is to understand how their connectivity emerges during development. The traditional model of brain development includes two phases: an early phase during which a coarse wiring of the nervous system is laid out, followed by a later phase during which the coarse connections are refined. In this model, the developmental events that underlie the coarse wiring are the result of predetermined genetic programs and occur independent of neural activity, whereas the refinement is a result of interactions between the

nervous system and the outside world. For example, the traditional view of visual system development is that a genetic program specifies the organization of projections from the retina to the brain and among visual areas within the brain, whereas once vision matures, neural activity driven by visual experience refines the coarse neuronal circuits into their adult pattern of connectivity.

This traditional model is slowly being modified to accommodate an overwhelming number of observations that neural activity and genetic programs interact to specify the composition and organization of neural circuits during all stages of development. Even at extremely early stages, well before synapses form, neurons and neuronal precursors exhibit spontaneous electrical and chemical activity. These early forms of activity, which often occur on a cell-by-cell basis and are not typically correlated across cells, influence developmental events such as neuronal differentiation, establishment of neurotransmitter phenotype, and neuronal migration (Owens and Kriegstein, 2002, Spitzer, 2006).

As neurons start to form synaptic connections and functional circuits begin to emerge, spontaneous activity becomes correlated across large groups of neighboring cells. This spontaneous network activity has been observed in many parts of the developing nervous system, and it serves a variety of purposes. In developing sensory epithelia, in particular the retina (Galli and Maffei, 1988, Meister et al., 1991) and cochlea (Tritsch et al., 2007), spontaneous network activity correlates action potential firing among projection neurons during a period of development when these projections are forming sensory maps (Torborg and Feller, 2005, Forsythe, 2007, Kandler et al., 2009). Spontaneous activity is also observed in developing spinal cord

(Landmesser and O'Donovan, 1984), where it contributes to motoneuron path-finding (Hanson et al., 2008), maturation of synapses (Gonzalez-Islas and Wenner, 2006), and development of pattern-generating circuits within the cord (Myers et al., 2005, Marder and Rehm, 2005). In forebrain structures such as the hippocampus (Ben-Ari et al., 1989, Garaschuk et al., 1998) and neocortex (Garaschuk et al., 2000, Corlew et al., 2004), as well as hindbrain (Gust et al., 2003), midbrain (Rockhill et al., 2009), and cerebellum (Watt et al., 2009), it has been postulated that spontaneous activity contributes to the development of local circuits (Moody and Bosma, 2005, Mohajerani and Cherubini, 2006).

This Review describes the cellular mechanisms that underlie the generation of correlated firing patterns in immature neural circuits soon after the onset of synapse formation. We do not attempt to review all of the mechanisms that underlie spontaneous activity in multiple brain areas. Rather, our goal is to highlight the remarkable parallels found in the mechanisms used by different circuits. Spontaneous activity in neurons is correlated by transient excitatory networks that are formed through a variety of mechanisms, such as a depolarizing action of GABA, transient synaptic connections, extrasynaptic transmission, and gap junction coupling. The recurrent excitatory connections within these networks amplify interactions between spontaneously active cells, initiating correlated network activity. In addition, these networks are highly resistant to perturbation — a pharmacological or genetic disruption of critical network components leads to an expression of alternative circuit mechanisms that generate activity similar to the endogenous pattern, suggesting that

redundancy is built into neural circuits to ensure that the spontaneous activity is maintained.

General features of spontaneous network activity patterns

Spontaneous network activation has been observed in multiple developing circuits, but has been best characterized in the retina, spinal cord and hippocampus. (A wide range of spontaneous activity patterns analogous to those observed in the hippocampus has also been described in neocortex (for a review, see Khazipov and Luhmann, 2006). The activity patterns in these diverse structures share several features during development. In all three cases, spontaneous network events are comprised of large, slow depolarizations crested by bursts of action potentials (Table 1). Another common feature is that excitatory interneurons have a role in the generation of spontaneous activity. Recently, spontaneous network activity has also been described in developing cochlea (Tritsch et al., 2007) and cerebellum (Watt et al., 2009). Although the details are not yet fully understood, the strategies used by the cochlea and cerebellum are comparable to those previously described in the retina, spinal cord, and hippocampus. Schematics of the functional circuits that mediate spontaneous network depolarizations in each of these brain structures are provided in Figure I-1.

The projection neurons of the retina, retinal ganglion cells, exhibit spontaneous bursts of action potentials separated by extended periods of silence during development (Galli and Maffei, 1988) (Figure I-1a). These bursts of action potentials spread as waves of depolarization across the retina (Meister et al., 1991, Wong et al.,

1993), which earned them the name retinal waves. Retinal waves propagate throughout the developing visual system, inducing similar burst patterns within the dorsal lateral geniculate nucleus of the thalamus (Mooney et al., 1996, Weliky and Katz, 1999) and in visual cortex (Hanganu et al., 2006). Spontaneous network activation appears very early in development, after retinal ganglion cells have extended axons to their primary targets in the brain, and lasts until the eyes open, which occurs at postnatal day 13-14 in mice. During this time, as the circuits that mediate retinal waves change, so too change the details of the resulting firing patterns (Table 1). In the latest stage, retinal waves briefly co-exist with visual responses, presumably using parallel circuitry.

In spinal cord, motoneurons exhibit episodes of large rhythmic depolarizations separated by extended periods of silence, a firing pattern that drives embryonic limb movements (Hamburger, 1963, Provine, 1972). This spontaneous network activity has been observed over an extended period of development, from before motoneurons innervate muscle fibers (Milner and Landmesser, 1999) until central pattern generator circuits are functional, which occurs in late embryonic development (Yvert et al., 2004, Ren and Greer, 2003, Xu et al., 2005). As in the retina, the circuits that mediate spontaneous activity in the spinal cord and the resulting pattern of activity change during development (Bekoff, 1976) (Figure I-1b).

In the developing hippocampus, pyramidal cells exhibit two distinct patterns of spontaneous correlated firing (Crepel et al., 2007). Synchronous plateau assemblies (SPAs), which in mice span the period from a few days before to a few days after birth, are characterized by bursts of plateau potentials and are correlated across 3-7

neurons. Later, hippocampal neurons exhibit giant depolarizing potentials (GDPs; Figure I-1c), which occur for a week, overlapping briefly with the end of the SPAs. GDPs are characterized by slow depolarizations that are correlated across many neurons and are differentiated from SPAs pharmacologically (Garaschuk et al., 1998, Allene et al., 2008, Leinekugel et al., 1997).

Prior to the onset of hearing, spontaneous bursts of action potentials have been recorded in the auditory nerve. These bursts follow a pattern similar to those in the retina: short active periods are followed by quiet periods that range from seconds to minutes, depending on the species (Gummer and Mark, 1994, Jones et al., 2001, Jones et al., 2007, Lippe, 1994). A recent study revealed that this activity originates in the developing cochlea, where a transient population of support cells spontaneously depolarizes hair cells (Tritsch et al., 2007) (Figure I-1d). Inner hair cells in turn depolarize spiral ganglion cells, the cochlear projection neurons. This correlated spontaneous activity dissipates at the onset of hearing (Jones et al., 2001, Lippe, 1994).

Recently, spontaneous network activation has been characterized in the developing cerebellum (Watt et al., 2009) (Figure I-1e). Here, Purkinje cells, which are the cerebellar projection neurons, fire bursts of action potentials that propagate from the apex toward the base of cerebellar lobules. Intervals between bursts are much shorter here compared to the other circuits described above. The spontaneous rhythmic activity in the cerebellum is found in the first postnatal week of development, preceding the formation of the primary inputs to Purkinje cells.

Early pacemaker networks in the nervous system

In the absence of external stimuli, what triggers the large correlated depolarizations that characterize spontaneous activity in developing circuits? In the adult nervous system, spontaneous firing in a variety of networks, such as motor circuits (Harris-Warrick, 2002), is driven by pacemaker neurons. Pacemaker neurons exhibit unstable membrane potentials driven by a cyclical interplay of depolarizing and hyperpolarizing conductances. Pacemakers in the adult nervous system are typically depolarized by either a hyperpolarization-activated cation conductance (Biel et al., 2009) or a persistently active sodium conductance (e.g. in respiratory system (Rybak et al., 2007)). Depolarization activates a calcium-activated potassium conductance, generating an afterhyperpolarization (AHP) (Bond et al., 2005). The AHP prevents further depolarization, and the duration of the AHP sets the period of depolarizing events. Such a complement of conductances in adult pacemaker neurons typically leads to membrane potential oscillations with a period of tens of milliseconds to seconds. However, spontaneous network depolarizations during development typically initiate with longer intervals between events. To initiate network activity with a range of periodicities, developing circuits use varying combinations of pacemaker-like intrinsic membrane properties and network interactions.

Perhaps the simplest example of the interaction pacemaker-like conductances and network properties is found in the developing cerebellum. Purkinje cells spontaneously fire in the absence of any synaptic input (Raman and Bean, 1997), and therefore serve as the pacemaker neurons. During development, network interactions in the form of depolarizing GABAergic synapses entrain nearby Purkinje cells to fire

in phase such that waves of depolarization propagate down a chain of Purkinje cells (Watt et al., 2009). Consistent with computational models (Watt et al., 2009), this leads to an inter-wave interval of about 100 msec.

Giant depolarizing potentials (GDPs) in the hippocampus are triggered by CA3 pyramidal cells, which spontaneously fire bursts of action potentials (reviewed in Ben-Ari, 2001). The bursts of CA3 pyramidal cells, both during development and in the adult, are driven by a persistent sodium current and are terminated by a slow AHP, which lasts 3-4 seconds and is mediated by a calcium-activated potassium conductance (Sipila et al., 2006, Sipila et al., 2005). Blockade of the AHP decreases the inter-event interval from 3 seconds to less than 2 seconds, suggesting that the frequency of GDPs is set by the kinetics of these conductances. Similar to cerebellum, network interactions mediated by recurrent excitatory connections between CA3 pyramidal cells and excitatory connections with GABAergic interneurons (as described below) entrain depolarizations among neighboring cells, thereby prolonging the AHP and setting the frequency of GDPs. A similar organization is observed in neocortex (Lischalk et al., 2009) and midbrain (Rockhill et al., 2009), where clusters of pacemaker neurons are the sites of repeated event initiation.

The periodicity of spontaneous activity in the developing retina is not fixed by the membrane conductances of the network's pacemaker neurons, as it is in cerebellum and hippocampus. Instead, the periodicity emerges from an interplay between the connectivity of the network and the properties of the developing retina's pacemaker neurons, as has been explored both computationally (Butts et al., 1999) and experimentally (Zheng et al., 2006). Early retinal waves are initiated by a class of

cholinergic interneurons called starburst amacrine cells (Zhou, 2001). During waves, depolarizations in starburst amacrine cells are followed by a slow AHP lasting 15-30 seconds (Zheng et al., 2006), which is roughly the minimum interval between event initiations. These extremely slow AHPs, which are similar to slow AHPs characterized in hippocampus, thalamus, and peripheral nervous system (Lancaster and Nicoll, 1987, Sah and Isaacson, 1995, Sah, 1996, Sah and Faber, 2002, Vogalis et al., 2003), are thought to be regulated by the cAMP/PKA second messenger pathway (Goaillard and Vincent, 2002, Neylon et al., 2006). Consistent with this hypothesis, elevating cAMP significantly reduces the duration of slow AHPs recorded in starburst amacrine cells (Zheng et al., 2006) and increases the frequency of retinal waves (Stellwagen et al., 1999). The conductance underlying the spontaneous depolarization of starburst amacrine cells is less clear. In contrast to the robustly firing pyramidal cells in the CA3 region of hippocampus or Purkinje cells in the cerebellum, individual starburst cells undergo cell autonomous spontaneous depolarizations with a frequency lower than the initiation rate of spontaneous network activity (Zheng et al., 2006). However, starburst cells are densely interconnected by excitatory, cholinergic synapses. It has been postulated that these synaptic interactions cause neighboring starburst cells to depolarize each other, generating a retinal wave and inducing a large calcium influx in each starburst cell. The calcium causes a large AHP, making starburst cells refractory to further depolarization. As more starburst cells recover from this refractory period the likelihood of another network depolarization increases (Butts et al., 1999). Hence, the minute-long interval between retinal waves is due to pacemaker conductances that are activated by network interactions (Hennig et al., 2009).

In contrast to the retina, hippocampus and cerebellum, no pacemaker neuron has been identified in the developing spinal cord. Rather, the periodicity of spontaneous network activity in the developing spinal cord is thought to be dependent on the properties of recurrent excitatory interactions in the network. The spinal cord contains cholinergic, glutamatergic, GABAergic, and glycinergic neurons, but all of the connections in the developing spinal cord are depolarizing (see below). Immature spinal neurons continuously release neurotransmitters onto one another, but the efficacy of synaptic connections changes as a function of activity (Chub and O'Donovan, 2001, Fedirchuk et al., 1999, Marchetti et al., 2005, Tabak et al., 2000, Chub et al., 2006). Immediately after an episode of spontaneous activity the network is most depressed, so the ongoing synaptic excitation within the network is not powerful enough to trigger another event. As the network recovers from the previous event the ongoing synaptic excitation increases in efficacy, until eventually the neurons reciprocally excite one another enough to trigger another network-encompassing event. An important component of the network in spinal cord is a population of GABAergic interneurons that form strong synapses onto motoneurons (Wenner and O'Donovan, 2001). During an episode of network activity, which can last as long as 60 seconds, sustained activation of $GABA_A$ receptors leads to a massive efflux of chloride (Chub and O'Donovan, 2001). As an episode progresses the intracellular concentration of chloride is reduced to such an extent that the reversal potential for chloride becomes more hyperpolarized than before the episode, causing GABA and glycine to be less excitatory. In this scenario, the long interval between events is due to chloride re-accumulation in motoneuron dendrites via chloride

transporters (Chub and O'Donovan, 2001, Marchetti et al., 2005, Chub et al., 2006). Evidence for a reduction in the excitatory drive is provided by the reduction of the size of $GABA_A$-mediated postsynaptic currents following a network event. In addition, blockade of the chloride-accumulating transporter NKCC1 can block spontaneous network activity during development (Marchetti et al., 2005), indicating that lowering levels of intracellular chloride reduce the excitability of the network.

Recent research has provided a model for the generation of spontaneous bursts of action potentials in the auditory nerve. In the developing rat cochlea, periodic release of ATP from inner supporting cells depolarizes inner hair cells, which then release glutamate onto the afferent dendrites of spiral ganglion neurons and initiate bursts of action potentials (Tritsch et al., 2007). Although ATP-mediated currents occur in hair cells at a rate of about three to four per minute, action potential bursts appear in spiral ganglion neurons only once per minute (Tritsch et al., 2007), possibly because only a subset of ATP-mediated currents are large enough to depolarize hair cells sufficiently to trigger glutamate release. At present, little is known about the mechanisms that regulate the timing of ATP release from supporting cells and thus the timing of action potential bursts in the auditory nerve. (Tritsch et al., 2007)

Transient features of developing networks

The patterns of spontaneous network activity observed during development differ in many ways from the activity patterns of the adult nervous system. A dramatic example is found in the retina: here, adult circuits are organized along a “vertical” axis, which limits the lateral spread of excitatory signals in order to preserve a high-

acuity representation of visual space. In contrast, during development spontaneous network activity in the form of retinal waves propagates laterally across large areas of tissue that represent several degrees of the visual field. This lateral spread of activity is a result of several connectivity features that are present only during a finite period of development, and which are described below.

Depolarizing GABA

A prominent feature of several developing circuits that is crucial for activity propagation is the excitatory action of GABA and glycine, which in the adult brain act as inhibitory neurotransmitters. This depolarizing action of canonically inhibitory transmitters is primarily due to high intracellular concentrations of chloride at early ages: when a $GABA_A$ receptor is activated, chloride exits the cell, which causes depolarization. As neurons mature, they change their complement of chloride transporters, which leads to a decrease in intracellular chloride (Ben-Ari, 2002). In the spinal cord, hippocampus, neocortex and cerebellum, the cells that will become inhibitory interneurons in adulthood are the primary source of depolarization during development (Ben-Ari et al., 2007, Blaesse et al., 2009). Although activation of $GABA_A$ receptors is depolarizing in the developing retina (Zhang et al., 2006, Sernagor et al., 2003, Leitch et al., 2005), $GABA_A$ receptor antagonists do not block retinal waves (though they do modulate wave properties (Stellwagen et al., 1999, Wang et al., 2007)), and GABA signaling is not required for spontaneous network activity in the developing cochlea.

Depolarizing GABA is critical for the generation of GDPs in the developing hippocampus (Garaschuk et al., 1998, Allene et al., 2008, Leinekugel et al., 1997). GDPs are blocked by ionotropic glutamate and $GABA_A$ receptor antagonists and the age at which activation of $GABA_A$ receptors is no longer depolarizing is the age at which GDPs disappear (Leinekugel et al., 1997). This is in contrast to the earlier form of spontaneous network activity in the hippocampus, SPAs, which are not dependent on $GABA_A$ signaling, but rather on L-type calcium channel activation and gap junction coupling (Crepel et al., 2007) (see table).

Spontaneous activity in the developing spinal cord is also strongly influenced by depolarizing GABA and glycine (O'Donovan et al., 1998). In the spinal cord, spontaneous network activity is blocked by $GABA_A$ receptor antagonists. (Note, this blockade is transient; activity returns after 30 min in $GABA_A$ receptor antagonists[101]. Also, see below.) As described above, episodes of bursting activity and the underlying waves of depolarization are likely to be initiated by massive GABA release, and then terminated by a switch in the chloride gradient such that GABA temporarily becomes less excitatory (Marchetti et al., 2005, Chub et al., 2006). Also similar to hippocampus, spontaneous network activity in spinal cord disappears around the time activation of $GABA_A$ receptors ceases to be excitatory (Yvert et al., 2004, Xu et al., 2005).

Depolarizing GABA is the sole source of coupling involved in generating spontaneous network activity in the developing cerebellum (Watt et al., 2009). GABAergic Purkinje cells, which are the primary projection neurons of the cerebellum, make local synaptic connections with neighboring Purkinje cells. These

local axon collaterals are not distributed uniformly within the cerebellar network. Instead, the density of Purkinje-Purkinje connections is higher for cells located closer to the base of each cerebellar lobule. Purkinje cells spontaneously spike at all ages, but the existence of depolarizing GABAergic connections between nearby Purkinje cells during the first postnatal week entrains the firing of neighboring Purkinje cells, generating a propagating wave that travels preferentially in the direction of higher-density local connections, i.e. towards the base of the cerebellar lobules. When $GABA_A$ signaling becomes inhibitory in the second postnatal week, a computational model predicts that Purkinje cells would still be entrained, but that the direction of propagation would switch (Watt et al., 2009), with waves starting from the base of a lobule and propagating toward the apex. Local axon collaterals among Purkinje cells persist until adulthood but form many fewer synaptic connections. Hence, as the cerebellum matures and the functional connections between nearby Purkinje cells are reduced, the substrate for propagation disappears.

Transient connections

The second feature of developing networks that is crucial for generating spontaneous network activity is the existence of circuit components that are uniquely expressed during development. These transient components, such as the local axon collaterals of Purkinje cells described above and expression of neurotransmitter receptors, provide a substrate for correlating activity across populations of cells that are not directly connected in the adult.

The retina provides another example of transient components that form a substrate for wave propagation. During the first postnatal week, retinal waves propagate via a network of starburst amacrine cells (Zhou, 2001). Immature starburst amacrine cells undergo spontaneous depolarizations and release both acetylcholine and GABA onto neighboring starburst amacrine cells (Zheng et al., 2006, Zheng et al., 2004). Hence, it has been proposed that cholinergic waves are initiated by spontaneous depolarizations in starburst amacrine cells and propagate via connections with other starburst amacrine cells. In contrast to its role in spinal cord, hippocampus and cerebellum, depolarizing GABA is not required for retinal wave propagation. Rather, retinal waves propagate through a recurrent cholinergic network of cells linked by nicotinic acetylcholine receptors (nAChRs), which are transiently expressed at synapses among starburst amacrine cells during development (Zheng et al., 2004). At the age when starburst amacrine cells stop expressing nAChRs and are therefore no longer connected via excitatory synapses, the cholinergic waves disappear (Zhou, 2001) and are replaced by glutamatergic waves, as discussed below.

Similar to the retina, spontaneous network activity in the spinal cord may also depends on connections that exist early in development but become functionally insignificant in the adult. During development, motoneurons form local excitatory connections with other motoneurons (Nishimaru et al., 2005) and with local GABAergic interneurons called Renshaw (Nishimaru et al., 2005, Mentis et al., 2005). Also, during development, Renshaw cells receive glutamatergic inputs from sensory neurons (Nishimaru et al., 2005, Mentis et al., 2006), Though motoneuron

inputs to Renshaw cells persist into adulthood, motoneuron-motoneuron synapses and sensory-neuron - Renshaw synapses do not remain functional (Mentis et al., 2006).

The developing cochlea uses a similar strategy to sustain spontaneous correlated activity early in development. Prior to the onset of hearing, hair cells are periodically depolarized through activation of purinergic receptors by ATP released from neighboring supporting cells (Tritsch et al., 2007). The supporting cells comprise a transient structure, Kölliker's organ, which is present only during a short period of development (Forsythe, 2007). Furthermore, preliminary studies in rats indicate that hair cells express purinergic receptors only for a transient period from a few days after birth to around the time of hearing onset [N. X. Tritsch and D. E. Bergles, "Developmental Regulation of Spontaneous Cochlear Activity", Association for Research in Otolaryngology, Annual Meeting, 2009]. Hence, the transient source of ATP-secreting cells and the transient expression of receptors are likely to dictate the period of development during which spontaneous activity in the cochlea is present.

Extrasynaptic glutamate

There is growing evidence that extrasynaptic transmission plays a part in propagating the waves of depolarization in developing networks before synaptic structures achieve their mature state (Demarque et al., 2002). In addition to mediating direct synaptic communication, neurotransmitters released from a presynaptic cell can "spill" out of the synaptic cleft and activate extrasynaptic receptors: on the postsynaptic cell, on the presynaptic terminal and on other neighboring neurons and glia. Extrasynaptic glutamate has been implicated in regulating the early

differentiation of neurons in the ventricular zone (LoTurco et al., 1995) and might modulate neuronal migration (Manent et al., 2005). Currently it is thought that at later developmental stages, retinal waves and hippocampal GDPs are mediated, at least in part, by extrasynaptic glutamate.

In the retina, during the period just prior to eye-opening, spontaneous correlated activity is no longer dependent on acetylcholine release from starburst amacrine cells, but rather on glutamate release from bipolar cells (for review see Torborg and Feller, 2005). In contrast to the starburst amacrine cells, whose processes form a dense lateral network, neighboring bipolar cells are not synaptically connected. Each bipolar cell has a very small axonal process, forming glutamatergic synapses on a small part of the total dendritic tree of its target ganglion cell. Recently we have demonstrated that retinal waves are accompanied by large transient increases in extrasynaptic glutamate (Blankenship et al., 2009). This extrasynaptic glutamate provides a possible source of depolarization that is not limited to cells directly postsynaptic to bipolar cell release sites.

Does extrasynaptic glutamate mediate wave propagation? Interestingly, elevating extrasynaptic glutamate by pharmacologically blocking glutamate transporters, which tightly regulate glutamate levels outside the synaptic cleft, significantly reduces variability in wave speed, making slow waves faster and fast waves slower (Blankenship et al., 2009). This observation indicates that extrasynaptic glutamate positively and negatively regulates wave propagation. Extrasynaptic glutamate is known to be both excitatory and inhibitory in the adult retina (Chen and Diamond, 2002, DeVries et al., 2006, Veruki et al., 2006). As there is no reliable way

to block extrasynaptic glutamate signaling independent of synaptic glutamate signaling, it is not know whether extrasynaptic glutamate transmission is required for wave propagation.

A role for extrasynaptic glutamate has also been demonstrated in developing cortex (Demarque et al., 2004, Milh et al., 2007), hippocampus (Cattani et al., 2007) and brain stem (Sharifullina and Nistri, 2006), where increasing extracellular glutamate profoundly alters the patterns of spontaneous network activation. In hippocampus, episodic elevations of extrasynaptic glutamate levels depolarize interneurons via activation of NMDA receptors, causing an increase in the frequency of events compared to endogenous GDPs (Cattani et al., 2007). Whether extrasynaptic glutamate plays a role in the endogenous activity patterns remains to be determined.

Gap junctions

Several studies have implicated gap junctions as potential substrates for propagating neural activity during development. There are three lines of evidence that support these claims. First, there are several examples of spontaneous network events that persist in the presence of a broad spectrum of neurotransmitter receptor antagonists and are thus non-synaptic. Such non-synaptic waves are detected embryonically in hippocampus (Crepel et al., 2007) and retina (Bansal et al., 2000, Syed et al., 2004), and they can be induced in cases when the synaptic pathways for mediating waves are disrupted (Singer et al., 2001) (Figure I-3 and see next section). Second, spontaneous network activity patterns can be suppressed by pharmacological blockade of gap junctions. Indeed, in the spinal cord, cochlea and retina, spontaneous

network activity is blocked by gap junction inhibitors (Tritsch et al., 2007, Milner and Landmesser, 1999, Syed et al., 2004, Singer et al., 2001, Hanson and Landmesser, 2003), at least at some stages of development. Unfortunately, gap junction blockers have several non-specific effects that could underlie the overall reduction of activity, including blockade of voltage-gated calcium channels that mediate synaptic transmission (Vessey et al., 2004, Takeda et al., 2005) , activation of large-conductance calcium-activated potassium channels (Takeda et al., 2005, Sheu et al., 2008, Wu et al., 2001), and inhibition of synaptic release (Tovar et al., 2009), which makes these experiments difficult to interpret. Third, transgenic mice lacking specific gap junction proteins (connexins) have altered spontaneous firing patterns. For example, in spinal cord the expression of a number of connexin proteins in motoneurons changes with development (Chang et al., 1999), and in mice lacking connexin 40 (Cx40), spontaneous activity is uncorrelated between motoneurons (Personius et al., 2007). In mice lacking Cx36, spontaneous network activity in the retina is altered such that retinal ganglion cells fire many more spikes between waves than observed in the wildtype (Torborg et al., 2005, Hansen et al., 2005), suggesting that Cx36-containing retinal gap junctions have a role in mediating the silences between waves.

Homeostatic regulation of spontaneous firing patterns

One of the striking features of spontaneous network activity during development is its robustness. Throughout their development, circuits use a multitude of strategies to spontaneously generate activity and, although the details of the

temporal and spatial correlations change, the overall pattern of activity remains the same – large depolarizations generated by excitatory synaptic inputs are followed by extended periods of silence.

The removal of a crucial component of a circuit showing spontaneous depolarizations often leads to compensation by the remaining components, providing further evidence of the robustness of the network activity (Turrigiano, 2006). This phenomenon was first described in the developing spinal cord, where extended blockade of receptors for a primary excitatory transmitter (acetylcholine during the early stage of development (Myers et al., 2005, Milner and Landmesser, 1999) and glutamate or GABA during a later stage (Chub and O'Donovan, 1998)) led to an initial block followed by a restoration of spontaneous network activity. Homeostatic compensation has also been observed *in ovo,* where recovery from blockade of glutamate or GABA-A receptors takes significantly longer than that observed in vitro (12 hours vs 30-60 minutes). A recent dissection of mechanisms that underlie a homeostatic phenomenon *in ovo* revealed that changes in synaptic strength (Gonzalez-Islas and Wenner, 2006, Wilhelm and Wenner, 2008) and changes in the expression of ion channels that control cellular excitability in motoneurons (Wilhelm et al., 2009) compensate for the loss of excitatory transmitter (Figure I-2).

A similar finding has been recently described in hippocampus (Sipila et al., 2009, Pfeffer et al., 2009). In transgenic mice lacking the chloride transporter NKCC1, GABA is not depolarizing in hippocampal neurons during development because the missing transporter is responsible for maintaining the high level of chloride in developing neurons. Yet the hippocampus of NKCC1-KO mice still exhibits

spontaneous network activity. Similar to the spinal cord, the compensation is due to an increase in excitability of CA3 neurons and potentially in synaptic strength (Sipila et al., 2009) (but see Pfeffer et al., 2009). Additionally, activity is maintained during acute blockade of GDPs by a strengthening of SPAs (Crepel et al., 2007).

Homeostatic compensation has also been observed in the circuits that mediate retinal waves (Figure I-3). Transgenic mice lacking choline acetyltransferase (ChAT), an enzyme crucial for acetylcholine production, do not exhibit the endogenous cholinergic waves. Instead, they exhibit compensatory waves, which are not blocked by any fast neurotransmitter receptor antagonists (Stacy et al., 2005), indicating that the compensatory mechanism here is different from the one observed in spinal cord and hippocampus. The compensatory waves are, however, blocked by gap junction antagonists (Stacy et al., 2005), leading to the hypothesis that they are an extension of an earlier, nonsynaptic wave-generating mechanism that has been observed in embryonic mice (Bansal et al., 2000) and rabbits (Syed et al., 2004). One of the interesting features of the compensatory retinal waves is that they require a few days to appear, suggesting that significant circuit rearrangements need to take place. A more complex form of compensation occurs in mice lacking the beta-2 subunit of nicotinic acetylcholine receptors. Under some experimental conditions, no wave activity is detected in these ß2-nAhR-KO mice (Bansal et al., 2000, McLaughlin et al., 2003), whereas in other recording conditions (Sun et al., 2008) -- characterized, for example, by increased temperature (D. Feldheim, personal communication) -- compensatory waves are observed. As these waves are not blocked by fast neurotransmitter receptor antagonists (Sun et al., 2008), they may be the same gap-

junction mediated waves as those in the transgenic mice lacking ChAT (Stacy et al., 2005). Although the circuit underlying these compensatory waves is not yet understood, one likely homeostatic mechanism is based on an increased excitability of retinal neurons, because bath application of voltage-gated calcium channel agonists leads to the generation of similar non-synaptic waves in both wildtype and ß2-nAChR-KO retinas (Singer et al., 2001, Torborg et al., 2004). Additionally, in ß2-nAChR-KO mice retinal waves dependent upon glutamatergic signaling appear 3-4 days earlier than in wildtype mice (Bansal et al., 2000), indicating that the absence of endogenous signaling induces an early maturation of the next stage of network activity.

The observation that transgenic mice with disrupted cholinergic circuitry exhibit a reappearance of non-synaptic waves suggests that normally, activity in the cholinergic circuit suppresses non-synaptic waves. Similarly, the disappearance of cholinergic waves depends on the maturation of glutamatergic circuits, suggesting that glutamate activity suppresses cholinergic circuit activity. Transgenic mice lacking the vesicular glutamate transporter VGLUT1 in bipolar cells continue to exhibit cholinergic waves at the age when cholinergic circuits disappear in wild-type mice (Blankenship et al., 2009). A similar switch from cholinergic to glutamatergic transmission has been observed in the developing hindbrain, however it is not yet known whether this transition is influenced by the absence of network activity as in the developing retina and spinal cord (Mochida et al., 2009).

Homeostatic regulation of spontaneous network activity has recently been observed in the developing hippocampus. In a knockout mouse lacking the chloride-accumulating transporter NKCC1, activation of $GABA_A$ receptors is never

depolarizing, and therefore the major depolarizing drive for GDPs is absent. Although GDPs are detectable (Sipila et al., 2009), fewer hippocampal neurons participate in the events (Pfeffer et al., 2009). In NKCC1 knockout mice, the compensatory activity was partially mediated by an increase in the intrinsic excitability of CA3 pyramidal cells rather than by a change in network properties as seen in spinal cord and retina (Sipila et al., 2009). To our knowledge, homeostatic regulation of spontaneous network activity has not been observed in developing cerebellum and cochlea.

Conclusions and future directions

A fundamental feature of developing neural circuits is the presence of spontaneous network activity, often taking the form of propagating waves. The circuits that mediate this activity rely on cell-intrinsic and synaptic properties that are observed for only a brief time during development. Robust compensatory mechanisms seem to be in place to ensure that spontaneous network activity is actively maintained throughout this crucial period of development.

Although tremendous insights have been gained into the mechanisms generating spontaneous activity, a remaining question concerns the purpose this activity serves during development. In developing sensory epithelia, such as retina and cochlea, propagating neural activity contains topographic information that may be crucial for the establishment of early sensory maps in the brain. Propagating activity in the spinal cord may be crucial for defining circuits within the cord that will serve as central pattern generators in adulthood, or for targeting motoneurons in neighboring spinal segments to neighboring muscles. Spontaneous activity in developing cortex

and hippocampus may serve to strengthen the networks mediating oscillatory activity in the adult. Answering these questions will require careful manipulations that can determine whether the pattern of activity is crucial for driving a given developmental event or whether the average level of activity that the pattern provides is simply permissive for other cues (Feller, 2009, Chalupa, 2009).

Continued insights into the mechanisms underlying early network activity, as well as an increased awareness of its crucial role in brain development, could have profound implications for clinical treatments of pregnant women. Alcohol, for example, is known to affect network activity patterns, and many regions of the brain are particularly sensitive to fetal exposure to alcohol. Alcohol disrupts normal firing patterns in the developing hippocampus (Galindo and Valenzuela, 2006), and extended fetal exposure prevents the normal development of primary sensory systems (Stromland, 2004, Medina et al., 2005). Another potential clinical implication relates to a decrease in spontaneous activity during birth -- a transient neuroprotective effect triggered by a large increase in oxytocin, a hormone that modulates the depolarizing action of GABA transmission (Tyzio et al., 2006). A deeper understanding of the mechanisms that mediate spontaneous activity during development will help to prevent neuropathologies associated with fetal exposure to neuroactive pharmacological agents.

Acknowledgement

This chapter is original work submitted as: Blankenship, AG; Feller, MB. Mechanisms underlying spontaneous patterned activity in developing neural circuits. Nature Reviews Neuroscience., and is included with permission from all authors. The dissertation author was the primary author of this paper.

References

Allene C, Cattani A, Ackman JB, Bonifazi P, Aniksztejn L, Ben-Ari Y, Cossart R (2008) Sequential generation of two distinct synapse-driven network patterns in developing neocortex. J Neurosci 28:12851-63.

Bansal A, Singer JH, Hwang BJ, Xu W, Beaudet A, Feller MB (2000) Mice lacking specific nicotinic acetylcholine receptor subunits exhibit dramatically altered spontaneous activity patterns and reveal a limited role for retinal waves in forming ON and OFF circuits in the inner retina. J Neurosci 20:7672-7681.

Bekoff A (1976) Ontogeny of leg motor output in the chick embryo: A neural analysis. Brain Res 106:271-291.

Ben-Ari Y (2002) Excitatory actions of gaba during development: The nature of the nurture. Nat Rev Neurosci 3:728-739.

Ben-Ari Y (2001) Developing networks play a similar melody. Trends Neurosci 24:353-360.

Ben-Ari Y, Gaiarsa JL, Tyzio R, Khazipov R (2007) GABA: A pioneer transmitter that excites immature neurons and generates primitive oscillations. Physiol Rev 87:1215-1284.

Ben-Ari Y, Cherubini E, Corradetti R, Gaiarsa JL (1989) Giant synaptic potentials in immature rat CA3 hippocampal neurones. J. Physiol 416:303-325.

Biel M, Wahl-Schott C, Michalakis S, Zong X (2009) Hyperpolarization-activated cation channels: From genes to function. Physiol Rev 89:847-885.

Blaesse P, Airaksinen MS, Rivera C, Kaila K (2009) Cation-chloride cotransporters and neuronal function. Neuron 61:820-838.

Blankenship AG, Ford KJ, Johnson J, Seal RP, Edwards RH, Copenhagen DR, Feller MB (2009) Synaptic and extrasynaptic factors governing glutamatergic retinal waves. Neuron 62:230-41.

Bloomfield SA, Volgyi B (2009) The diverse functional roles and regulation of neuronal gap junctions in the retina. Nat Rev Neurosci 10:495-506.

Bond CT, Maylie J, Adelman JP (2005) SK channels in excitability, pacemaking and synaptic integration. Curr Opin Neurobiol 15:305-311.

Butts DA, Feller MB, Shatz CJ, Rokhsar DS (1999) Retinal waves are governed by collective network properties. J Neurosci 19:3580-3593.

Cattani AA, Bonfardin VD, Represa A, Ben-Ari Y, Aniksztejn L (2007) Generation of slow network oscillations in the developing rat hippocampus after blockade of glutamate uptake. J Neurophysiol 98:2324-36.

Chalupa LM (2009) Retinal waves are unlikely to instruct the formation of eye-specific retinogeniculate projections. Neural Dev 4:25.

Chang Q, Gonzalez M, Pinter MJ, Balice-Gordon RJ (1999) Gap junctional coupling and patterns of connexin expression among neonatal rat lumbar spinal motor neurons. J Neurosci 19:10813-28.

Chen S, Diamond JS (2002) Synaptically released glutamate activates extrasynaptic NMDA receptors on cells in the ganglion cell layer of rat retina. J Neurosci 22:2165-73.

Chub N, O'Donovan MJ (2001) Post-episode depression of GABAergic transmission in spinal neurons of the chick embryo. J Neurophysiol 85:2166-2176.

Chub N, O'Donovan MJ (1998) Blockade and recovery of spontaneous rhythmic activity after application of neurotransmitter antagonists to spinal networks of the chick embryo. J Neurosci 18:294-306.

Chub N, Mentis GZ, O'donovan MJ (2006) Chloride-sensitive MEQ fluorescence in chick embryo motoneurons following manipulations of chloride and during spontaneous network activity. J Neurophysiol 95:323-330.

Corlew R, Bosma MM, Moody WJ (2004) Spontaneous, synchronous electrical activity in neonatal mouse cortical neurones. J Physiol 560:377-90. Epub 2004 Aug 5.

Crepel V, Aronov D, Jorquera I, Represa A, Ben-Ari Y, Cossart R (2007) A parturition-associated nonsynaptic coherent activity pattern in the developing hippocampus. Neuron 54:105-20.

Demarque M, Represa A, Becq H, Khalilov I, Ben-Ari Y, Aniksztejn L (2002) Paracrine intercellular communication by a Ca2+- and SNARE-independent release of GABA and glutamate prior to synapse formation. Neuron 36:1051-1061.

Demarque M, Villeneuve N, Manent JB, Becq H, Represa A, Ben-Ari Y, Aniksztejn L (2004) Glutamate transporters prevent the generation of seizures in the developing rat neocortex. J Neurosci 24:3289-94.

DeVries SH, Li W, Saszik S (2006) Parallel processing in two transmitter microenvironments at the cone photoreceptor synapse. Neuron 50:735-48.

Fedirchuk B, Wenner P, Whelan PJ, Ho S, Tabak J, O'Donovan MJ (1999) Spontaneous network activity transiently depresses synaptic transmission in the embryonic chick spinal cord. J Neurosci 19:2102-2112.

Feller MB (2009) Retinal waves are likely to instruct the formation of eye-specific retinogeniculate projections. Neural Dev 4:24.

Forsythe ID (2007) Hearing: A fantasia on kolliker's organ. Nature 450:43-44.

Galindo R, Valenzuela CF (2006) Immature hippocampal neuronal networks do not develop tolerance to the excitatory actions of ethanol. Alcohol 40:111-118.

Galli L, Maffei L (1988) Spontaneous impulse activity of rat retinal ganglion cells in prenatal life. Science 242:90-1.

Garaschuk O, Hanse E, Konnerth A (1998) Developmental profile and synaptic origin of early network oscillations in the CA1 region of rat neonatal hippocampus. J Physiol (Lond) 507:219-36.

Garaschuk O, Linn J, Eilers J, Konnerth A (2000) Large-scale oscillatory calcium waves in the immature cortex. Nat Neurosci 3:452-9.

Goaillard JM, Vincent P (2002) Serotonin suppresses the slow afterhyperpolarization in rat intralaminar and midline thalamic neurones by activating 5-HT (7) receptors. J Physiol 541:453-465.

Gonzalez-Islas C, Wenner P (2006) Spontaneous network activity in the embryonic spinal cord regulates AMPAergic and GABAergic synaptic strength. Neuron 49:563-75.

Gummer AW, Mark RF (1994) Patterned neural activity in brain stem auditory areas of a prehearing mammal, the tammar wallaby (macropus eugenii). Neuroreport 5:685-688.

Gust J, Wright JJ, Pratt EB, Bosma MM (2003) Development of synchronized activity of cranial motor neurons in the segmented embryonic mouse hindbrain. J Physiol 550:123-133.

Hamburger V (1963) Some aspects of the embryology of behavior. Q Rev Biol 38:342-365.

Hanganu IL, Ben-Ari Y, Khazipov R (2006) Retinal waves trigger spindle bursts in the neonatal rat visual cortex. J Neurosci. 26:6728-36.

Hansen KA, Torborg CL, Elstrott J, Feller MB (2005) Expression and function of the neuronal gap junction protein connexin 36 in developing mammalian retina. J Comp Neurol 493:309-20.

Hanson MG, Landmesser LT (2003) Characterization of the circuits that generate spontaneous episodes of activity in the early embryonic mouse spinal cord. J Neurosci 23:587-600.

Hanson MG, Milner LD, Landmesser LT (2008) Spontaneous rhythmic activity in early chick spinal cord influences distinct motor axon pathfinding decisions. Brain Res Rev 57:77-85.

Harris-Warrick RM (2002) Voltage-sensitive ion channels in rhythmic motor systems. Curr Opin Neurobiol 12:646-651.

Hennig MH, Adams C, Willshaw D, Sernagor E (2009) Early-stage waves in the retinal network emerge close to a critical state transition between local and global functional connectivity. J Neurosci 29:1077-1086.

Jones TA, Jones SM, Paggett KC (2001) Primordial rhythmic bursting in embryonic cochlear ganglion cells. J Neurosci 21:8129-8135.

Jones TA, Leake PA, Snyder RL, Stakhovskaya O, Bonham B (2007) Spontaneous discharge patterns in cochlear spiral ganglion cells before the onset of hearing in cats. J Neurophysiol 98:1898-1908.

Kandler K, Clause A, Noh J (2009) Tonotopic reorganization of developing auditory brainstem circuits. Nat Neurosci 12:711-717.

Khazipov R, Luhmann HJ (2006) Early patterns of electrical activity in the developing cerebral cortex of humans and rodents. Trends Neurosci 29:414-418.

Lancaster B, Nicoll RA (1987) Properties of two calcium-activated hyperpolarizations in rat hippocampal neurones. J Physiol 389:187-203.

Landmesser LT, O'Donovan MJ (1984) Activation patterns of embryonic chick hind limb muscles recorded in ovo and in an isolated spinal cord preparation. J Physiol 347:189-204.

Leinekugel X (2003) Developmental patterns and plasticities: The hippocampal model. J Physiol Paris 97:27-37.

Leinekugel X, Medina I, Khalilov I, Ben-Ari Y, Khazipov R (1997) Ca2+ oscillations mediated by the synergistic excitatory actions of GABA (A) and NMDA receptors in the neonatal hippocampus. Neuron 18:243-55.

Leinekugel X, Khazipov R, Cannon R, Hirase H, Ben-Ari Y, Buzsaki G (2002) Correlated bursts of activity in the neonatal hippocampus in vivo. Science 296:2049-52.

Leitch E, Coaker J, Young C, Mehta V, Sernagor E (2005) GABA type-A activity controls its own developmental polarity switch in the maturing retina. J Neurosci 25:4801-4805.

Lippe WR (1994) Rhythmic spontaneous activity in the developing avian auditory system. J Neurosci 14:1486-1495.

Lischalk JW, Easton CR, Moody WJ (2009) Bilaterally propagating waves of spontaneous activity arising from discrete pacemakers in the neonatal mouse cerebral cortex. Dev Neurobiol 69:407-414.

LoTurco JJ, Owens DF, Heath MJ, Davis MB, Kriegstein AR (1995) GABA and glutamate depolarize cortical progenitor cells and inhibit DNA synthesis. Neuron 15:1287-1298.

Manent JB, Demarque M, Jorquera I, Pellegrino C, Ben-Ari Y, Aniksztejn L, Represa A (2005) A noncanonical release of GABA and glutamate modulates neuronal migration. J Neurosci 25:4755-4765.

Marchetti C, Tabak J, Chub N, O'Donovan MJ, Rinzel J (2005) Modeling spontaneous activity in the developing spinal cord using activity-dependent variations of intracellular chloride. J Neurosci 25:3601-3612.

Marder E, Rehm KJ (2005) Development of central pattern generating circuits. Curr Opin Neurobiol 15:86-93.

McLaughlin T, Torborg CL, Feller MB, O'Leary DD (2003) Retinotopic map refinement requires spontaneous retinal waves during a brief critical period of development. Neuron 40:1147-1160.

Medina AE, Krahe TE, Ramoa AS (2005) Early alcohol exposure induces persistent alteration of cortical columnar organization and reduced orientation selectivity in the visual cortex. J Neurophysiol 93:1317-1325.

Meister M, Wong RO, Baylor DA, Shatz CJ (1991) Synchronous bursts of action potentials in ganglion cells of the developing mammalian retina. Science 252:939-43.

Mentis GZ, Siembab VC, Zerda R, O'Donovan MJ, Alvarez FJ (2006) Primary afferent synapses on developing and adult renshaw cells. J Neurosci 26:13297-13310.

Mentis GZ, Alvarez FJ, Bonnot A, Richards DS, Gonzalez-Forero D, Zerda R, O'Donovan MJ (2005) Noncholinergic excitatory actions of motoneurons in the neonatal mammalian spinal cord. Proc Natl Acad Sci U S A 102:7344-7349.

Milh M, Becq H, Villeneuve N, Ben-Ari Y, Aniksztejn L (2007) Inhibition of glutamate transporters results in a "suppression-burst" pattern and partial seizures in the newborn rat. Epilepsia 48:169-74.

Milner LD, Landmesser LT (1999) Cholinergic and GABAergic inputs drive patterned spontaneous motoneuron activity before target contact. J Neurosci 19:3007-3022.

Mochida H, Sato K, Momose-Sato Y (2009) Switching of the transmitters that mediate hindbrain correlated activity in the chick embryo. Eur J Neurosci 29:14-30.

Mohajerani MH, Cherubini E (2006) Role of giant depolarizing potentials in shaping synaptic currents in the developing hippocampus. Crit Rev Neurobiol 18:13-23.

Moody WJ, Bosma MM (2005) Ion channel development, spontaneous activity, and activity-dependent development in nerve and muscle cells. Physiol Rev 85:883-941.

Mooney R, Penn AA, Gallego R, Shatz CJ (1996) Thalamic relay of spontaneous retinal activity prior to vision. Neuron 17:863-874.

Myers CP, Lewcock JW, Hanson MG, Gosgnach S, Aimone JB, Gage FH, Lee KF, Landmesser LT, Pfaff SL (2005) Cholinergic input is required during embryonic development to mediate proper assembly of spinal locomotor circuits. Neuron 46:37-49.

Neylon CB, Fowler CJ, Furness JB (2006) Regulation of the slow afterhyperpolarization in enteric neurons by protein kinase A. Auton Neurosci 126-127:258-263.

Nishimaru H, Restrepo CE, Ryge J, Yanagawa Y, Kiehn O (2005) Mammalian motor neurons corelease glutamate and acetylcholine at central synapses. Proc Natl Acad Sci U S A 102:5245-5249.

O'Donovan MJ, Chub N, Wenner P (1998) Mechanisms of spontaneous activity in developing spinal networks. J Neurobiol 37:131-145.

Owens DF, Kriegstein AR (2002) Is there more to GABA than synaptic inhibition? Nat Rev Neurosci 3:715-727.

Personius KE, Chang Q, Mentis GZ, O'Donovan MJ, Balice-Gordon RJ (2007) Reduced gap junctional coupling leads to uncorrelated motor neuron firing and precocious neuromuscular synapse elimination. Proc Natl Acad Sci U S A 104:11808-11813.

Pfeffer CK, Stein V, Keating DJ, Maier H, Rinke I, Rudhard Y, Hentschke M, Rune GM, Jentsch TJ, Hubner CA (2009) NKCC1-dependent GABAergic excitation drives synaptic network maturation during early hippocampal development. J Neurosci 29:3419-3430.

Provine RR (1972) Ontogeny of bioelectric activity in the spinal cord of the chick embryo and its behavioral implications. Brain Res 41:365-378.

Raman IM, Bean BP (1997) Resurgent sodium current and action potential formation in dissociated cerebellar purkinje neurons. J Neurosci 17:4517-4526.

Ren J, Greer JJ (2003) Ontogeny of rhythmic motor patterns generated in the embryonic rat spinal cord. J Neurophysiol 89:1187-1195.

Rockhill W, Kirkman JL, Bosma MM (2009) Spontaneous activity in the developing mouse midbrain driven by an external pacemaker. Dev Neurobiol .

Rybak IA, Abdala AP, Markin SN, Paton JF, Smith JC (2007) Spatial organization and state-dependent mechanisms for respiratory rhythm and pattern generation. Prog Brain Res 165:201-220.

Sah P (1996) Ca (2+)-activated K+ currents in neurones: Types, physiological roles and modulation. Trends Neurosci 19:150-154.

Sah P, Faber ES (2002) Channels underlying neuronal calcium-activated potassium currents. Prog Neurobiol 66:345-353.

Sah P, Isaacson JS (1995) Channels underlying the slow afterhyperpolarization in hippocampal pyramidal neurons: Neurotransmitters modulate the open probability. Neuron 15:435-441.

Sernagor E, Young C, Eglen SJ (2003) Developmental modulation of retinal wave dynamics: Shedding light on the GABA saga. J Neurosci 23:7621-7629.

Sharifullina E, Nistri A (2006) Glutamate uptake block triggers deadly rhythmic bursting of neonatal rat hypoglossal motoneurons. J Physiol 572:407-23.

Sheu SJ, Bee YS, Chen CH (2008) Resveratrol and large-conductance calcium-activated potassium channels in the protection of human retinal pigment epithelial cells. J Ocul Pharmacol Ther 24:551-555.

Singer JH, Mirotznik RR, Feller MB (2001) Potentiation of L-type calcium channels reveals nonsynaptic mechanisms that correlate spontaneous activity in the developing mammalian retina. J Neurosci 21:8514-22.

Sipila ST, Huttu K, Voipio J, Kaila K (2006) Intrinsic bursting of immature CA3 pyramidal neurons and consequent giant depolarizing potentials are driven by a persistent na+ current and terminated by a slow Ca2+ -activated K+ current. Eur J Neurosci 23:2330-8.

Sipila ST, Huttu K, Soltesz I, Voipio J, Kaila K (2005) Depolarizing GABA acts on intrinsically bursting pyramidal neurons to drive giant depolarizing potentials in the immature hippocampus. J Neurosci 25:5280-5289.

Sipila ST, Huttu K, Yamada J, Afzalov R, Voipio J, Blaesse P, Kaila K (2009) Compensatory enhancement of intrinsic spiking upon NKCC1 disruption in neonatal hippocampus. J Neurosci 29:6982-6988.

Spitzer NC (2006) Electrical activity in early neuronal development. Nature 444:707-712.

Stacy RC, Demas J, Burgess RW, Sanes JR, Wong RO (2005) Disruption and recovery of patterned retinal activity in the absence of acetylcholine. J Neurosci 25:9347-9357.

Stellwagen D, Shatz CJ, Feller MB (1999) Dynamics of retinal waves are controlled by cyclic AMP. Neuron 24:673-685.

Stromland K (2004) Visual impairment and ocular abnormalities in children with fetal alcohol syndrome. Addict Biol 9:153-7; discussion 159-60.

Sun C, Warland DK, Ballesteros JM, van der List D, Chalupa LM (2008) Retinal waves in mice lacking the beta2 subunit of the nicotinic acetylcholine receptor. Proc Natl Acad Sci U S A 105:13638-13643.

Syed MM, Lee S, Zheng J, Zhou ZJ (2004) Stage-dependent dynamics and modulation of spontaneous waves in the developing rabbit retina. J Physiol 560:533-49.

Tabak J, Senn W, O'Donovan MJ, Rinzel J (2000) Modeling of spontaneous activity in developing spinal cord using activity-dependent depression in an excitatory network. J Neurosci 20:3041-3056.

Takeda Y, Ward SM, Sanders KM, Koh SD (2005) Effects of the gap junction blocker glycyrrhetinic acid on gastrointestinal smooth muscle cells. Am J Physiol Gastrointest Liver Physiol 288:G832-41.

Torborg C, Wang CT, Muir-Robinson G, Feller MB (2004) L-type calcium channel agonist induces correlated depolarizations in mice lacking the beta2 subunit nAChRs. Vision Res 44:3347-3355.

Torborg CL, Feller MB (2005) Spontaneous patterned retinal activity and the refinement of retinal projections. Prog. Neurobiol. 76:213-35.

Torborg CL, Hansen KA, Feller MB (2005) High frequency, synchronized bursting drives eye-specific segregation of retinogeniculate projections. Nat Neurosci 8:72-8.

Tovar KR, Maher BJ, Westbrook GL (2009) Direct actions of carbenoxolone on synaptic transmission and neuronal membrane properties. J Neurophysiol 102:974-978.

Tritsch NX, Yi E, Gale JE, Glowatzki E, Bergles DE (2007) The origin of spontaneous activity in the developing auditory system. Nature 450:50-5.

Turrigiano G (2006) Maintaining your youthful spontaneity: Microcircuit homeostasis in the embryonic spinal cord. Neuron 49:481-483.

Tyzio R, Cossart R, Khalilov I, Minlebaev M, Hubner CA, Represa A, Ben-Ari Y, Khazipov R (2006) Maternal oxytocin triggers a transient inhibitory switch in GABA signaling in the fetal brain during delivery. Science 314:1788-1792.

Veruki ML, Morkve SH, Hartveit E (2006) Activation of a presynaptic glutamate transporter regulates synaptic transmission through electrical signaling. Nat Neurosci 9:1388-96.

Vessey JP, Lalonde MR, Mizan HA, Welch NC, Kelly ME, Barnes S (2004) Carbenoxolone inhibition of voltage-gated ca channels and synaptic transmission in the retina. J Neurophysiol 92:1252-6.

Vogalis F, Storm JF, Lancaster B (2003) SK channels and the varieties of slow after-hyperpolarizations in neurons. Eur J Neurosci 18:3155-3166.

Wang CT, Blankenship AG, Anishchenko A, Elstrott J, Fikhman M, Nakanishi S, Feller MB (2007) GABA (A) receptor-mediated signaling alters the structure of spontaneous activity in the developing retina. J Neurosci 27:9130-9140.

Watt AJ, Cuntz H, Mori M, Nusser Z, Sjostrom PJ, Hausser M (2009) Traveling waves in developing cerebellar cortex mediated by asymmetrical purkinje cell connectivity. Nat Neurosci 12:463-73. Epub 2009 Mar 15.

Weliky M, Katz LC (1999) Correlational structure of spontaneous neuronal activity in the developing lateral geniculate nucleus in vivo. Science 285:599-604.

Wenner P, O'Donovan MJ (2001) Mechanisms that initiate spontaneous network activity in the developing chick spinal cord. J Neurophysiol 86:1481-98.

Wilhelm JC, Wenner P (2008) GABA (A) transmission is a critical step in the process of triggering homeostatic increases in quantal amplitude. Proc Natl Acad Sci U S A 105:11412-11417.

Wilhelm JC, Rich MM, Wenner P (2009) Compensatory changes in cellular excitability, not synaptic scaling, contribute to homeostatic recovery of embryonic network activity. Proc Natl Acad Sci U S A 106:6760-6765.

Wong RO, Meister M, Shatz CJ (1993) Transient period of correlated bursting activity during development of the mammalian retina. Neuron 11:923-38.

Wu SN, Jan CR, Chiang HT (2001) Fenamates stimulate BKCa channel osteoblast-like MG-63 cells activity in the human. J Investig Med 49:522-533.

Xu H, Whelan PJ, Wenner P (2005) Development of an inhibitory interneuronal circuit in the embryonic spinal cord. J Neurophysiol 93:2922-2933.

Yvert B, Branchereau P, Meyrand P (2004) Multiple spontaneous rhythmic activity patterns generated by the embryonic mouse spinal cord occur within a specific developmental time window. J Neurophysiol 91:2101-2109.

Zhang LL, Pathak HR, Coulter DA, Freed MA, Vardi N (2006) Shift of intracellular chloride concentration in ganglion and amacrine cells of developing mouse retina. J Neurophysiol 95:2404-2416.

Zheng J, Lee S, Zhou ZJ (2006) A transient network of intrinsically bursting starburst cells underlies the generation of retinal waves. Nat Neurosci. 9:363-71. Epub 2006 Feb 5.

Zheng JJ, Lee S, Zhou ZJ (2004) A developmental switch in the excitability and function of the starburst network in the mammalian retina. Neuron 44:851-864.

Zhou ZJ (2001) The function of the cholinergic system in the developing mammalian retina. Prog Brain Res 131:599-613.

Figure I-1: Circuits mediating spontaneous network activity during development.

a. Retina: There are three distinct circuits that mediate retinal waves at different stages of development (for review, see Torborg and Feller, 2005). Not shown is the circuit that mediates waves perinatally. The cholinergic circuit that mediates waves during the first postnatal week consists of cholinergic interneurons (starburst amacrine cells, blue) and projection neurons (retinal ganglion cells, grey). Starburst amacrine cells form excitatory synaptic connections with other starburst amacrine cells and retinal ganglion cells (for details, see Figure 3). It is postulated that wave propagation is mediated by excitatory connections among starburst amacrine cells, which in turn release acetylcholine that depolarizes the ganglion cells. Waves are initiated by spontaneous depolarization in starburst amacrine cells that are amplified by recurrent excitatory connections, and the interval between waves is set by a slow after-hyperpolarization in the starburst cells. The circuit that mediates glutamatergic waves consists of glutamatergic interneurons (bipolar cells, green), inhibitory interneurons (amacrine cells, pink), and retinal ganglion cells. One hypothesis is that bipolar cells are coupled by high levels of extrasynaptic glutamate (green cloud), which spills out of the synaptic cleft.
b. Spinal cord: A schematic of the circuit mediating spontaneous network activity in each segment of the developing the spinal cord (O'Donovan et al., 1998, Hanson and Landmesser, 2003). The circuit consists of glutamatergic (green) and GABAergic (red) interneurons, and the cholinergic projection neurons (motoneurons, blue) which transiently make local nAChR-mediated connections with local interneurons during development. It is postulated that spontaneous network events initiate in motoneurons, which depolarize a population of GABAergic interneurons, Renshaw cells (R-interneurons). The primary source of depolarization that mediates propagation of spontaneous network activity in the spinal cord changes with development -- early activity is largely dependent on cholinergic transmission from motoneurons, with GABAergic and glutamatergic transmission becoming more dominant as the animal matures). The circuits that mediate event propagation along the length of the cord are not described here. Event initiation is due to a slow buildup of synaptic activity via recurrent excitatory connections until an event threshold is reached. During an event, strong activation of GABAA receptors lowers the intracellular chloride concentration, which diminishes the depolarizing force of GABA. The inter-event interval is set by the time it takes to restore chloride concentrations such that he depolarizing action of GABA is restored (Marchetti et al., 2005). Schematic modified from (Hanson and Landmesser, 2003).

a. Retina

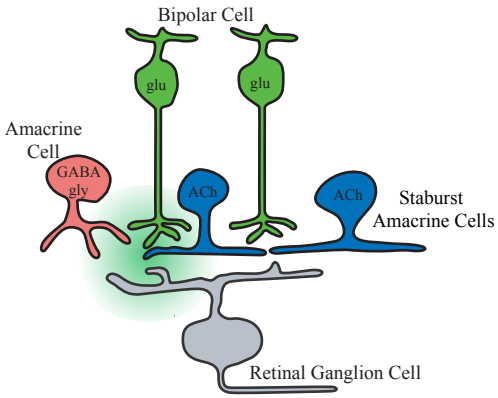

b. Spinal Cord

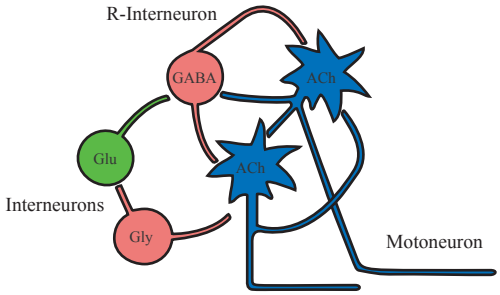

c. Hippocampus: A schematic of the circuit mediating giant depolarizing potentials (GDPs) during the first postnatal week in rodents (for review, see Leinekugel, 2003). The circuit consists of pyramidal cells (green) and local GABAergic interneurons (pink) in both the CA3 region and CA1 regions of the hippocampus. GDPs are most likely to initiate in the CA3 region, where intrinsic bursting activity in CA3 pyramidal cells is coupled with network interactions mediated by depolarizing GABA and recurrent excitatory connections. The inter-event interval is set by an after-hyperpolarization in CA3 neurons (Sipila et al., 2006, Sipila et al., 2005).

d. Cochlea: The circuit consists of glutamatergic inner hair cells (green), a transient population of inner support cells (orange) located in a developmentally transient structure called Kölliker's organ, and the projection neurons (Tritsch et al., 2007) (spiral ganglion cells, gray). Spontaneous network activity in the cochlea is initiated by a diffuse release of ATP (orange cloud) from inner support cells, which drives depolarization in nearby inner hair cells by activating both metabotropic and ionotropic ATP receptors. Inner hair cells in turn release glutamate, which depolarizes spiral ganglion cells via activation of ionotropic glutamate receptors. The mechanisms determining the inter-event interval are not known.

e. Cerebellum: The circuit mediating spontaneous network activity in the cerebellum consists solely of projection neurons (Watt et al., 2009), which are GABAergic Purkinje cells. Purkinje cells are transiently connected via local axon collaterals, which entrain the spontaneous firing of nearby Purkinje cells via depolarizing GABA signaling. The direction of propagation is dictated by the asymmetric wiring of local collaterals with Purkinje cells located toward to base of the lobule receiving more connections than those located toward the apex.

c. Hippocampus

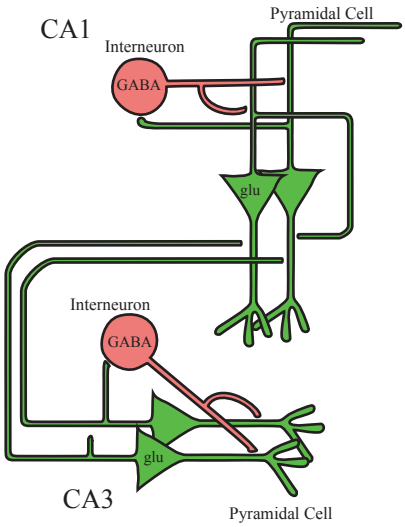

d. Cochlea

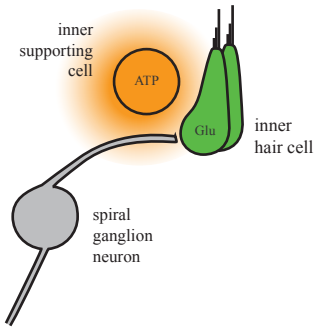

e. Cerebellum

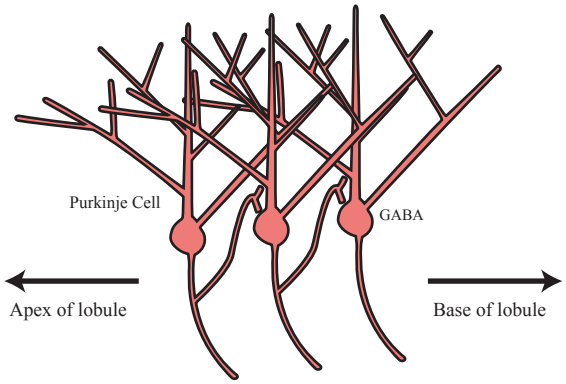

Figure I-1, continued

Figure I-2: Homeostatic regulation of spontaneous network activity in spinal cord.

When a part of the spinal cord network is blocked, activity becomes temporarily less frequent, but quickly recovers to pre-block levels. Here we provide schematics of the changes that take place after activity blockade.
a. Schematic of the circuits mediating activity in developing spinal cord. Neurons are color-coded by the transmitter they release. ACh, acetylcholine, blue; Glu, glutamate, green; Gly, glycine pink; GABA, pink.
b. Motoneurons provide a crucial drive in the generation of activity. Motoneurons receive input from other motoneurons and from interneurons. nAChR, nicotinic acetylcholine receptor; GABAA-R, GABAA receptor; iGluR, ionotropic glutamate receptor.
c. When GABAA receptors are blocked in ovo, activity becomes temporarily less frequent but recovers (Gonzalez-Islas and Wenner, 2006). After 12 hours of GABAA-R blockade, motoneurons become more excitable, an effect which is mediated by an increase in the density of sodium current and a decrease in the density of potassium current (Wilhelm et al., 2009) (right). Bottom, schematics illustrating an increase in motoneuron excitability. Bottom curve is current injection into a motoneuron, top curve is membrane potential. A more excitable motoneuron fires more action potentials in response to the same stimulus. INa, sodium current, represented by sodium channels; IK, potassium current, represented by potassium channels.
d. When GABAA receptors are blocked for long periods of time (24-48 hours) glutamatergic and GABAergic postsynaptic currents in motoneurons increase in size (Wilhelm and Wenner, 2008). The exact mechanisms underlying this increase in postsynaptic current are not fully understood, but are schematized here as increases in the number of glutamate and GABAA receptors.

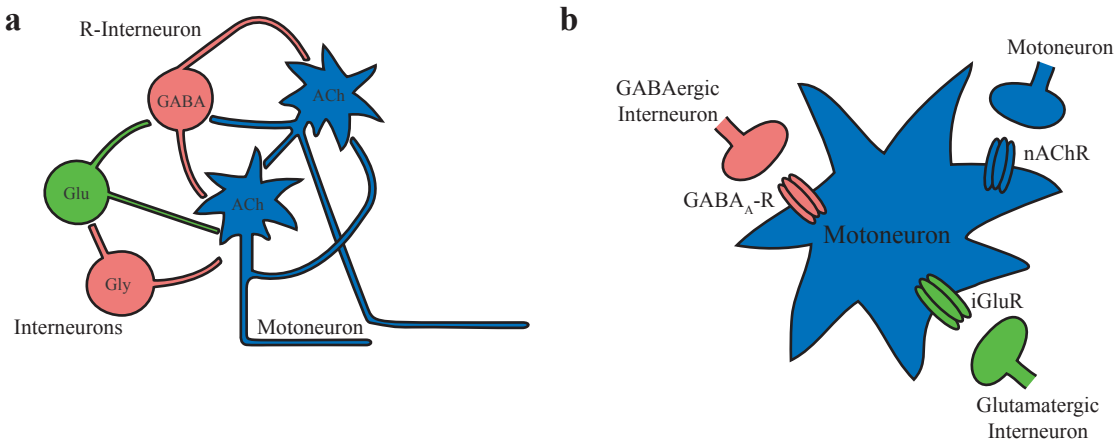

c. Short-latency homeostasis - increased excitability

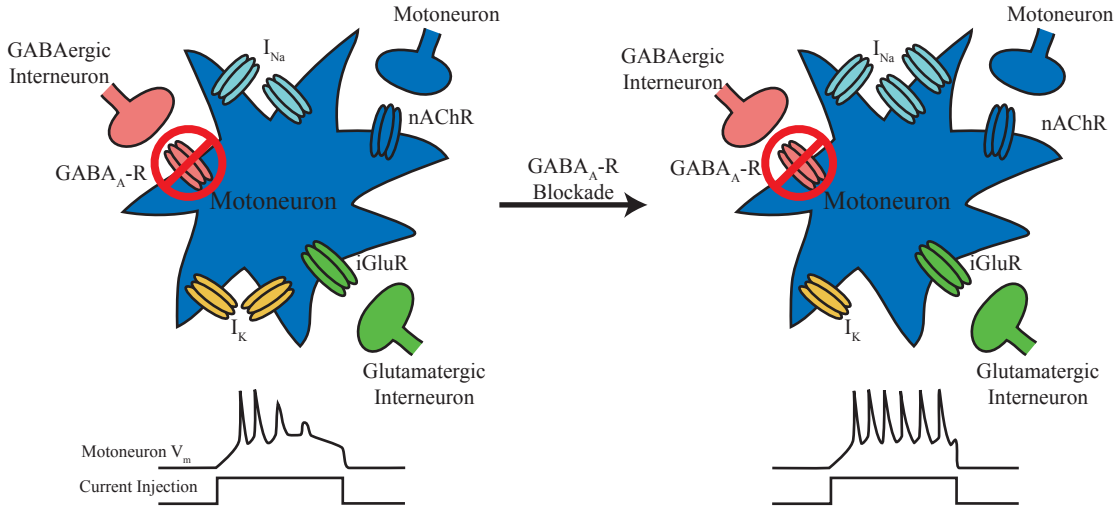

d. Long-latency homeostasis - increased synaptic strength

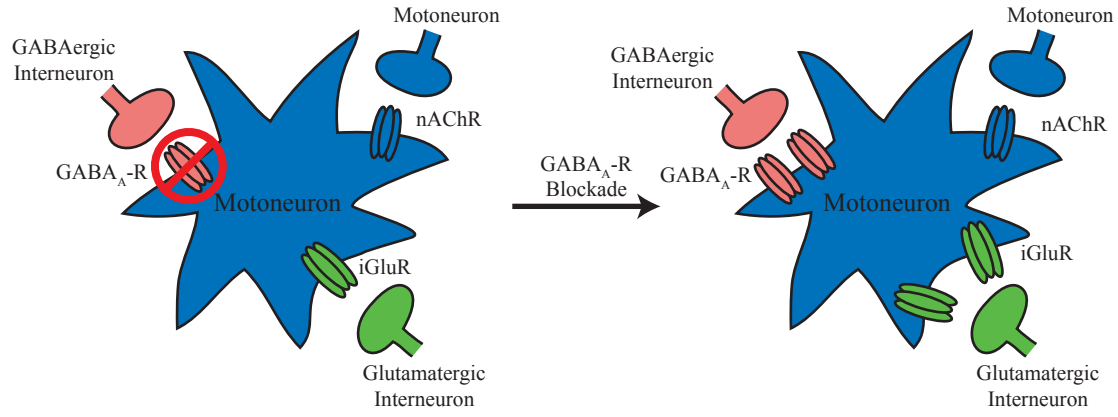

Figure I-3: Homeostatic regulation of spontaneous network activity in retina.

In the absence of a requisite circuit component, the retina regresses to the previous wave-generating mechanism. Here we provide schematics of the circuits that mediate retinal waves at different ages and diagrams of the changes thought to take place when one form of activity is disrupted.
a. Perinatally in mice, waves are mediated by a non-synaptic circuit, thought to be mediated by gap junction coupling (inset). Here the coupling is shown to be between retinal ganglion cells, although the location of the relevant coupling is not known.
b. During the first postnatal week, starburst amacrine cells (blue) form synaptic connections with other starburst amacrine cells and retinal ganglion cells (gray). Retinas from mice lacking ACh in retina exhibit non-synaptic waves (Stacy et al., 2005), potentially through a reactivation of the earlier, perinatal circuit.
c: In the few days before eye opening in mice, waves are mediated by glutamatergic circuits. Inset: Glutamatergic bipolar cells (green), which make glutamatergic synapses onto amacrine and ganglion cells and have no direct connections with each other, release glutamate that is detected both synaptically and extrasynaptically (Blankenship et al., 2009). After the first postnatal week, starburst cells no longer express nAChRs (Zheng et al., 2004). Retinas from mice in which bipolar cells do not release glutamate exhibit waves mediated by the cholinergic network (Blankenship et al., 2009).

a. Non-synaptic/gap junction coupling

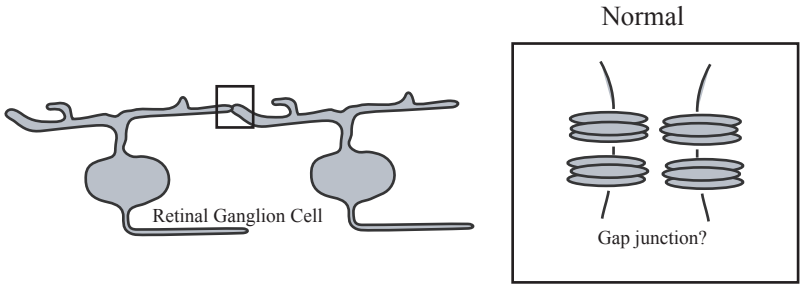

b. No ACh --> nonsynaptic waves

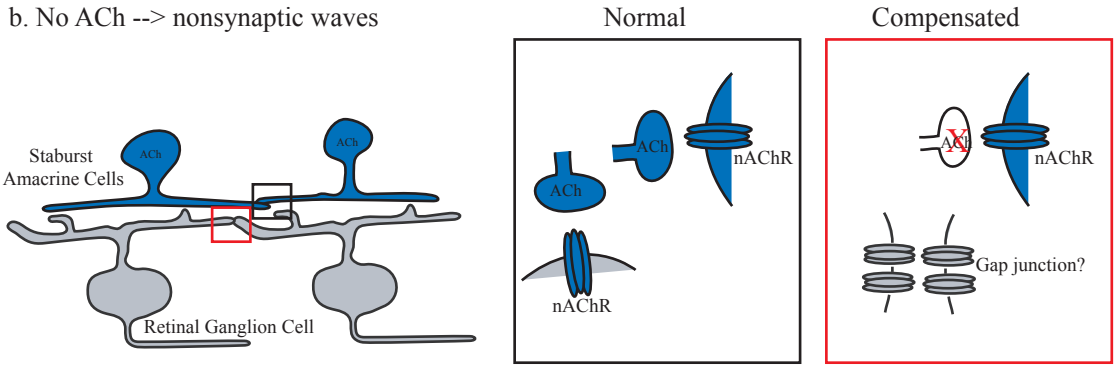

c. No glutamate --> maintained cholinergic waves

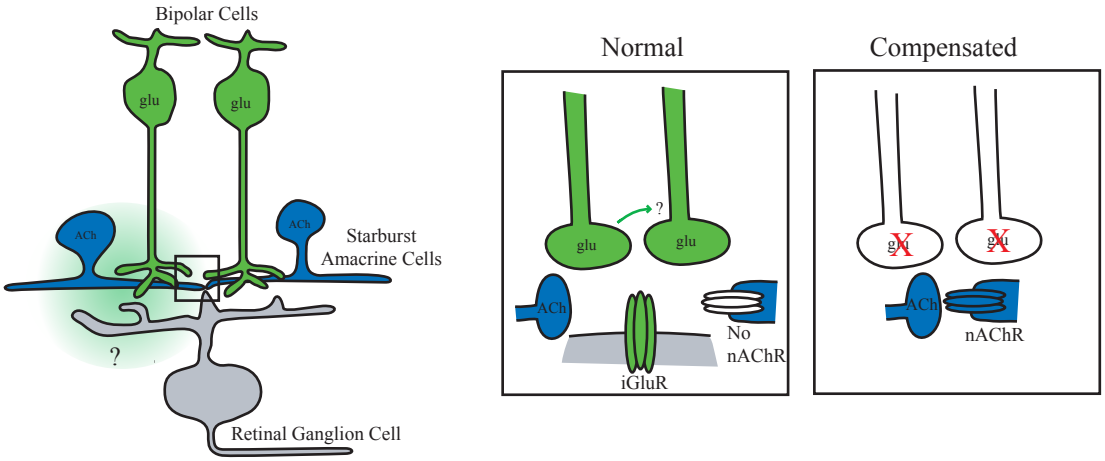

Table I-1: Summary of important features of spontaneous network activity recorded in rodents.

See text for references.

E, embryonic; P, postnatal; GCL, ganglion cell layer; SPA, synchronous plateau assembly; GDP, giant depolarizing potential

	Retina			Spinal Cord		Hippocampus		Cochlea	Cerebellum
Stage	1. E17-P1	2. P1-P10	3. P10-P14	1. E12-E15	2. E15-E18	1. E18 – P5 (SPAs)	2. P3-P10 (GDPs)	P7-P10	P4-P6
Description of projection neuron firing patterns	Bursts that propagate over limited region of GCL	Bursts that propagate over large region of GCL	Clusters of bursts that propagate over large GCL	Bursts of oscillatory activity that propagate within and between segments	Bursts of oscillatory activity that propagate within and between segments	Calcium spikes correlated over few pyramidal cells	Bursts correlated across CA3 and CA1 subfields	Bursts of action potentials; correlation pattern unknown	Traveling waves of action potentials that propagate from apex to base of cerebellar lobules
Inter-event interval	30 s	1 – 2 min	1 min	2- 3 min	1 min	8 s	3-10 s	5-60 s	100 ms
Mechanisms of Initiation	Unknown	Spontaneous calcium spikes in starburst amacrine cells	Unknown	Network interactions	Network interactions	Spontaneous calcium spikes in pyramidal cells	Intrinsic bursts in CA3 interneurons	Unknown	Spontaneous firing in Purkinje neurons
Primary source of depolarization	Gap junctions	nAChR	iGluR	nACh, $GABA_A$, Glycine receptors	iGlu, nACh, glycine, $GABA_A$ receptors	L-type calcium channels and gap junctions	$GABA_A$ and NMDA receptors	ATP release from supporting cells in Kölliker's organ	$GABA_A$ receptors

Table I-1, continued.

	Retina			**Spinal Cord**		**Hippocampus**		**Cochlea**	**Cerebellum**
Stage	1. E17-P1	2. P1-P10	3. P10-P14	1. E12-E15	2. E15-E18	1. E18 – P5 (SPAs)	2. P3-P10 (GDPs)	P7-P10	P4-P6
State of network at end	Maturation of cholinergic circuit	Maturation of glutamatergic circuits	Onset of vision	Loss of requisite role for nAChR signaling	GABA signaling becomes inhibitory	Maturation of GDP circuits	GABA signaling becomes inhibitory	Kölliker's organ disappears	GABA signaling becomes inhibitory
Recorded in vivo	No	Yes (Galli and Maffei, 1988)	Yes (Weliky and Katz, 1999, Hanganu et al., 2006)	Yes (chick (Provine, 1972))	Yes (chick (Provine, 1972))	No	Yes (Leinekugel et al., 2002)	Yes (Lippe, 1994)	No

II. Synaptic and Extrasynaptic Factors Governing Glutamatergic Retinal Waves

Summary

In the few days prior to eye-opening in mice, the excitatory drive underlying waves switches from cholinergic to glutamatergic. Here, we describe the unique synaptic and spatiotemporal properties of waves generated by the retina's glutamatergic circuits. First, knockout mice lacking vesicular glutamate transporter type 1 do not have glutamatergic waves, but continue to exhibit cholinergic waves, demonstrating for the first time that the two wave generating circuits are linked. Second, simultaneous outside-out patch and whole-cell recordings reveal that retinal waves are accompanied by transient increases in extrasynaptic glutamate, directly demonstrating the existence of glutamate spillover during waves. Third, the initiation rate and propagation speed of retinal waves, as assayed by calcium imaging, are sensitive to pharmacological manipulations of spillover and inhibition, demonstrating a role for both signaling pathways in shaping the spatiotemporal properties of glutamatergic retinal waves.

Introduction

Spontaneous activity in developing circuits plays a multitude of important roles. For example, in the developing visual system spontaneous activity in the retina is critical for neuronal survival (Goldberg et al., 2002), neuronal path finding (Nicol et al., 2007), and in the refinement and maintenance of visual maps (for reviews, see Huberman et al., 2008; Torborg and Feller, 2005; Wong, 1999). Indeed, similar

functions have been assigned to spontaneous activity in the cochlea (Tritsch et al., 2007), spinal cord (Gonzalez-Islas and Wenner, 2006; Hanson et al., 2008), hippocampus and cortex (Leinekugel, 2003; Mohajerani and Cherubini, 2006), indicating that spontaneous activity may represent a general strategy used by the developing nervous system to assemble neural circuits (Feller, 1999).

We study this phenomenon in the developing retina, which exhibits propagating bursts of action potentials termed retinal waves. Retinal waves persist in a period of development during which the retina is rapidly maturing (Morgan and Wong, 2006; Sernagor et al., 2001). These changes in retinal circuitry are reflected by changes in the mechanisms that mediate waves, which have been divided into three stages (for review, see Torborg and Feller, 2005). Stage I retinal waves (embryonic day 16 – postnatal day 0 [P0] in mice) are blocked by gap junction blockers but are only weakly affected by antagonists to fast neurotransmitter receptors. Stage II waves (P0-P10) are blocked by nicotinic acetylcholine receptor (nAChR) antagonists. Stage III waves (P10-P14) are blocked by ionotropic glutamate receptor antagonists and not nAChR antagonists. The transition from Stage II to Stage III waves occurs when bipolar cell axons begin to make synapses within the inner plexiform layer (Fisher, 1979; Morgan et al., 2008) and light responses are first detected (Demas et al., 2003; Tian and Copenhagen, 2003).

The mechanisms underlying Stage II waves and their role in visual system development have been well characterized (Huberman et al., 2008; Torborg and Feller, 2005). However, there is little understanding of Stage III waves. Recently, it has been proposed that glutamate acting outside of the synaptic cleft provides a source

of depolarization before mature synaptic structures are established (Demarque et al., 2002). There is also evidence that glutamate spillover, in which glutamate spills out of the synaptic cleft and activates extrasynaptic glutamate receptors, plays a role in circuit development. Spillover in hippocampus has been detected as early as P14, with a developmental reduction in glutamate spillover correlated with an increase in the expression of glutamate transporters (Diamond, 2005), and may be critical for activation of "silent synapses" (Balland et al., 2008). In developing neocortex (Demarque et al., 2004; Milh et al., 2007), hippocampus (Cattani et al., 2007) and brainstem (Sharifullina and Nistri, 2006) blockade of glutamate transporters profoundly alters spontaneous firing patterns, indicating that regulation of spillover has implications for network function. Furthermore, ambient levels of extracellular glutamate regulate spontaneous activity in perinatal neocortex (Allene et al., 2008).

Here, we describe several experiments that provide key insights into the mechanisms underlying glutamatergic Stage III waves. First, we use a knockout mouse lacking glutamate release from bipolar cells to demonstrate that the maturation of glutamate signaling is required for the cessation of cholinergic Stage II waves. Second, we use glutamate receptor-containing outside-out patches to establish that Stage III waves induce spontaneous increases in glutamate spillover. Third, we use calcium imaging to determine how manipulating glutamate spillover and inhibition alters the spatiotemporal properties of waves.

Results

RGCs receive excitatory and inhibitory input during waves

Throughout this study we use synaptic inputs onto RGCs to monitor retinal waves. Therefore it is critical to establish the correspondence between synaptic inputs and network activation. We performed simultaneous current and voltage clamp recordings from neighboring RGCs while monitoring spontaneous calcium increases in the region around these cells (Figure II-1A,B). Because bath-loading of calcium indicators is significantly less effective in mouse retinas older than P4 (Bansal et al., 2000) we used the multicell bolus loading method to label cells in the RGC layer of P10-P13 mouse retinas with Oregon Green BAPTA-1-AM (Ohki et al., 2005; Stosiek et al., 2003). Simultaneous calcium imaging, whole-cell voltage clamp (V_{hold}=-60 mV) and current clamp recordings revealed that correlated increases in calcium indicative of retinal waves were concurrent with RGCs firing bursts of action potentials and receiving excitatory input (Figure II-1B,C). Retinal waves were always accompanied by compound excitatory synaptic currents (cEPSCs) in RGCs (n=6 cells in 6 retinas). Hence, Stage III waves represent waves of depolarization in RGCs that are driven by synaptic input, and cEPSCs reliably indicate the presence of retinal waves.

What inputs do RGCs receive during retinal waves? Simultaneously monitoring excitatory currents in one RGC (V_{hold} = -60 mV) and inhibitory currents in another (V_{hold} = 0 mV) revealed that RGCs receive both excitatory and inhibitory synaptic inputs during retinal waves (Figure II-1D). Wave-associated cEPSCs were blocked by a combination of the AMPA/Kainate receptor antagonist DNQX (20-50

μM) and the NMDA receptor antagonist AP5 (50 μM, n=6 pairs; Figure II-1D), suggesting that during retinal waves RGCs receive direct excitatory inputs from bipolar cells, which are the primary glutamatergic input to RGCs (Bansal et al., 2000; Demas et al., 2006; Syed et al., 2004; Wong et al., 2000). Wave-associated inhibitory synaptic currents (cIPSCs) were also blocked by DNQX and AP5, indicating that RGCs receive feedforward inhibition from amacrine cells during retinal waves.

The $GABA_A$ antagonist gabazine (5 μM) and the glycine antagonist strychnine (4 μM) together (n=11), but neither alone (n=6 cells in gabazine, n=5 cells in strychnine), blocked all cIPSCs recorded from RGCs, establishing that RGCs receive both GABAergic and glycinergic inputs during waves (Figure II-1E).

In the recordings of the excitatory synaptic inputs RGCs receive during retinal waves, we observed that some cEPSCs and cIPSCs occurred in clusters (Figure II-1F), which is visible in a histogram of inter-cEPSC intervals (Figure II-1G).

Transition between Stage II and Stage III waves requires VGLUT1 but not VGLUT3

Stage III waves are blocked by ionotropic glutamate receptor antagonists, but the source of glutamate is not known. In the adult retina, bipolar cells are the primary source of glutamatergic inputs to RGCs, but there is a class of amacrine cells which express vesicular glutamate transporter 3 (VGLUT3) on their synaptic vesicles and form synapses onto RGCs (Haverkamp and Wassle, 2004; Johnson et al., 2004). Bipolar cells express only VGLUT1 (Fremeau et al., 2004; Wassle et al., 2006). (Photoreceptors also express VGLUT1, however they are not thought to contribute to Stage III waves since our experiments are carried out in bright light, which

hyperpolarizes photoreceptors.) To determine which cell supplies the glutamate required for Stage III waves, we examined mice lacking either VGLUT1 or VGLUT3.

We monitored retinal waves by recording wave-associated synaptic currents from pairs of RGCs in P10 – P12 VGLUT1 -/- mice and in age-matched littermate VGLUT1 +/- controls (Figure II-2A,B). In VGLUT1 +/- retinas, as in wild type retinas, wave-associated synaptic currents were blocked by a combination of either DNQX (20 μM) or NBQX (20 μM) and AP5 (50 μM, n=10 cells in 5 mice), whereas wave-associated synaptic currents were not blocked by DHßE, a nicotinic acetylcholine receptor antagonist (8 μM, n=11 cells in 5 mice; Figure II-2A,C). Conversely, wave-associated synaptic currents in VGLUT1 -/- retinas were not blocked by DNQX or NBQX and AP5 (n=13 cells in 4 mice), but were instead blocked by DHßE (n=12 cells in 4 mice; Figure II-2B,D), demonstrating that VGLUT1-/- mice do not have Stage III glutamatergic waves but rather have maintained Stage II cholinergic waves. These results indicate that 1) Stage III waves require glutamate release from bipolar cells or photoreceptors and that 2) glutamatergic signaling is necessary for the cessation of Stage II waves.

In contrast to VGLUT1 -/- RGCs, all compound PSCs were blocked by DNQX and AP5 in both VGLUT3 +/- (n=8 cells in 4 mice) and VGLUT3 -/- RGCs (n=6 cells in 4 mice; data not shown). Hence, we conclude that glutamate release from VGLUT3-positive amacrine cells is not required for Stage III retinal waves and that bipolar cells are the source of glutamatergic currents recorded in RGCs during Stage III waves (Figure II-1).

Outside-out patch recordings detect spillover during waves

Spontaneous release of glutamate from bipolar cells is necessary for the generation of Stage III waves. However, at this age glutamatergic synaptic structures (Morgan et al., 2008; Sherry et al., 2003) and transmission (Tian and Copenhagen, 2001) are not yet mature. We detected very few spontaneous synaptic events in between retinal waves (Figure II-1D), indicating that there are fewer glutamate synapses than detected in later stages of development (Tian and Copenhagen, 2001). We found that cEPSCs associated with retinal waves were extremely slow (Figure II-1D), suggestive of spillover-mediated currents (Bergles et al., 1999).

Is there glutamate spillover during retinal waves? To directly detect extrasynaptic glutamate, we used glutamate receptor-containing outside-out patches (Allen, 1997; Copenhagen and Jahr, 1989; Maeda et al., 1995), a technique that has also been used to detect extrasynaptic ACh (Hume et al., 1983; Young and Poo, 1983) and GABA (Isaacson et al., 1993). Patches of membrane excised from RGC somas in the outside-out patch configuration respond to pressure-applied glutamate, indicating that they contain sufficient numbers of glutamate receptors to detect extrasynaptic glutamate (see Experimental Procedures). To test whether there is glutamate spillover during Stage III retinal waves, we monitored extracellular glutamate in the inner plexiform layer with outside-out patches while monitoring cEPSCs in RGCs (Figure II-3). Most wave-associated cEPSCs were accompanied by glutamate currents in outside-out patches (Figure II-3; currents were present in 6/6 patches; 65±26% of cEPSCs were accompanied by patch currents). Wave-associated patch currents reversed at 0 mV, consistent with activation of glutamate receptors (Figure II-3A).

These data indicate that retinal waves are accompanied by episodic increases in the amount of glutamate spillover.

There is a significant amount of GABA and glycine release during retinal waves (Figure II-1). To ensure that GABA and glycine currents (Isaacson et al., 1993) were not contaminating our recordings we repeated these experiments while blocking $GABA_A$ and glycine receptors using solutions containing 5μM gabazine and 4μM strychnine. In addition, to increase the current through NMDA receptors, we also performed these experiments in 0 Mg^{2+}. There was no significant increase in the percent of wave-associated cEPSCs accompanied by measurable spillover currents under these pharmacological conditions (79±6%, n=3 patches, p=.42, unpaired t test vs. control; Figure II-3B), suggesting that GABA and glycine currents do not contribute significantly to wave-associated currents in outside-out patches.

Calcium imaging reveals Stage III waves occur in clusters

We have demonstrated for the first time that Stage III waves are accompanied by robust glutamate spillover (Figure II-3). Our next goal was to assay the role of glutamate spillover in circuit function. To do so we performed a detailed characterization of Stage III wave properties by visualizing intracellular calcium concentration in many cells over several hundred microns simultaneously. This method has been used extensively to determine the spatiotemporal properties of Stage II waves but has been limited in its application to Stage III waves due to poor loading of calcium indicators at older ages (Bansal et al., 2000; Feller et al., 1997; Sernagor et al., 2000; Wong et al., 1995; Zhou and Zhao, 2000). In retinas loaded with the

multicell bolus loading technique (Stosiek et al., 2003) (Figure II-1), Stage III waves induced a large change in fluorescence and therefore the time evolution and the spatial boundaries of waves were clearly distinguishable (Figure II-4A).

First, we assayed wave initiation rates. Stage III waves were similar to Stage II waves in that they initiated at several locations across the imaged region, and over time the entire ganglion cell layer participated in waves. However, Stage III waves were different from Stage II waves in that they often occurred in episodes during which a cluster of 2-5 waves initiated rapidly in roughly the same location of the retina (Figure II-4B,C). These episodes were separated by much longer intervals, after which a distinct wave or cluster of waves initiated in a different region of the retina (Figure II-4B-D).

Second, we assayed wave propagation speed (see Experimental Procedures and Figure II-5), which is reflective of the coupling that underlies the sequential recruitment of bipolar cells into retinal waves. Stage III waves propagate at a mean velocity of 198 μm/s with a very large variability across retinas (standard deviation=68 μm/s, n=341 waves recorded in 34 P10-P13 retinas, Figure II-4E). This high variability indicates that the coupling mechanisms that underlie wave propagation are likely to be easily modulated by environmental factors. These velocities are comparable to those previously reported for mice (Muir-Robinson et al., 2002), rabbit (Syed et al., 2004) and ferret (Feller et al., 1997; Wong et al., 1993), and significantly lower than turtle (Sernagor and Grzywacz, 1999; Sernagor et al., 2003) and previous reports of Stage III waves in mice based on multielectrode array (MEA) recordings (Demas et al., 2003). The different measurements of Stage III wave velocities in mice

obtained using calcium imaging and the multielectrode array are due to the methods used to compute velocity (see Experimental Procedures).

Enhancing spillover alters wave frequency and speed

Traditionally, glutamate spillover is studied at the level of intercellular communication between pairs of cells. Our goal was to assay the role of glutamate spillover in the function of an entire circuit. To do so we assayed the effects of different manipulations of glutamate spillover on the spatiotemporal properties of Stage III waves.

First, we monitored the effects of enhancing glutamate spillover by blocking excitatory amino acid transporters (EAATs), which remove glutamate from the extracellular space. To characterize the effects of the non-transportable blocker of EAATs TBOA (25 μM) on glutamatergic synaptic input to RGCS and glutamate spillover we used whole-cell voltage clamp and outside-out patch recordings. The presence of TBOA increased the amount of glutamatergic activity recorded in RGCs (Figure II-6A,B), and in TBOA 73±12% of wave-associated cEPSCs were accompanied by measurable glutamate spillover, (a significant increase over control patches; 55±6% in control, n=4 patches, p=.04).

The presence of TBOA significantly altered the spatiotemporal properties of retinal waves as assayed by calcium imaging. Waves initiated much more frequently with very few quiescent periods between waves (Figure II-6C,D). The presence of TBOA dramatically shifted the distribution of inter-wave intervals such that the vast majority of intervals were less than 10 seconds (Figure II-6E).

A second dramatic effect we observed was that TBOA reduced the variability of wave propagation speed. In contrast to the wide range of propagation speeds recorded in control retinas (Figure II-4E), waves in TBOA propagated within a significantly narrower range of velocities (mean±SD: 145±14 μm/s in TBOA vs. 173±79 μm/s in control, n = 8 retinas; t test, p=0.33; Levene's test of variance, p=0.001; Figure II-6F). Interestingly, the effect of TBOA depended on control wave propagation speed. For retinas with waves slower than 140 microns per second TBOA significantly increased wave propagation speed (n=3, $p<0.02$ for each retina), for retinas with waves faster than 200 microns/sec TBOA significantly decreased wave propagation speed (n=4, $p<0.02$ for each retina), and for one retina with waves propagating near 150 μm/s TBOA had no effect (n=1, p=.16). Indeed, the magnitude of the TBOA-induced change in wave propagation speed was strongly correlated with the control propagation speed (linear regression $r^2=0.985$; Figure II-6G). Furthermore, in a subset of retinas that exhibited waves of widely varying propagation speeds, TBOA reduced the variability across waves within a retina (Figure II-7). The dramatic reduction in variability of propagation speed caused by TBOA leads to the hypothesis that variations in ambient levels of glutamate may control the spatial and temporal structure of correlations induced by retinal waves.

Are the TBOA-induced changes in wave properties due to effects of spillover on the Stage III wave-generating circuitry, or does TBOA induce waves generated by a novel mechanisms as observed in developing neocortex, hippocampus and brainstem (Cattani et al., 2007; Demarque et al., 2004; Milh et al., 2007; Sharifullina and Nistri, 2006)? If the retina contains a circuit that supports waves independent of the Stage III

wave-generating circuitry, TBOA may induce waves in retinas not capable of generating Stage III waves. To test this, we performed calcium imaging while applying TBOA to retinas during Stage II waves and to adult retinas. TBOA did not induce waves in P5-P6 retinas; on the contrary, it made Stage II waves less frequent (IWI, mean±SD = 107±36 s in control, 226±49 s in TBOA, n=5 retinas, p = .01; Figure II-8), and did not induce waves in adult retinas (n=8 P22-P24 retinas). Hence, enhancing glutamate spillover enhanced wave activity only during Stage III. Furthermore, like Stage III waves in the absence of TBOA (Figure II-9; Wong et al., 2000) but unlike TBOA-induced activity in other brain areas, wave-associated cEPSCs in TBOA were not blocked by AP5 alone (n=6/7 cells in 4 retinas) but were blocked by a combination of AP5 and DNQX (n=5/5 cells in 3 retinas). Though these data do not directly implicate glutamate spillover in wave propagation, they are consistent with the model that glutamate signaling via spillover is a component of the Stage III wave generating circuit.

As a second manipulation of glutamate spillover, we took advantage of glutamate transporters' high sensitivity to temperature (Wadiche and Kavanaugh, 1998) by altering the temperature of the ACSF. We found a significant decrease in inter-wave intervals and increase in wave propagation speed for elevated temperatures (Figure II-10). However, there was a significant increase in propagation speed and a shift in the IWI distribution as a function of temperature in the presence of TBOA, similar to the temperature effects observed in control solutions. Hence we cannot distinguish whether the effects of elevated temperatures on the spatiotemporal

properties of waves were due to glutamate spillover or other temperature-dependent physiological processes.

Waves persist in AMPA/kainate or NMDA receptor blockade

Unfortunately, there is no unambiguous way to block glutamate spillover without also inhibiting conventional synaptic transmission. However, in many parts of the brain, glutamate spillover exerts its effects by preferentially activating NMDA receptors, which have a high affinity for glutamate and are therefore more likely to be activated by the lower concentrations of glutamate outside of the synaptic cleft (Chen and Diamond, 2002; Higgs and Lukasiewicz, 1999). In RGCs, over 90% of NMDA receptors are localized extrasynaptically while AMPA receptors, conversely, are expressed almost exclusively in synapses (Zhang and Diamond, 2006). Therefore, one way to test the role of glutamate spillover in the retinal wave-generating circuit is to block AMPA/Kainate receptors.

Bath application of NBQX, a selective AMPA/kainate receptor antagonist, did not block Stage III waves as assayed with calcium imaging (n=5, Figure II-9A,B). This demonstrates that activation of NMDA receptors provides sufficient depolarization to support retinal waves. This is consistent with previous results from calcium imaging in ferrets (Wong et al., 2000). However, these results differ from a report previous from our lab indicating that CNQX or DNQX are sufficient to block waves (Bansal et al., 2000). This difference could be due to poorer sensitivity in previous calcium imaging experiments or potential non-specificity of CNQX and DNQX.

Though waves persist in AMPA/kainate receptor antagonists, we observed a reduction in their frequency (Figure II-9C). AMPA/kainate receptor antagonists had no effect on wave propagation speed (mean±SD, 229±37μm/s in NBQX vs. 198±17 μm/sec in control, n=5, p=0.22; Figure II-9D), indicating that glutamate signaling via AMPA/kainate receptors determines the initiation rate but not the propagation speed of Stage III waves.

Next, we assayed the role of NMDA receptor activation in determining the spatiotemporal properties of Stage III waves. Similar to blockade of AMPA/kainate receptors and consistent with previous results we found that blockade of NMDA receptors by bath application of AP5 (50 μM) did not block waves or change the speed of wave propagation (205±16μm/s in AP5 vs. 193±35 in control, n=5, p=0.47, Figure II-9E,F,H), although the initiation rate was slightly shifted to higher inter-wave intervals (Figure II-9G).

These results suggest that both synaptic and extrasynaptic glutamate receptors contribute to the depolarizations during Stage III waves. However, they do not distinguish which aspects of wave propagation are mediated by synaptic vs. extrasynaptic glutamate receptor activation. First, the subcellular distribution of AMPA and NMDA receptors in the retina at this age is not known, and it may differ from adult as there is robust reorganization of glutamatergic synapses during development (Morgan et al., 2008). Second, in cerebellum glutamate spillover has been shown to activate AMPA receptors in neighboring synapses (DiGregorio et al., 2002), so an alternative interpretation is that glutamate spillover-mediated activation of both NMDA and AMPA receptors is required for wave propagation. Furthermore,

during circuit development the distinction between synaptic and extrasynaptic signaling may represent a false dichotomy given the dramatic rearrangements of glutamate receptors that occur at this age (Morgan et al., 2008).

Disinhibition and enhanced spillover show similar effects

Elevating glutamate spillover increased the initiation rate of retinal waves. Previously, it was established that blocking $GABA_A$ and glycine receptors also increased the frequency of Stage III waves (Fischer et al., 1998; Kerschensteiner and Wong, 2008; Syed et al., 2004; Zhou, 2001). Application of gabazine (5 μM) and strychnine (4μM) increased the frequency of cEPSCs recorded in RGCs (Figure II-1E), indicating that GABA and glycine normally suppress glutamate release from bipolar cells. These observations lead to the hypothesis that the initiation rate of retinal waves is determined by the balance of excitation and inhibition at the level of bipolar cells. To test this hypothesis, we compared the effects of TBOA and the blockade of inhibition on the spatiotemporal properties of waves.

Waves initiated much more frequently in $GABA_A$ and glycine receptor antagonists (5 μM gabazine and 4 μM strychnine; Figure II-11A-C). As in TBOA, this rapid initiation of waves eliminated the bimodal distribution of inter-wave intervals observed in control conditions, and replaced it with a smooth distribution in which the inter-wave interval for the vast majority of waves is less than 10 seconds.

Blockade of $GABA_A$ and glycine receptors slightly reduced wavefront propagation speed (mean±SD 172±18 μm/s in GZ+STR, 199±32 μm/s in control, n=8 retinas, p=.05; Figure II-11D). Furthermore, although the change in propagation

speed caused by gabazine and strychnine on a per-retina basis was correlated with the initial propagation speed (linear regression $r^2 = .7$; Figure II-11E), gabazine and strychnine did not reduce the variability in mean wave propagation speed among retinas (Levene test, p=0.1). However, for these experiments variability in propagation speed in control retinas was lower than for the TBOA experiments and therefore direct comparisons cannot be made.

This supports the hypothesis that the depolarization state of bipolar cells, set by spillover and inhibition, is a critical determinant of initiation rate. A schematic of these functional circuits consistent with the pharmacology presented here is provided in Figure II-12 and discussed below.

Discussion

We have explored the role of synaptic and extrasynaptic signaling in the generation of Stage III retinal waves. First, knockout mice lacking VGLUT1 did not have glutamatergic retinal waves but continued to exhibit cholinergic waves, demonstrating that glutamatergic signaling causes the disappearance of Stage II waves. Second, we provided direct evidence that glutamate spillover is a robust feature of Stage III retinal waves, demonstrating for the first time spontaneous episodic elevations in extrasynaptic glutamate in the developing retina. Third, elevating levels of glutamate spillover significantly reduced the variance in wave propagation speed, indicating that fluctuating endogenous levels of glutamate influence the propagation properties of retinal waves. In addition, wave initiation rates are reduced by blockade of either NMDA or AMPA receptors, indicating that

initiation rates are influenced bidirectionally by levels of glutamate signaling. Last, blocking inhibition had similar effects on the spatiotemporal properties of waves as elevating glutamate spillover, supporting a model in which spontaneous initiation of Stage III waves is dictated by the balance of excitation and inhibition onto bipolar cells.

Role for glutamate signaling in transition from Stage II to Stage III

What role do glutamate waves play in development? Our observation that VGLUT1 -/- retinas do not have normal Stage III waves demonstrates that synaptic transmission from photoreceptors or bipolar cells is necessary for Stage III waves. Interestingly, while VGLUT1 +/- littermates have Stage III waves, VGLUT1 -/- mice have Stage II-like waves. This suggests that in wild type retinas the onset of glutamatergic signaling may turn off the Stage II wave-generating circuitry.

A similar phenomenon has been seen in a mouse lacking choline acetyl transferase (ChAT), the enzyme that synthesizes acetylcholine, in a portion of the retina (Stacy et al., 2005). During the period of development normally occupied by the cholinergic Stage II waves, ChAT-knockout retina exhibits spontaneous activity that is blocked by gap junction blockers but not by nAChR or ionotropic glutamate receptor antagonists (Stacy et al., 2005), indicating a persistence of mechanisms that mediate Stage I waves (for review, see Torborg and Feller, 2005) . These findings suggest that the retina turns on a different form of spontaneous activity when one form is blocked, revealing powerful homeostatic mechanisms that ensure spontaneous activity is always present.

Role for glutamate spillover in circuit function

Glutamate spillover has been described in the adult retina (Chen and Diamond, 2002; DeVries et al., 2006; Veruki et al., 2006). A major goal of this study was to determine whether glutamate spillover exists at a stage in development when functional glutamatergic synapses are first forming. We found that retinal waves are accompanied by robust glutamate spillover by using glutamate receptor-containing outside-out patches (Figure II-3). It is possible that the presence of a recording pipette in the inner plexiform layer locally disrupts glutamate clearance, contributing to the spillover currents we see. However, glutamate spillover between pairs of bipolar cells has been measured in the adult retina, consistent with our conclusion that spillover occurs in the IPL (Veruki et al., 2006). This finding may have implications for spontaneous activity in other developing circuits that exhibit glutamate receptor-dependent spontaneous activity while glutamatergic synapses are still being formed, as in cortex (Dupont et al., 2006; Minlebaev et al., 2008) and hippocampus (Ben-Ari et al., 2004; Kasiyanov et al., 2008).

We demonstrated a role for glutamate spillover in shaping the spatiotemporal properties of retinal waves in two ways. First, altering the level of glutamate spillover altered the rate of wave initiations, i.e. the rate at which retinas entered the active state. Reducing signaling via ionotropic glutamate receptors by blocking either AMPA/kainate or NMDA receptors reduced the frequency of wave initiations (Figure II-9), while increasing glutamate spillover by blocking glutamate transporters dramatically increased the frequency of wave initiations (Figure II-6). A similar

increase in wave initiations was observed when inhibition was blocked (Figure II-11 and Fischer et al., 1998; Kerschensteiner and Wong, 2008; Syed et al., 2004; Zhou, 2001).

Second, altering the level of glutamate spillover affected wavefront propagation speed. Wavefront propagation is a measure of the rate at which bipolar cells are recruited into waves. In control conditions, Stage III waves propagate with a highly variable wavefront propagation speed. Though wavefront propagation varied across waves within a retina (Figure II-7), it varied most significantly across preparations, with a few retinas supporting very rapid waves with propagation speeds greater than 250 μm/s (Figure II-4D, Figure II-5). Surprisingly, TBOA reduced the variability in propagation speed by causing all waves to propagate at speeds near 150 μm/s (Figure II-6, Figure II-7).

Based on this observation, we propose that glutamate activates two distinct processes: one that positively regulates wave speed, such as activation of ionotropic glutamate receptors, and one that negatively regulates it, such as activation of presynaptic mGluRs. In this scenario variation in propagation speed from retina to retina may have to do with varying ambient levels of glutamate, perhaps due to variations in the effectiveness of transporters. In TBOA, there is maximum activation of both positive and negative regulators of wave speed and therefore there is less variation across retinas.

We propose a model that is consistent with these experimental observations (Figure II-12). Stage III waves are initiated by spontaneous depolarizations in bipolar cells, and coupled to surrounding bipolar cells via spillover. In this way, bipolar cells

function in a manner similar to starburst amacrine cells during the cholinergic stage II waves. The strong depolarization provided by a wave also excites inhibitory circuits, which contribute to the delay between waves. Hence, the balance of excitation and inhibition onto bipolar cells sets the initiation rate. The question remains – how does spillover couple bipolar cells when its function in the adult retina is to inhibit release from neighboring bipolar cells? More experiments are required to determine whether glutamate release from one bipolar cell directly depolarizes its neighbor during development via conductances that are not described in adult or whether there is an intermediate excitatory cell.

In summary, we have demonstrated that an absence of glutamate signaling prevents the transition from Stage II to Stage III waves. In addition, there is robust inhibitory signaling and glutamate spillover during Stage III waves, both of which shape the spatiotemporal properties of waves. These findings represent key insights into the features of transient circuits that mediate spontaneous activity during development.

Experimental procedures

Animals. C57Bl/6 mice obtained from Harlan were used for all WT recordings. VGLUT1 knockout mice (Fremeau et al., 2004) and VLGUT3 knockout mice (Seal et al., 2008) were generated as reported previously. Heterozygous littermates were used as controls for experiments using VGLUT1- and VGLUT3-null mice. All animal procedures were approved by the University of California, Berkeley; University of California, San Diego; or University of California, San Francisco

Institutional Animal Care and Use Committees and conformed to the National Institutes of Health *Guide for the Care and Use of Laboratory Animals*, the Public Health Service Policy, and the Society for Neuroscience Policy on the Use of Animals in Neuroscience Research.

Whole-Mount Retinal Preparation. P10 – P24 mice were anesthetized with halothane or isoflurane and decapitated. Retinas were isolated in artificial cerebrospinal fluid (ACSF) (in mM: 119.0 NaCl, 26.2 $NaHCO_3$, 11 glucose, 2.5 KCl, 1.0 K_2HPO_4, 2.5 $CaCl_2$, 1.3 $MgCl_2$) and mounted RGC side up on filter paper. Retinas were incubated at room temperature in bubbled (95% O2 / 5% CO2) ACSF until transfer to the recording chamber, where they were constantly superfused with bubbled ACSF (32-34°C unless otherwise specified).

Electrophysiology and Pharmacology. Whole-cell current and voltage clamp recordings were made from whole-mount retinas. Retinas were visualized with differential interference contrast optics on a Zeiss Axioskop 2 FS Plus microscope with an Achroplan 40x water immersion objective. The inner limiting membrane of the retina was removed with a glass recording pipette and RGCs were targeted under control of a micromanipulator (MP-225; Sutter Instruments). RGCs were identified by their large somas and the presence of a voltage-gated sodium conductance. Recording pipettes (Garner Glass or Sutter Instruments) were pulled (PP-830; Narishige) with a tip resistance of 3-6 MΩ and filled with either a cesium gluconate (for all voltage-clamp recordings; in mM: 100 CsOH, 100 gluconic acid, 1.7 CsCl, 40 HEPES, 10 EGTA, 5 $MgCl_2$, 1 QX-314, 2 Na_2ATP, and 0.3 Na-GTP; pH adjusted to 7.25 with CsOH; E_{Cl} = -60 mV) or potassium gluconate internal solution (for current-

clamp recordings; in mM: 98.3 K-gluconate, 40 HEPES, 1.7 KCl, 0.6 EGTA, 5 $MgCl_2$, 2 Na_2ATP, and 0.3 Na-GTP; pH adjusted to 7.25 with KOH). Data were acquired using pCLAMP 9 recording software and a Multiclamp 700A amplifier (Molecular Devices), sampled at 5 kHz and low-pass filtered at 1 kHz. 6,7-Dinitroquinoxaline-2,3-dione disodium salt (DNQX), D-(-)-2-Amino-5-phosphonopentanoic acid (AP5), 2,3-Dioxo-6-nitro-1,2,3,4-tetrahydrobenzo [f]quinoxaline-7-sulfonamide disodium salt (NBQX), SR-95531 hydrobromide (gabazine), strychnine, and Dihydro-ß-erythroidine hydrobromide (DHßE) were added to ACSF as stock solutions prepared at ≥1000x concentration in water. DL-threo-b-Benzyloxyaspartic acid (TBOA) stock solution was prepared at ≥1000x in dimethyl sulfoxide. All antagonists were acquired from Tocris; all other chemicals were acquired from Sigma-Aldrich. Data were analyzed in pCLAMP, IGOR Pro (Wavemetrics Inc.) or MATLAB (Mathworks).

To calculate inter-cEPSC intervals in whole-cell voltage clamp recordings, cEPSCs were identified by eye. For Figure II-2, a cluster was defined as a series of cEPSCs separated by not more than 10 s.

Outside-out patches were excised from RGC somas > 500 µm away from the simultaneously recorded RGC. Cesium gluconate was used for outside-out patch recordings. To confirm that patches contained glutamate receptors, L-glutamate was pressure-applied (5 psi) to patches at a concentration of 1mM in a solution containing (in mM): 150 NaCl, 2.5 KCl, 10 Hepes, pH 7.4. Patches were inserted to a depth of 10 µm in the inner plexiform layer, within 10 µm of the recorded RGC's soma. All patch traces included were low-pass filtered (Bessel, 8-pole) at 150 Hz for clarity.

Calcium Imaging. Retinas were bulk loaded with the calcium indicator Oregon Green 488 BAPTA-1 AM (OGB-1 AM; Invitrogen) using the multicell bolous loading technique (Stosiek et al., 2003). OGB-1 AM was prepared at a concentration of 10mM in a solution of 2% pluronic in DMSO, which was then diluted 1/10 in a solution containing (in mM): 150 NaCl, 2.5 KCl, 10 Hepes, pH 7.4 (Stosiek et al., 2003). The OGB-1 AM solution was pressure ejected from a borosilicate glass micropipette (Garner Glass or Sutter Instruments) using a PV-820 Pneumatic PicoPump (World Precision Instruments) at a pressure of 10 – 20 psi. The pipette was positioned just under the inner limiting membrane and dye was injected for 700 ms in 3-5 locations per retina. Epifluorescent calcium imaging was performed on a Zeiss Axioskop 2 FS Plus microscope using a 10x or 40x water immersion objective (Zeiss Achroplan), with illumination provided by a Sutter Lambda LS and controlled by a Uniblitz shutter. Images were acquired at 2-4 Hz in MetaMorph (Universal Imaging Corporation).

Calcium Imaging Analysis. Stage III retinal waves exhibited clusters of rapidly initiating waves, and therefore we often observed waves in regions that still had elevated calcium from a preceding wave. This property required a method of analysis that relied upon the accurate definition of wave boundaries. Therefore, fluorescence intensity image time series were processed using custom MATLAB (Mathworks) programs to define wave boundaries in the following manner. Images were spatially filtered using a two-dimensional mean filter which averaged over a 31 x 31 micron box. For each frame, the fractional change in fluorescence intensity $\Delta F/F = (F(t)-F_{avg})/F_{avg}$ was computed, where F(t) is the fluorescence intensity at time t and

F_{avg} is the fluorescence intensity at each pixel averaged over the entire time series. Wave boundaries were defined as contiguous pixels that had a change in ΔF/F greater than 2% within 1 second. Contiguous regions from one frame to the next were considered to be part of one wave. In order to exclude spontaneous calcium transients in individual RGCs, we defined waves as having a minimum size of 960 μm^2. These values for the time and threshold were determined to best match the wave boundaries as determined by visual inspection. This process generated binary images of wave regions at each point in time on which subsequent analysis was compiled (Fig. 4). Inter-wave intervals were determined at 25 points on a 5X5 grid evenly spaced over the imaged region. Given our temporal filter of 1 second to reliably define waves, we could not determine inter-wave intervals of less than 2 seconds. We did not estimate the total area covered by waves because many waves initiated or ended outside of the imaged area.

Velocity of the wavefront was computed for waves covering greater than one quarter of the imaged region and lasting longer than 2 seconds. Here the term velocity refers to the magnitude of displacement over time without regard to direction. Smaller and shorter duration waves were excluded because they are difficult to distinguish from local bursts of synchronous activity. Velocity was measured by first projecting the path of the wavefront onto an isotemporal map such that the wave boundaries at each time are represented by a continuous line (Figure II-5). The furthest distance traveled during the last frame of a wave was used as an ending point for tracing the path of the wavefront. Points along the wave path were selected by finding the shortest distance from the point at time *t* and the wavefront at time *t-1*. Wave paths

were examined by eye for each wave to ensure they met the above criteria. Paths were excluded from analysis if waves propagated over regions containing patches of retina where uneven loading of calcium indicator prevented accurate measurement of the wavefront. Velocity was calculated by averaging the distance traveled between each consecutive time point then multiplying by the image acquisition rate (4Hz for all analyses of wave spatiotemporal properties). Some wavefronts propagated in a start-stop manner. For these waves pauses, where the distance between wavefronts at consecutive time points is 0, were not included in the averaging when computing velocity.

Computing velocity based on wavefronts defined by calcium imaging leads to lower values than wave velocities measured using spikes recorded on an MEA (Demas et al., 2003; Demas et al., 2006). The two methods lead to similar values for velocities for smoothly propagating waves with circular wavefronts (Figure II-5, right). However, waves with more complex wavefronts, such as those that propagate in a saltatory manner (Figure II-5, left) or split into two distinct wavefronts, yield different values when measured with calcium imaging and with an MEA.

Statistics. Paired t-tests were used for all paired comparisons. For multiple comparisons, a repeated measures ANOVA with a Newman-Keuls post hoc test was used. Levene's test was used to compare variances. Alpha was always 0.05.

Acknowledgement

This chapter, in full, is a reprint of the material as it appears in: Blankenship, AG; Ford, KJ; Johnson, J; Seal, RP; Edwards, RH; Copenhagen, DR; Feller, MB.

Synaptic and Extrasynaptic Factors Governing Glutamatergic Retinal Waves. Neuron, vol. 62, 2009, and is included with permission from all authors. The dissertation author was the primary author of this paper.

References

Allen, T. G. (1997). The 'sniffer-patch' technique for detection of neurotransmitter release. Trends Neurosci *20*, 192-197.

Allene, C., Cattani, A., Ackman, J. B., Bonifazi, P., Aniksztejn, L., Ben-Ari, Y., and Cossart, R. (2008). Sequential generation of two distinct synapse-driven network patterns in developing neocortex. J Neurosci *28*, 12851-12863.

Balland, B., Lachamp, P., Kessler, J. P., and Tell, F. (2008). Silent synapses in developing rat nucleus tractus solitarii have AMPA receptors. J Neurosci *28*, 4624-4634.

Bansal, A., Singer, J. H., Hwang, B. J., Xu, W., Beaudet, A., and Feller, M. B. (2000). Mice lacking specific nicotinic acetylcholine receptor subunits exhibit dramatically altered spontaneous activity patterns and reveal a limited role for retinal waves in forming ON and OFF circuits in the inner retina. J Neurosci *20*, 7672-7681.

Ben-Ari, Y., Khalilov, I., Represa, A., and Gozlan, H. (2004). Interneurons set the tune of developing networks. Trends Neurosci *27*, 422-427.

Bergles, D. E., Diamond, J. S., and Jahr, C. E. (1999). Clearance of glutamate inside the synapse and beyond. Curr Opin Neurobiol *9*, 293-298.

Cattani, A. A., Bonfardin, V. D., Represa, A., Ben-Ari, Y., and Aniksztejn, L. (2007). Generation of slow network oscillations in the developing rat hippocampus after blockade of glutamate uptake. J Neurophysiol *98*, 2324-2336.

Chen, S., and Diamond, J. S. (2002). Synaptically released glutamate activates extrasynaptic NMDA receptors on cells in the ganglion cell layer of rat retina. J Neurosci *22*, 2165-2173.

Copenhagen, D. R., and Jahr, C. E. (1989). Release of endogenous excitatory amino acids from turtle photoreceptors. Nature *341*, 536-539.

Demarque, M., Represa, A., Becq, H., Khalilov, I., Ben-Ari, Y., and Aniksztejn, L. (2002). Paracrine intercellular communication by a Ca2+- and SNARE-independent release of GABA and glutamate prior to synapse formation. Neuron *36*, 1051-1061.

Demarque, M., Villeneuve, N., Manent, J. B., Becq, H., Represa, A., Ben-Ari, Y., and Aniksztejn, L. (2004). Glutamate transporters prevent the generation of seizures in the developing rat neocortex. J Neurosci *24*, 3289-3294.

Demas, J., Eglen, S. J., and Wong, R. O. (2003). Developmental loss of synchronous spontaneous activity in the mouse retina is independent of visual experience. J Neurosci *23*, 2851-2860.

Demas, J., Sagdullaev, B. T., Green, E., Jaubert-Miazza, L., McCall, M. A., Gregg, R. G., Wong, R. O., and Guido, W. (2006). Failure to maintain eye-specific segregation in nob, a mutant with abnormally patterned retinal activity. Neuron *50*, 247-259.

DeVries, S. H., Li, W., and Saszik, S. (2006). Parallel processing in two transmitter microenvironments at the cone photoreceptor synapse. Neuron *50*, 735-748.

Diamond, J. S. (2005). Deriving the glutamate clearance time course from transporter currents in CA1 hippocampal astrocytes: transmitter uptake gets faster during development. J Neurosci *25*, 2906-2916.

DiGregorio, D. A., Nusser, Z., and Silver, R. A. (2002). Spillover of glutamate onto synaptic AMPA receptors enhances fast transmission at a cerebellar synapse. Neuron *35*, 521-533.

Dupont, E., Hanganu, I. L., Kilb, W., Hirsch, S., and Luhmann, H. J. (2006). Rapid developmental switch in the mechanisms driving early cortical columnar networks. Nature *439*, 79-83.

Feller, M. B. (1999). Spontaneous correlated activity in developing neural circuits. Neuron *22*, 653-656.

Feller, M. B., Butts, D. A., Aaron, H. L., Rokhsar, D. S., and Shatz, C. J. (1997). Dynamic processes shape spatiotemporal properties of retinal waves. Neuron *19*, 293-306.

Fischer, K. F., Lukasiewicz, P. D., and Wong, R. O. (1998). Age-dependent and cell class-specific modulation of retinal ganglion cell bursting activity by GABA. J Neurosci *18*, 3767-3778.

Fisher, L. J. (1979). Development of synaptic arrays in the inner plexiform layer of neonatal mouse retina. J Comp Neurol *187*, 359-372.

Fremeau, R. T., Jr., Kam, K., Qureshi, T., Johnson, J., Copenhagen, D. R., Storm-Mathisen, J., Chaudhry, F. A., Nicoll, R. A., and Edwards, R. H. (2004). Vesicular glutamate transporters 1 and 2 target to functionally distinct synaptic release sites. Science *304*, 1815-1819.

Goldberg, J. L., Espinosa, J. S., Xu, Y., Davidson, N., Kovacs, G. T., and Barres, B. A. (2002). Retinal ganglion cells do not extend axons by default: promotion by neurotrophic signaling and electrical activity. Neuron *33*, 689-702.

Gonzalez-Islas, C., and Wenner, P. (2006). Spontaneous network activity in the embryonic spinal cord regulates AMPAergic and GABAergic synaptic strength. Neuron *49*, 563-575.

Hanson, M. G., Milner, L. D., and Landmesser, L. T. (2008). Spontaneous rhythmic activity in early chick spinal cord influences distinct motor axon pathfinding decisions. Brain Res Rev *57*, 77-85.

Haverkamp, S., and Wassle, H. (2004). Characterization of an amacrine cell type of the mammalian retina immunoreactive for vesicular glutamate transporter 3. J Comp Neurol *468*, 251-263.

Higgs, M. H., and Lukasiewicz, P. D. (1999). Glutamate uptake limits synaptic excitation of retinal ganglion cells. J Neurosci *19*, 3691-3700.

Huberman, A. D., Feller, M. B., and Chapman, B. (2008). Mechanisms Underlying Development of Visual Maps and Receptive Fields. Annu Rev Neurosci *31*, 479-509.

Hume, R. I., Role, L. W., and Fischbach, G. D. (1983). Acetylcholine release from growth cones detected with patches of acetylcholine receptor-rich membranes. Nature *305*, 632-634.

Isaacson, J. S., Solis, J. M., and Nicoll, R. A. (1993). Local and diffuse synaptic actions of GABA in the hippocampus. Neuron *10*, 165-175.

Johnson, J., Sherry, D. M., Liu, X., Fremeau, R. T., Jr., Seal, R. P., Edwards, R. H., and Copenhagen, D. R. (2004). Vesicular glutamate transporter 3 expression identifies glutamatergic amacrine cells in the rodent retina. J Comp Neurol *477*, 386-398.

Kasiyanov, A., Fujii, N., Tamamura, H., and Xiong, H. (2008). Modulation of network-driven, GABA-mediated giant depolarizing potentials by SDF-1alpha in the developing hippocampus. Dev Neurosci *30*, 285-292.

Kerschensteiner, D., and Wong, R. O. (2008). A precisely timed asynchronous pattern of ON and OFF retinal ganglion cell activity during propagation of retinal waves. Neuron *58*, 851-858.

Leinekugel, X. (2003). Developmental patterns and plasticities: the hippocampal model. J Physiol Paris *97*, 27-37.

Maeda, T., Shimoshige, Y., Mizukami, K., Shimohama, S., Kaneko, S., Akaike, A., and Satoh, M. (1995). Patch sensor detection of glutamate release evoked by a single electrical shock. Neuron *15*, 253-257.

Milh, M., Becq, H., Villeneuve, N., Ben-Ari, Y., and Aniksztejn, L. (2007). Inhibition of glutamate transporters results in a "suppression-burst" pattern and partial seizures in the newborn rat. Epilepsia *48*, 169-174.

Minlebaev, M., Ben-Ari, Y., and Khazipov, R. (2008). NMDA Receptors Pattern Early Activity in the Developing Barrel Cortex In Vivo. Cereb Cortex.

Mohajerani, M. H., and Cherubini, E. (2006). Role of giant depolarizing potentials in shaping synaptic currents in the developing hippocampus. Crit Rev Neurobiol *18*, 13-23.

Morgan, J. I., and Wong, R. O. (2006). Development of cell types and synaptic connections in the retina. In WEBVISION: The organization of the retina and the visual system, H. Kolb, E. Fernandez, and R. Nelson, eds. (Salt Lake City), pp. http://webvision.med.utah.edu/.

Morgan, J. L., Schubert, T., and Wong, R. O. (2008). Developmental patterning of glutamatergic synapses onto retinal ganglion cells. Neural Develop *3*, 8.

Muir-Robinson, G., Hwang, B. J., and Feller, M. B. (2002). Retinogeniculate axons undergo eye-specific segregation in the absence of eye-specific layers. J Neurosci *22*, 5259-5264.

Nicol, X., Voyatzis, S., Muzerelle, A., Narboux-Neme, N., Sudhof, T. C., Miles, R., and Gaspar, P. (2007). cAMP oscillations and retinal activity are permissive for ephrin signaling during the establishment of the retinotopic map. Nat Neurosci *10*, 340-347.

Ohki, K., Chung, S., Ch'ng, Y. H., Kara, P., and Reid, R. C. (2005). Functional imaging with cellular resolution reveals precise micro-architecture in visual cortex. Nature *433*, 597-603. Epub 2005 Jan 2019.

Seal, R. P., Akil, O., Yi, E., Weber, C. M., Grant, L., Yoo, J., Clause, A., Kandler, K., Noebels, J. L., Glowatzki, E., *et al.* (2008). Sensorineural deafness and seizures in mice lacking vesicular glutamate transporter 3. Neuron *57*, 263-275.

Sernagor, E., Eglen, S. J., and O'Donovan, M. J. (2000). Differential effects of acetylcholine and glutamate blockade on the spatiotemporal dynamics of retinal waves. J Neurosci *20*.

Sernagor, E., Eglen, S. J., and Wong, R. O. (2001). Development of retinal ganglion cell structure and function. Prog Retin Eye Res *20*, 139-174.

Sernagor, E., and Grzywacz, N. M. (1999). Spontaneous activity in developing turtle retinal ganglion cells: pharmacological studies. J Neurosci *19*, 3874-3887.

Sernagor, E., Young, C., and Eglen, S. J. (2003). Developmental modulation of retinal wave dynamics: shedding light on the GABA saga. J Neurosci *23*, 7621-7629.

Sharifullina, E., and Nistri, A. (2006). Glutamate uptake block triggers deadly rhythmic bursting of neonatal rat hypoglossal motoneurons. J Physiol *572*, 407-423.

Sherry, D. M., Wang, M. M., Bates, J., and Frishman, L. J. (2003). Expression of vesicular glutamate transporter 1 in the mouse retina reveals temporal ordering in development of rod vs. cone and ON vs. OFF circuits. J Comp Neurol *465*, 480-498.

Stacy, R. C., Demas, J., Burgess, R. W., Sanes, J. R., and Wong, R. O. (2005). Disruption and recovery of patterned retinal activity in the absence of acetylcholine. J Neurosci *25*, 9347-9357.

Stosiek, C., Garaschuk, O., Holthoff, K., and Konnerth, A. (2003). In vivo two-photon calcium imaging of neuronal networks. Proc Natl Acad Sci U S A *100*, 7319-7324. Epub 2003 May 7330.

Syed, M. M., Lee, S., Zheng, J., and Zhou, Z. J. (2004). Stage-dependent dynamics and modulation of spontaneous waves in the developing rabbit retina. J Physiol *560*, 533-549.

Tian, N., and Copenhagen, D. R. (2001). Visual deprivation alters development of synaptic function in inner retina after eye opening. Neuron *32*, 439-449.

Tian, N., and Copenhagen, D. R. (2003). Visual stimulation is required for refinement of ON and OFF pathways in postnatal retina. Neuron *39*, 85-96.

Torborg, C. L., and Feller, M. B. (2005). Spontaneous patterned retinal activity and the refinement of retinal projections. Prog Neurobiol *76*, 213-235. Epub 2005 Nov 2008.

Tritsch, N. X., Yi, E., Gale, J. E., Glowatzki, E., and Bergles, D. E. (2007). The origin of spontaneous activity in the developing auditory system. Nature *450*, 50-55.

Veruki, M. L., Morkve, S. H., and Hartveit, E. (2006). Activation of a presynaptic glutamate transporter regulates synaptic transmission through electrical signaling. Nat Neurosci *9*, 1388-1396.

Wadiche, J. I., and Kavanaugh, M. P. (1998). Macroscopic and microscopic properties of a cloned glutamate transporter/chloride channel. J Neurosci *18*, 7650-7661.

Wassle, H., Regus-Leidig, H., and Haverkamp, S. (2006). Expression of the vesicular glutamate transporter vGluT2 in a subset of cones of the mouse retina. J Comp Neurol *496*, 544-555.

Wong, R. O., Chernjavsky, A., Smith, S. J., and Shatz, C. J. (1995). Early functional neural networks in the developing retina. Nature *374*, 716-718.

Wong, R. O., Meister, M., and Shatz, C. J. (1993). Transient period of correlated bursting activity during development of the mammalian retina. Neuron *11*, 923-938.

Wong, R. O. L. (1999). Role of retinal waves in visual system development. Annual Review of Neuroscience *22*.

Wong, W. T., Myhr, K. L., Miller, E. D., and Wong, R. O. (2000). Developmental changes in the neurotransmitter regulation of correlated spontaneous retinal activity. J Neurosci *20*, 351-360.

Young, S. H., and Poo, M. M. (1983). Spontaneous release of transmitter from growth cones of embryonic neurones. Nature *305*, 634-637.

Zhang, J., and Diamond, J. S. (2006). Distinct perisynaptic and synaptic localization of NMDA and AMPA receptors on ganglion cells in rat retina. J Comp Neurol *498*, 810-820.

Zhou, Z. J. (2001). A critical role of the strychnine-sensitive glycinergic system in spontaneous retinal waves of the developing rabbit. J Neurosci *21*, 5158-5168.

Zhou, Z. J., and Zhao, D. (2000). Coordinated transitions in neurotransmitter systems for the initiation and propagation of spontaneous retinal waves. J Neurosci *20*, 6570-6577.

Figure II-1: Simultaneous calcium imaging and whole-cell recording show compound excitatory and inhibitory synaptic inputs are correlated with retinal waves

(A) Fluorescence image of retinal ganglion cell layer loaded with the calcium indicator OGB-1 AM using the multicell bolus loading technique. Pseudocolor overlay represents the fractional change in fluorescence over baseline (ΔF/F) in a single frame at the peak of a retinal wave (frame taken from the wave marked by an asterisk in B). Black triangles represent whole-cell patch clamp electrodes. Scale bar: 15 μm
(B) Simultaneous calcium imaging (top), whole-cell current (middle) and voltage (bottom, Vm = -60mV) clamp traces recorded over 3 min. Time course of ΔF/F is averaged over the entire field of view. Vertical scale: 4% ΔF/F, 25mV, 100pA; Horizontal scale: 30 s.
(C) Simultaneous calcium imaging (top), whole-cell current (middle) and voltage (bottom, Vm = -60 mV) clamp traces recorded during the wave in the boxed region of B. Dots on calcium imaging trace represent the average fluorescence intensity at each time point, with no filtering. Vertical scale: 2% ΔF/F, 20mV, 70pA; Horizontal scale: 2 s.
(D) Left, whole-cell voltage clamp recordings from two neighboring RGCs reveal that RGCs receive both excitatory (-60 mV, top) and inhibitory (0 mV, bottom) compound synaptic inputs (cEPSCs and cIPSCs) during retinal waves. Recording is 3 min long. Right, Whole-cell voltage clamp recordings from the same pair as in left panel, in the presence of 20 μM DNQX and 50 μM AP5. Recording is 3 min long. Numbered boxes represent events expanded in F. Vertical scale bar: 100 pA for top trace, 500 pA for bottom trace; Horizontal scale bar: 30 s.
(E) Dual whole-cell voltage clamp recording of wave-associated cEPSCs (top; Vm = -60 mV) and cIPSCs (bottom; Vm = 0mV) in control (left), in 4 μM strychnine (middle), and in the presence of 5 μM gabazine and 4 μM strychnine (right). Recordings in each condition are 2.5 minutes long. Vertical scale bar: 200 pA; Horizontal scale bar: 20 s.
(F) Expanded timescale of the boxed areas in D. Top: -60 mV; Bottom: 0 mV. Small currents in top trace of (3) are unclamped IPSCs. Scale bar for (1) and (2): Vertical: 50 pA for top traces, 250 pA for bottom traces; Horizontal: 1 s. Scale bar for (3): Vertical: 20 pA for top trace, 100 pA for bottom trace; Horizontal: 125 ms
(G) Histogram of intervals between peaks of wave-associated cEPSCs. Bin size is 2 s. n = 2,654 intervals from 46 cells.

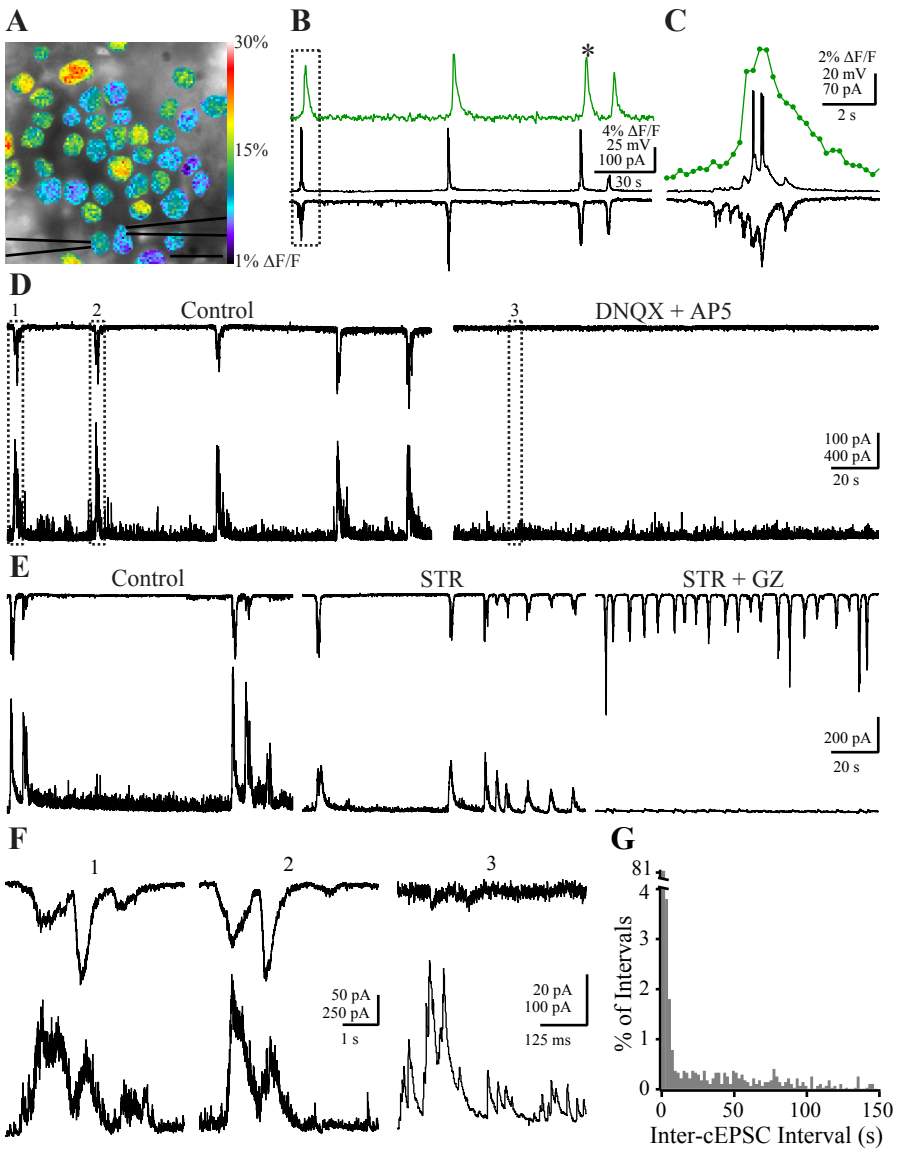
A
30%
15%
1% ΔF/F
B
4% ΔF/F
25 mV
100 pA
30 s
C
2% ΔF/F
20 mV
70 pA
2 s
D
1
2
Control
3
DNQX + AP5
100 pA
400 pA
20 s
E
Control
STR
STR + GZ
200 pA
20 s
F
1
2
3
50 pA
250 pA
1 s
20 pA
100 pA
125 ms
G
81
4
3
2
1
0
% of Intervals
0
50
100
150
Inter-cEPSC Interval (s)

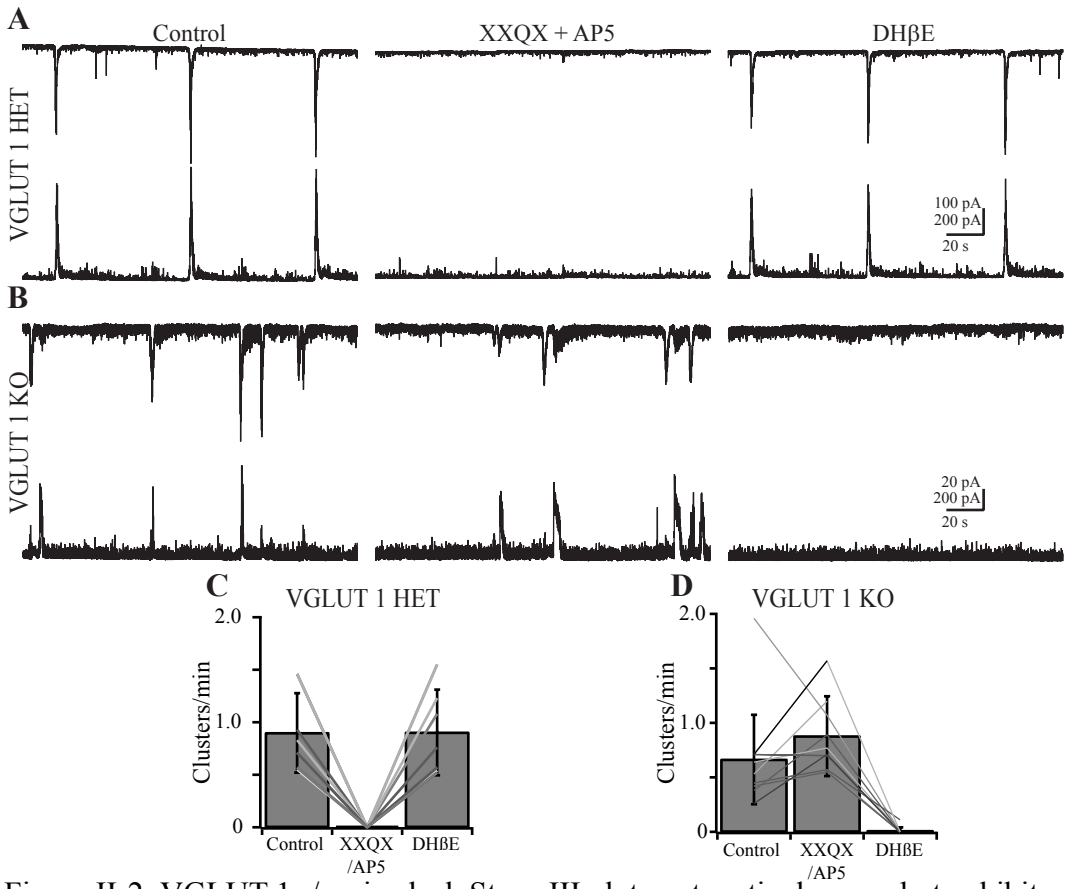

Figure II-2: VGLUT 1 -/- mice lack Stage III glutamate retinal waves but exhibit extended Stage II cholinergic waves

(A) Dual whole-cell voltage clamp recordings from neighboring RGCs in a P11 VGLUT 1 +/- retina. Wave-associated cEPSCs (top, Vm = -60 mV) and cIPSCs (bottom, Vm = 0 mV) are shown in control (left), in the presence of the glutamate receptor antagonists DNQX (20 µM) or NBQX (20 µM) and D-AP5 (50 µM, middle), and in the presence of the nicotinic acetylcholine receptor antagonist DHßE (8 µM, right). Recordings are 3 min long. n=10 cells in 5 mice for XXQX and AP5, n=11 cells in 5 mice for DHßE. XXQX = DNQX or NBQX. Vertical scale bar: 100 pA for top traces, 200 pA for bottom traces; Horizontal scale bar: 20 s.
(B) Same experiment as in A in a P12 VGLUT1 -/- retina. Recordings are 3 min long. n=13 cells in 4 mice for XXQX and AP5, n=12 cells in 4 mice for DHßE. XXQX = DNQX or NBQX. Vertical scale bar: 100 pA for top traces, 200 pA for bottom traces; Horizontal scale bar: 20 s.
(C) Effects of ionotropic glutamate and nicotinic acetylcholine receptor antagonists on frequency of cEPSC clusters in VGLUT1 +/-. Bars are mean±SD, lines are individual cells.
(D) Effects of ionotropic glutamate and nicotinic acetylcholine receptor antagonists on frequency of cEPSC clusters in VGLUT1 -/-. Bars are mean±SD, lines are individual cells.

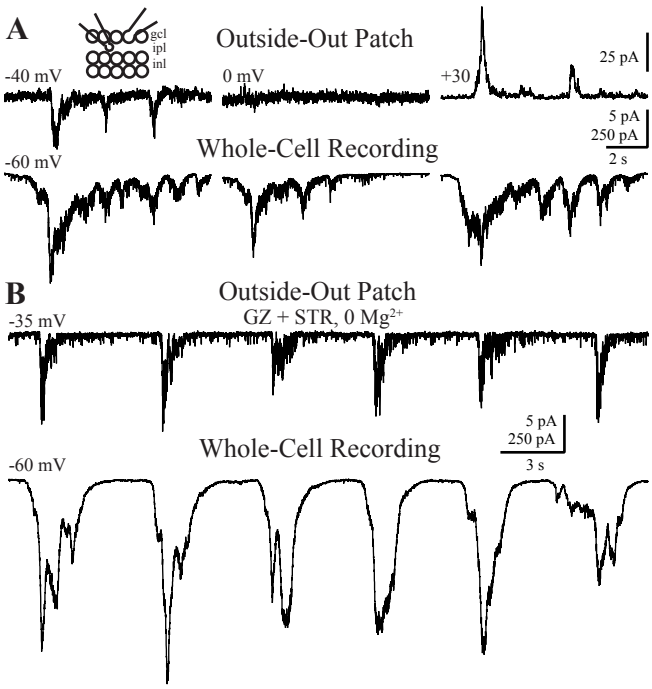

Figure II-3: Glutamate spillover occurs during waves

(A) Simultaneous outside-out patch (top) and whole-cell (bottom) recordings from a single patch-RGC pair. RGC Vm = -60 mV; patch Vm = -40 mV (left), 0mV (middle) and +30 mV (right). Inset, schematic of recording configuration. Outside-out patch pipette was positioned in the IPL near the recorded RGC. Vertical scale bar: 5 pA for top left and middle traces, 25 pA for top right trace, 250 pA for bottom traces; Horizontal scale bar: 2 s.

(B) Thirty-second-long voltage clamp recording from an outside-out patch (top, Vm = -35 mV) and RGC (bottom, Vm = -60 mV) in the presence of 5 µM gabazine (GZ), 4 µM strychnine (STR) and 0 Mg2+. Vertical scale bar: 5 pA for top trace, 250 pA for bottom trace; Horizontal scale bar: 3 s.

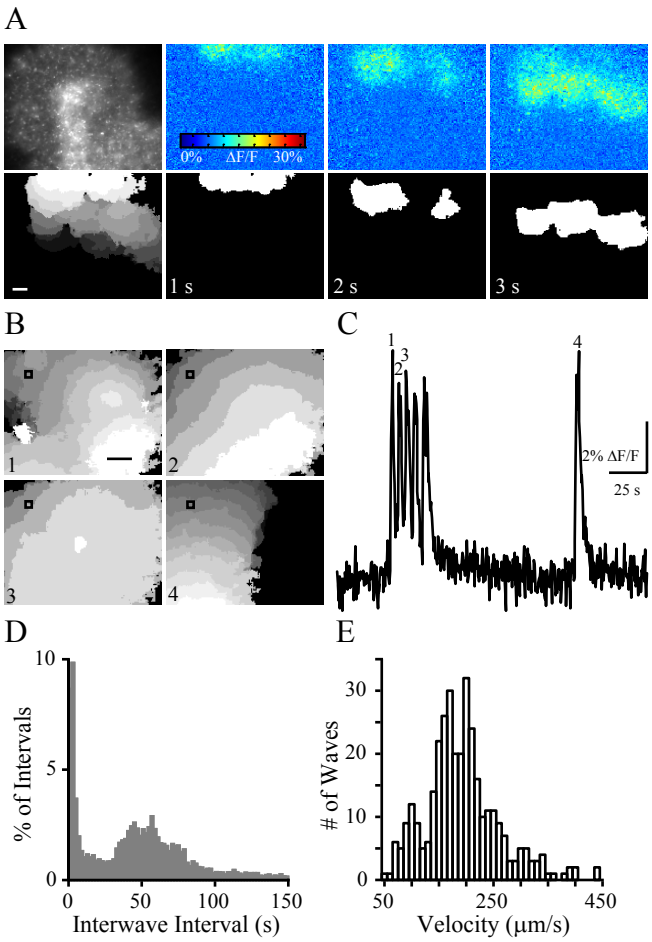

Figure II-4: Calcium imaging reveals Stage III waves occur in episodic clusters

(A) Top Left frame is a fluorescence image showing loading of calcium indicator. Right frames are ΔF/F pseudocolor images during 3 seconds of a retinal wave. Bottom: Left frame, the spatial extent of propagation of a single wave. Each gray-scale value represents the active area in one frame, with a 4 Hz frame rate. White is the first frame in which the wave was detected, dark gray the last. Right frames are binarized wave front (white; see Supplemental Experimental Procedures) showing progression of the same wave as in the top three frames. Scale: 100 μm.
(B) Spatial extent of wave propagation of four waves marked by numbers in C. Colors are as in bottom left frame of A.
(C) Time course of the ΔF/F recorded over 120 s from the 30x30 μm region of interest in B. Waves depicted in B are numbered. The first 5 waves follow within 3-5 seconds of one another. Conversely, the last wave is not followed rapidly by other waves. Vertical scale bar: 2% ΔF/F; Horizontal scale bar: 25 s.
(D) Histogram of inter-wave intervals. Bin size is 2 s. n=22,204 IWIs from 69 retinas.
(E) Histogram of wave velocities. Bin size is 10 s. n=341 waves from 34 retinas.

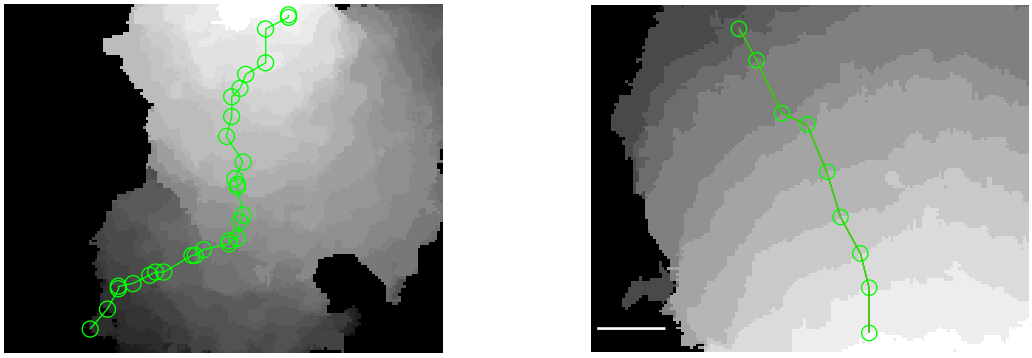

116 μm/s 313 μm/s

Figure II-5: Examples of images used to compute wave propagation speed.

Equal shades of gray represent the wave boundary at a given time, with darker shades corresponding to later time points during the wave. The width of isotemporal regions is indicative of the distance traveled during the interval between frames (250 ms). The green line represents the path of the wave and green circles represent the points along the wave boundaries where the distance measurements are taken to determine velocity (see Methods). The wave on the left has an average velocity of 116 μm/sec whereas the wave on the right has an average velocity of 313 μm/sec. Scale bar 100 μm.

Figure II-6: The effects of increased glutamate spillover on spatiotemporal properties of Stage III waves

(A) Outside-out patch recording (top; Vm = -40 mV) and RGC whole-cell voltage clamp recording of cEPSCs in an RGC (bottom, -60 mV) in control ACSF (left) and in 25 μM TBOA (right). Dotted line represents baseline holding current before TBOA application. Recordings are 2 min long. Vertical scale bar: top, 4 pA; bottom, 100pA. Horizontal scale bar: 20 s.
(B) Cumulative histogram summarizing effects of TBOA on inter-cEPSC interval measured from whole-cell recordings. n=4 cells in control, n=3 cells in 25 μM TBOA, n=3 cells in rinse. Black is control, dotted line is TBOA.
(C) Summary of spontaneous calcium transients during three sequential ten second intervals. Gray value corresponds to the time during which that region of the retina was active. Black is baseline; white is activity at 0 s, with increasing time depicted as darker grays. If a region of the retina was active more than once, the time of the most recent activity is displayed. Top: Control. Bottom: 25 μM TBOA. Scale bar = 100 μm
(D) Time course of ΔF/F averaged over a 30 μm x 30 μm region in the center of the retina in C. Top: Control ACSF; Bottom: TBOA.
(E) Summary cumulative probability distribution of inter-wave intervals (IWIs). Black line is control, dotted line is TBOA. Shaded areas represent standard error of the mean (n=9 retinas).
(F) Summary of effects of TBOA on propagation speed. Individual dots represent single retinas; lines connect a retina's speed in control and TBOA.
(G) TBOA-induced change in wave propagation speed plotted versus propagation speed in control. Dots represent average speed of all waves in individual retinas; error bars are standard deviation.

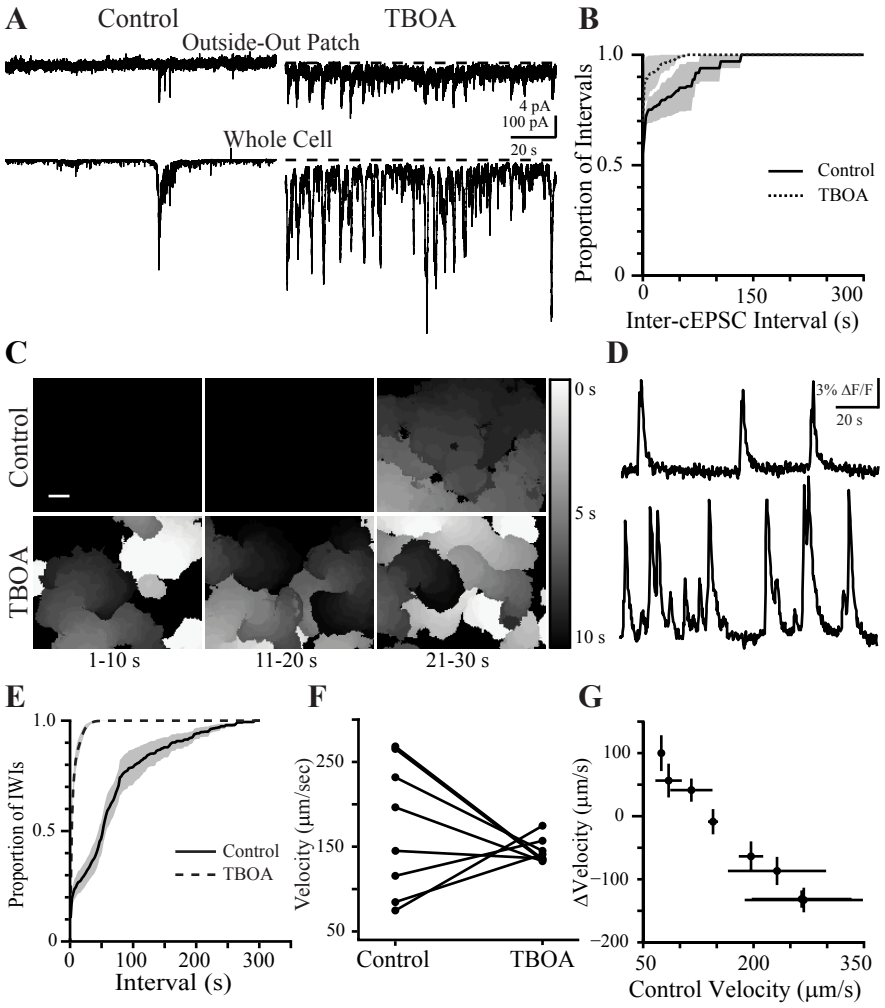
A
Control
TBOA
Outside-Out Patch
4 pA
100 pA
20 s
Whole Cell
B
Proportion of Intervals
1.0
0.5
0
0
150
300
Inter-cEPSC Interval (s)
Control
TBOA
C
Control
TBOA
0 s
5 s
10 s
1-10 s
11-20 s
21-30 s
D
3% ΔF/F
20 s
E
Proportion of IWIs
1.0
0.5
0
0
100
200
300
Interval (s)
Control
TBOA
F
Velocity (μm/sec)
250
150
50
Control
TBOA
G
ΔVelocity (μm/s)
100
0
−100
−200
50
200
350
Control Velocity (μm/s)

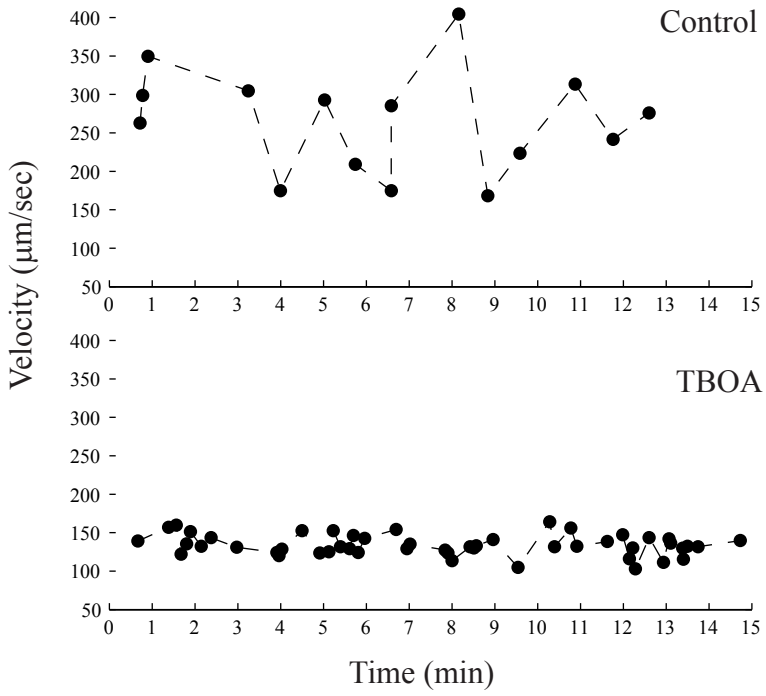

Figure II-7: Blocking glutamate transporters decreases the variability of wave propagation speed.

Plots of propagation speed vs. time in a single retina. Each dot represents one wave. Top, control; bottom, 25 μM TBOA.

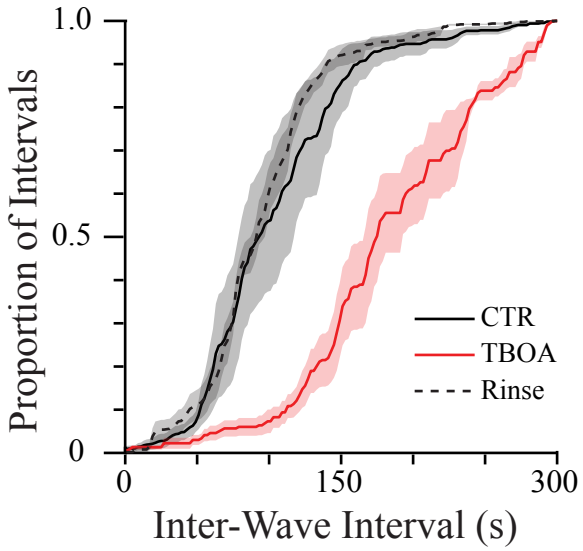

Figure II-8: TBOA reduces wave frequency during Stage II waves.

Cumulative histogram summarizing effect of 25 µM TBOA on inter-wave intervals during Stage II waves. n=5 retinas, aged P5-P6. Black is control, red is 25 µM TBOA, dotted line is rinse. Shaded areas represent standard error of the mean.

Figure II-9: Inter-wave interval, but not propagation speed, is affected by NMDA or AMPA/kainate receptor blockade

(A) Progression of a wave recorded with calcium imaging during bath application of 20 μM NBQX. Each grayscale value represents the active area in one frame, with a 4 Hz frame rate. White is the first frame in which the wave was detected, dark gray the last. Black square is the 30x30 μm region from which the traces in B are derived. Scale bar = 100 μm.
(B) Time course of the ΔF/F in retinas in control (top) and during bath application of NBQX (bottom). Asterisk indicates the wave shown in A. Vertical scale bar: 5% Δ F/F; Horizontal scale bar: 50 s.
(C) Cumulative probability distribution of inter-wave intervals (IWIs). Black line is control, dotted line is NBQX. Shaded areas represent standard error of the mean.
(D) Summary of effects of NBQX on propagation speed. Individual dots represent single retinas; lines connect a retina's speed in control and NBQX.
(E) Progression of a wave recorded with calcium imaging during bath application of 50 μM AP5. Colors are as in A. Black square is the 30x30 μm region from which the traces in F are derived. Scale bar: 100 μm.
(F) Time course of the ΔF/F in control (top) and during bath application of 50 μM AP5 (bottom). Asterisk indicates the wave shown in E. Vertical scale bar: 5% ΔF/F; Horizontal scale bar: 50 s.
(G) Cumulative probability distribution of inter-wave intervals (IWIs). Black line is control, dotted line is AP5. Shaded areas represent standard error of the mean.
(H) Summary of effects of AP5 on propagation speed. Individual dots represent single retinas; lines connect a retina's speed in control and AP5.

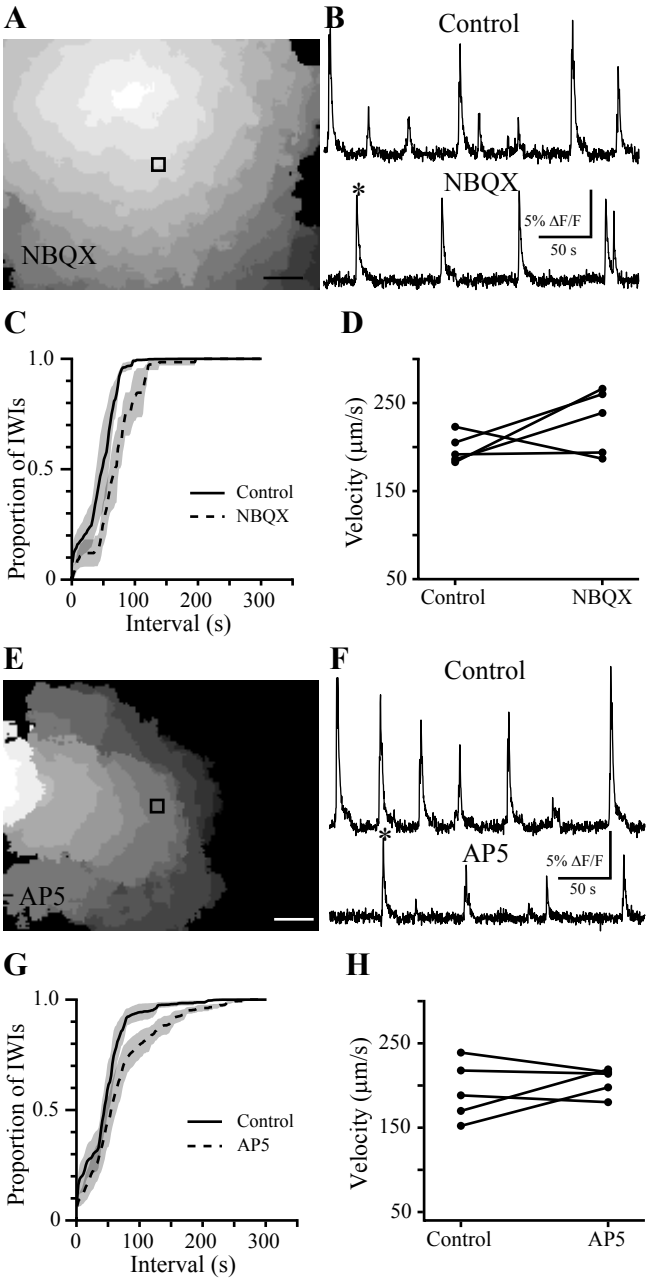
A
B
Control
NBQX
NBQX
5% ΔF/F
50 s
C
D
Proportion of IWIs
1.0
0.5
0
Control
NBQX
0
100
200
300
Interval (s)
Velocity (μm/s)
250
150
50
Control
NBQX
E
F
Control
AP5
AP5
5% ΔF/F
50 s
G
H
Proportion of IWIs
1.0
0.5
0
Control
AP5
0
100
200
300
Interval (s)
Velocity (μm/s)
250
150
50
Control
AP5

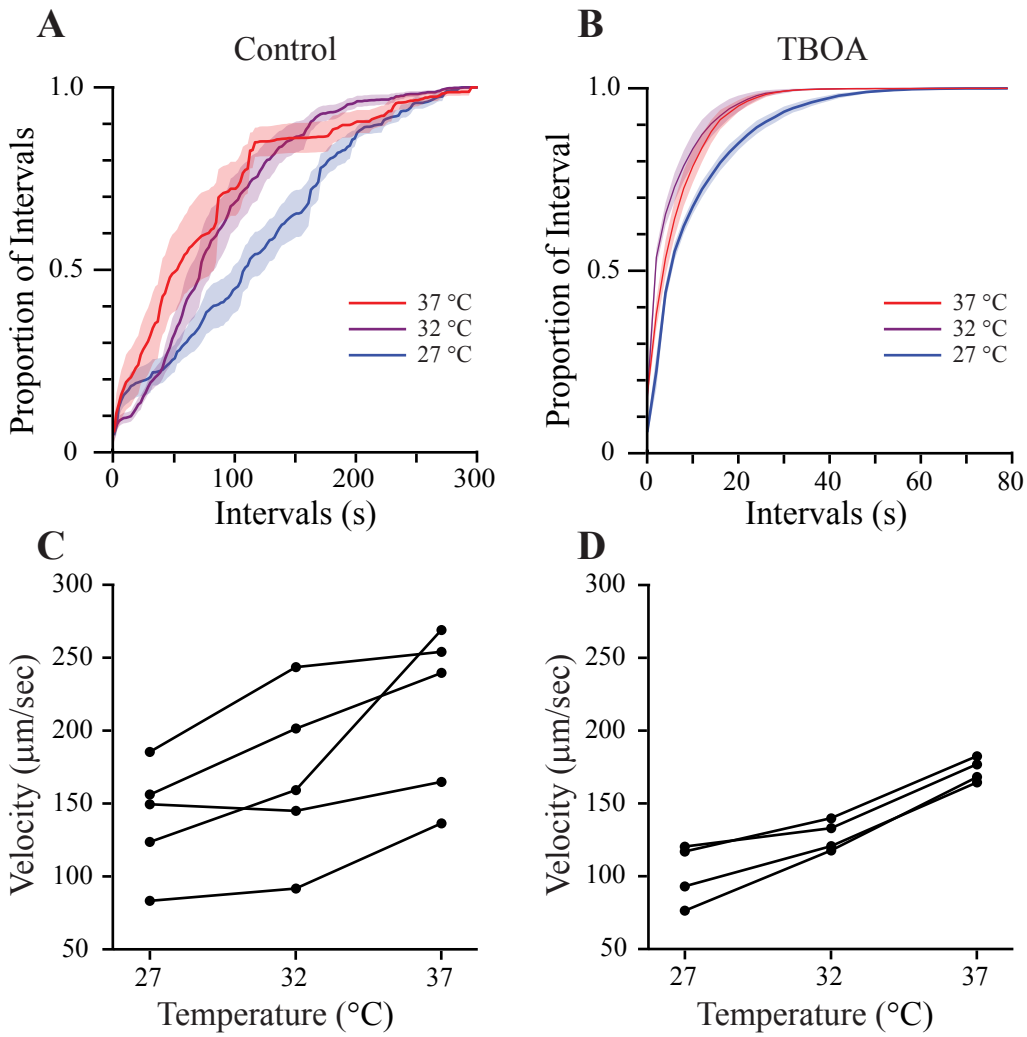

Figure II-10: Temperature effects on spatiotemporal properties of Stage III waves

(A) Cumulative histogram summarizing effects of different bath temperatures on inter-wave intervals. Shaded areas represent standard error of the mean.
(B) Cumulative histogram summarizing effects of different bath temperatures on inter-wave intervals in the presence of 25 µM TBOA. Shaded areas represent standard error of the mean.
(C) Effects of temperature on propagation speed. Individual dots represent single retinas; lines connect a retina's speed at three different temperatures.
(D) Effects of temperature on propagation speed in the presence of 25 µM TBOA. Note there was a reduction in the across-retina variability in the presence of TBOA as described in Figure 5. Since the effects of changing temperature on the spatiotemporal properties of waves followed the same trends in the presence of TBOA, we could not differentiate effects of temperature on glutamate transporters from effects on other physiological processes.

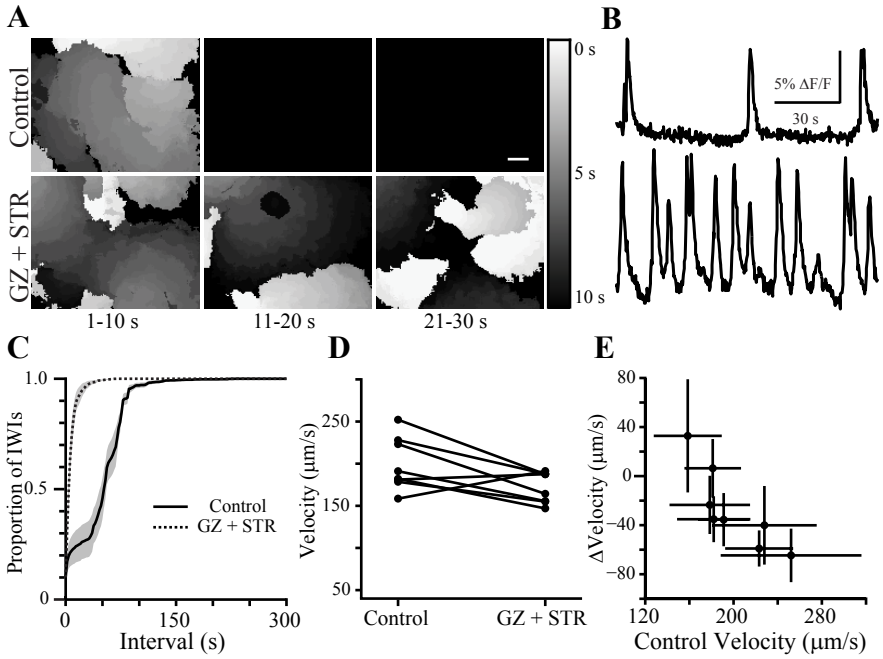

Figure II-11: Effects of blocking inhibition on the spatiotemporal properties of retinal waves

(A) Summary of spontaneous calcium transients during three sequential 10 second intervals. Gray value corresponds to the time during which that region of the retina was active. Black is baseline; white is activity at 0 s, with increasing time depicted as darker grays. If a region of the retina was active more than once, the time of the most recent activity is displayed. Top: Control. Bottom: 5 μM gabazine (GZ) and 4 μM strychnine (STR). Scale bar = 100 μm
(B) Time course of ΔF/F averaged over a 30 μm x 30 μm region in the center of the retina in A. Top: Control. Bottom: gabazine and strychnine.
(C) Summary cumulative probability distribution of inter-wave intervals (IWIs). Black line is control, dotted line is gabazine and strychnine. Shaded areas represent standard error of the mean.
(D) Effects of gabazine and strychnine on propagation speed. Individual dots represent single retinas; lines connect a retina's speed in control and GZ + STR. n=8 retinas.
(E) GZ+STR-induced change in wave propagation speed plotted versus propagation speed in control. Dots represent average speed of all waves in individual retinas; error bars are standard deviation.

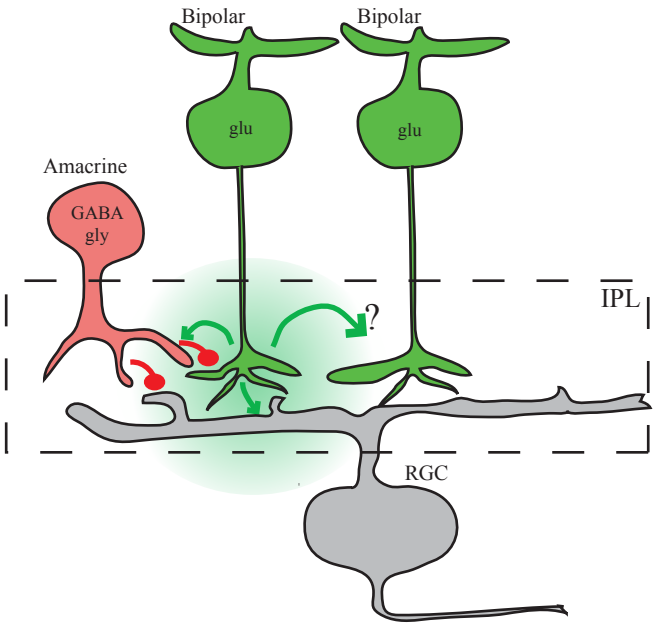

Figure II-12: Schematic of functional circuit organization of mammalian retina during Stage III waves

Glutamatergic (glu) bipolar cells (green) provide excitatory input (green) to RGCs (gray) and amacrine cells (red). In turn, glycinergic (gly) and GABAergic (GABA) amacrine cells (here both represented by a generic red cell) provide direct inhibition (red) to RGCs as well as inhibit release from bipolar cells. The mechanism by which glutamate spillover (green cloud) depolarizes neighboring bipolar cells is unknown.

III. Neuronal connexin 45 does not contribute to retinal wave function

Summary

Gap junctions are widely expressed in the developing nervous system, and adult retinal neurons are extensively connected by gap junctions. Here we investigate the role of gap junctions in shaping spontaneous activity in the developing retina. Pharmacological manipulations have led to conflicting results in the role of gap junctions in retinal waves. Therefore we have studied the role of retinal waves in transgenic mice lacking gap junction proteins, called connexins. There are two connexins expressed in the inner retina: Connexin 36 (Cx36) and Cx45. In previous studies our lab showed that Cx36ko mice exhibit normal retinal waves. Here we study retinal waves in a mouse in which the gap junction protein connexin 45 is knocked out and a GFP reporter is knocked in (Cx45ko). Using GFP expression, we found that Cx45 is expressed in amacrine and ganglion cells the developing retina. Using calcium imaging and whole cell recordings, we found that Cx45ko retinas exhibited normal retinal waves. In order to test whether compensation occurs in single-connexin knockout mice we generated a Cx36-Cx45 double knockout (Cx36-45dko). Whole cell recordings revealed that Cx36-45dko retinas also exhibit retinal waves. Hence, although gap junctions are present during development, they do not play a role in the generation of retinal waves

Introduction

Gap junctions mediate electrical coupling among cells. Gap junctions are comprised of transmembrane proteins called connexins. Connexins are widely expressed in the central nervous system, and gap junction coupling has been shown to coordinate neural activity in various brain areas (Connors and Long, 2004) including the adult retina (Sohl et al., 2005). In several regions of the CNS, expression of gap junctions is high early in development and is downregulated on a timescale that corresponds to the maturation of chemical synapses, indicating that it is important for intercellular communication before functional synaptic circuits have formed (Roerig and Feller, 2000).

Gap junction coupling has been described in the developing retina, where it has been implicated in regulating spontaneous firing. Tracer coupling experiments in the developing retina reveal that RGCs form gap junctions with other RGCs as well as amacrine cells (Penn et al., 1994, Singer et al., 2001). Bath application of gap junction blockers has had varying effects on the propagation of retinal waves ranging from no effect to a complete blockade (Singer et al., 2001, Syed et al., 2004, Wong et al., 1998, Catsicas et al., 1998). One possible reason for the variable effects is that pharmacological agents that block gap junctions also have several non-specific effects (Connors and Long, 2004), such as blockade of voltage-gated calcium channels that mediate synaptic transmission in the outer retina (Vessey et al., 2004), activation of potassium channels (Takeda et al., 2005, Sheu et al., 2008, Wu et al., 2001), and inhibition of synaptic release (Tovar et al., 2009). Therefore, to study the role of

specific connexins in generating spontaneous firing patterns, we have turned to using connexin knockout mice.

There are 20 identified connexins in the mouse genome. Approximately half of these have been detected in the CNS and only three (Cx36, Cx45, and Cx57) have been unambiguously observed in neurons (Connors and Long, 2004, Sohl et al., 2005). All three of these connexins have been detected in the retina. Cx36 and Cx45 have been observed in the inner mammalian retina (Guldenagel et al., 2000, Sohl et al., 2000), suggesting that one or both of these connexins could be involved in correlating RGC firing during development. The other neuronal connexin, Cx57, has been localized to horizontal cells (Deans and Paul, 2001, Hombach et al., 2004, Huang et al., 2005), an interneuron in the outer retina that has not yet been implicated in retinal waves. Using mice in which the Cx36 coding sequence has been replaced by a reporter gene (Deans and Paul, 2001, Deans et al., 2002), it was found that Cx36 is expressed in several cell types early in development, and that Cx36ko mice exhibit increased spontaneous firing of RGCs. However, Cx36ko mice have normal retinal wave propagation (Hansen et al., 2005, Torborg et al., 2005).

Here, we address the role of Cx45 in retinal wave generation using a knockout mouse. First, we find that Cx45 is expressed in the developing retina. Second, we find that Cx45ko mice have retinal waves from birth until eye opening, as measured by calcium imaging and whole-cell recording. Third, we show that, as in wild type, late-stage retinal waves in Cx45ko are blocked by ionotropic glutamate receptor antagonists. Finally, we show that a mouse lacking both Cx36 and Cx45 has late-stage retinal waves that are blocked by ionotropic glutamate receptor antagonists.

Together, these results suggest that neuronal gap junctions are not required for the generation of retinal waves.

Results

The expression pattern of Cx45 in the developing retina is not known, although it is well-characterized in the adult. Because germline deletion of Cx45 results in embryonic lethality (Kruger et al., 2000, Kumai et al., 2000), we used a mouse in which the endogenous *Cx45* gene is replaced by a floxed *Cx45* gene with an EGFP reporter (Cx45fl, Maxeiner et al., 2005). Cre-mediated deletion of the Cx45 coding sequence was achieved by crossing *Cx45f/fl* mice with mice expressing Cre recombinase under control of the neuron-directed Nestin promoter (Nestin-cre mice) (Tronche et al., 1999), yielding Cx45fl/fl:Nestin-cre(+) mice, which we will refer to as Cx45ko. Cx45ko mice lack Cx45 protein wherever the Nestin promoter is active, and once the *Cx45fl* allele has been converted to the *Cx45del* allele, EGFP expression is controlled by the Cx45 promoter. We examined cross sections of retinas at P4 and P9 and found that GFP is expressed in the developing inner retina. Using immunohistochemistry to visualize GABA expression we found that GFP colocalizes with GABA at P4 and P9 (Figure III-1). These results indicate that Cx45 is expressed in the developing retina and may therefore be involved in generating retinal waves.

To determine whether retinas can generate waves in the absence of Cx45, we loaded retinas from Cx45ko mice with fluorescent calcium indicators and monitored fluorescence over time in large pieces of retina (896 x 670 μm). To determine whether Cx45 is required for stage II retinal waves we bath loaded retinas from P0-P4

Cx45ko mice with the calcium indicator fura-2 AM (Feller et al., 1996, Wong et al., 1995). To test the role of Cx45 in stage III retinal waves, we bulk loaded P10-P13 retinas with the calcium indicator OGB-1AM. We observed waves in both P0-P4 (n=5 mice) and P10-P13 retinas, indicating that Cx45 is not required for stage II or stage III retinal waves (Figure III-2A-C).

In some cases, when a component of the retinal circuit required for wave generation is disrupted, waves are generated using a compensatory circuit mechanism (for review, see Blankenship and Feller, submitted). Therefore, although waves are present in Cx45ko retinas, it is possible that they are generated by a different circuit than in wild type retinas. To test the possibility that stage III waves in Cx45ko are generated by a compensatory circuit we applied the ionotropic glutamate receptor antagonists DNQX (10μM) and AP5 (50μM), which block stage III waves in wild type retinas. Stage III retinal waves in Cx45ko mice were blocked by DNQX and AP5, suggesting that waves in Cx45ko mice are not different from those in wild type mice (Figure III-2C,D).

Cx45 is expressed in GABAergic amacrine cells, which modulate glutamate release from bipolar cells. Therefore we monitored transmitter release in Cx45ko mice using whole-cell voltage clamp recordings from RGCs (Blankenship et al., 2009). We found that Cx45ko RGCs received wave-associated compound excitatory postsynaptic currents (cEPSCs) during stage II (P1-P8; frequency in Cx45ko 0.63 ± 0.25 cEPSC clusters /min, n=11 cells in 6 mice, Cx45fl 0.5 ± .2 cEPSC clusters /min, n=12 cells in 6 mice; Figure III-3A, B) and stage III (P10-P13; frequency in Cx45ko 0.55 ± 0.58 cEPSC clusters /min, n=35 cells in 13 mice; Cx45fl 0.5 ± 0.58 cEPSC clusters/min

n=16 cells in 6 mice; Figure III-3C-E). Using simultaneous dual whole-cell voltage-clamp recordings from neighboring RGCs we also found that Cx45ko RGCs receive correlated compound inhibitory postsynaptic currents (cIPSCs) during waves (n=3 pairs; Figure III-3C). We observed some cells that did not receive cEPSCs during both stage II (Cx45ko n=1/11 cells, Cx45fl n=1/12 cells) and stage III (Cx45ko n=8/35 cells in 4/13 mice; Cx45fl n=3/16 cells in 3/6 mice).

To confirm that the cEPSCs that RGCs receive during stage III waves in Cx45ko are glutamatergic, we applied glutamate receptor antagonists while performing whole cell recordings. cEPSCs were blocked in Cx45fl retinas (n=3 cells in 2 mice; Figure III-3D), and were blocked in 10/12 cells in Cx45ko retinas (frequency reduced from 1.15 ± 0.47 to .01 ± .04 cEPSC clusters/min, n=12 cells in 4 mice; Figure III-3E).

One possible interpretation of our finding that mice lacking either of the neuronal connexins found in the inner retina, Cx36 and Cx45, still exhibit retinal waves is that gap junctions containing either connexin alone are sufficient to support wave propagation. To test this hypothesis we generated Cx36-Cx45 double knockout mice and monitored retinal activity using whole-cell voltage clamp recordings. We found that Cx36-45dko RGCs received cEPSCs during stage III waves (frequency 0.77 ± 0.31 cEPSC clusters/min, n=9 cells in 3 mice; Figure III-4A), and that RGCs receive cIPSCs during waves (n=2 pairs, Figure III-4A). and that these currents were blocked by DNQX and AP5 (n=6 cells in 2 mice; Figure III-4B). These findings suggest that there has not been compensation in Cx45ko mice by Cx36.

Discussion

We have examined the role of Cx45 in generating retinal waves. First, we showed that Cx45 was expressed in the developing retina. Second, we showed that retinas lacking Cx45 generate retinal waves as measured by calcium imaging, and that late-stage waves in Cx45ko were blocked by glutamate receptor antagonists, as they are in WT retinas. These results demonstrate that Cx45 is not required for wave generation. Third, we showed that RGCs in Cx45ko retinas received normal cEPSCs during retinal waves, indicating that Cx45 does not dramatically shape RGC inputs in the developing retina. Finally, we showed that a mouse lacking both of the connexins expressed in the adult inner retina, Cx36 and Cx45, receives normal wave-associated cEPSCs. Together, these results show that Cx45 and Cx36 are not required for retinal wave generation.

Gap junction blockers have had varying effects on retinal wave propagation. There are three basic categories of gap junction antagonists. First, there are the glycyrrhizinic acid derivatives, which include the widely used carbenoxolone; alcohols, such as octanol; antimalarial drugs, such as mefloquine; and fenamates, such as meclofenamic acid (Connors and Long, 2004, Harks et al., 2001, Pan et al., 2007). Carbenoxolone has been observed to block waves measured by calcium imaging in E16 chick at concentrations between 25 and 50 μM (Wong et al., 1998). However, 50μM carbenoxolone had no effect on stage II or stage III waves as measured by multielectrode array recordings in mice (Stacy et al., 2005, Kerschensteiner and Wong, 2008), whereas 100μM carbenoxolone slightly reduced stage II wave frequency (Stacy et al., 2005). In rabbit, concentrations of carbenoxolone up to

200μM had no effect on waves measure by calcium imaging (Syed et al., 2004). Similarly mixed results have been seen with 18-α- and 18-ß-glycyrrhetinic acid. In rabbit, 15μM 18-ß- glycyrrhetinic acid restricted propagation of waves measured by calcium imaging, and 75μM blocked both stage II and stage III waves, whereas 18-α-glycyrrhetinic acid had no effect (Syed et al., 2004). Studies in mouse have found that 18-α-glycyrrhetinic acid (25μM) decreased stage II wave frequency and size as measured by calcium imaging (Singer et al., 2001). In E16 chick, both 18-α- and 18-ß-glycyrrhetinic acid blocked waves (50μM, Wong et al., 1998). Octanol blocked stage II waves measured by calcium imaging in rabbit (100μM, Syed et al., 2004) and dramatically reduced wave frequency in E9-E10 chick (2mM, Catsicas et al., 1998). Finally, meclofenamic acid (200μM) increased stage III wave frequency in mice as measured with multielectrode array recordings (Kerschensteiner and Wong, 2008).

There are several potential explanations for these variable effects. First is that although all of these agents have been demonstrated to directly block gap junction coupling as assayed either with tracer coupling or direct measurements of the junctional conductance , they also have several non-specific effects (Connors and Long, 2004, Vessey et al., 2004, Takeda et al., 2005, Sheu et al., 2008, Wu et al., 2001, Tovar et al., 2009). Also, gap junction antagonists need to be bath applied for at least 30 minutes to completely block coupling (Veruki and Hartveit, 2009, Cruikshank et al., 2004). Therefore, short bath application times might lead to different effects than longer applications.

Another possible interpretation of the finding that gap junction antagonists block waves and knockout mice have normal waves is that a distinct connexin is

transiently expressed during development, as has been demonstrated in developing spinal cord {{316 Chang,Q. 1999}} and hypothalamus (Arumugam et al., 2005). We have carried out preliminary studies in which we used RT-PCR to search for transient expression of connexins in the developing retina. We have screened 8 of the 20 connexin genes found in the mouse genome (Cx30.3, Cx31.1, Cx32, Cx36, Cx40, Cx45, Cx46, Cx57; S. Guerrero, K.J. Ford & M.B. Feller, unpublished observations). None of these genes are transiently expressed in the developing retina. These data argue against the theory that there is developmentally transient expression of connexins in the retina, although we cannot rule out the possibility that other connexins are transiently expressed.

Our results do not rule out a role for Cx57-containing gap junctions in wave generation. Cx57 is expressed in horizontal cells, an interneuron that provides feedback inhibition at the photoreceptor-to-bipolar-cell synapse. Horizontal cells, which are immunoreactive for GABA (Brandon, 1985), are unlikely to be involved in retinal waves. $GABA_A$ receptor antagonists do no block waves (Firth et al., 2005). Furthermore, retinal waves are not sensitive to transmission at the photoreceptor-to-bipolar-cell synapse, because our experiments are done under bright lighting conditions, when photoreceptors are hyperpolarized, and blocking the photoreceptor-to-ON-bipolar-cell synapse with APB does not block waves (Kerschensteiner and Wong, 2008). However, horizontal cell signaling has not yet been characterized during development, so there remains the possibility that they play a role via an unidentified mechanism or via Cx57-mediated coupling.

We found that a small percentage of RGCs in Cx45ko and Cx45fl mice did not receive cEPSCs. The rarity of the phenomenon and the fact that it was seen in both Cx45ko and Cx45fl mice suggest that the lack of waves in some cells was not a result of Cx45 deletion but rather experimental variability. In addition, the gross properties of waves as determined by calcium imaging were not altered. Hence we conclude Cx45 is not required for the initiation or propagation of retinal waves.

Together, our results show that the two known neuronal connexins expressed in the inner retina are not required for wave generation. However, given that it is not yet known how glutamate release from bipolar cells is correlated during stage III waves (Blankenship et al., 2009), gap junctions remain an intriguing possibility. Preliminary studies indicate that bipolar cell dendrites are coupled via gap junctions composed of a yet-to-be identified connexin (M. tachibana, FASEB meeting on Retinal Neurobiology, 2008). Furthermore, hemichannels composed of pannexins (Scemes et al., 2007), which are transiently expressed in the retina (Dvoriantchikova et al., 2006, Ray et al., 2005), may play a role in propagating retinal waves. To fully determine whether gap junctions play a role in wave propagation will require the generation of new tools to acutely and selectively eliminate gap junction coupling.

Methods

Animals. All procedures were approved by the Institutional Animal Care and Use Committee at The University of California, San Diego or the University of California, Berkeley.

Retinal preparation. Mice (P10-P13) were deeply anesthetized with halothane or isoflurane and decapitated. Eyes were removed, and retinas isolated in artificial cerebrospinal fluid (ACSF; in mM: 119.0 NaCl, 26.2 $NaHCO_3$, 11 glucose, 2.5 KCl, 1.0 K_2HPO_4, 2.5 $CaCl_2$, 1.3 $MgCl_2$). For physiology, retinas were mounted RGC layer-up on filter paper (Millipore). For histology, retinas were fixed in paraformaldehyde (4% in PBS).

Physiology. Retinas were visualized on an upright microscope (Zeiss Axioskop 2 FS Plus or Olympus BX51WI) and were continually superfused with ACSF. RGCs were exposed by using a glass recording pipette to remove the inner limiting membrane over a small region of the retina. Recording pipettes (3-6 MΩ) were filled with internal containing either Cesium Gluconate (in mM: 75 gluconic acid, 149.9 CsOH, 10 EGTA, 20 HEPES, 1 QX-314, 2 ATP-Mg, 0.3 GTP-Na, pH adjusted to 7.25 with CsOH) or Potassium Gluconate (in mM: : 128 K-gluconate, 10 HEPES, 12 KCl, 5 EGTA, 1 $MgCl_2$, 0.5 $CaCl_2$, 2 Na_2ATP, and 0.5 Na-GTP; pH adjusted to 7.25 with KOH or, alternatively, in mM: 98.3 K-gluconate, 40 HEPES, 1.7 KCl, 0.6 EGTA, 5 $MgCl_2$, 2 Na_2ATP, and 0.3 Na-GTP; pH adjusted to 7.25 with KOH). 6,7-Dinitroquinoxaline-2,3-dione disodium salt (DNQX), and D-(-)-2-Amino-5-phosphonopentanoic acid (AP5) were acquired from Tocris; all other chemicals were acquired from Sigma or Fisher.

Calcium Imaging. Retinas from P0-P4 mice were loaded with fura-2 AM by bath application. Because bath application does not effectively load older retinas (Bansal et al., 2000), we used the multicell bolus loading technique to load retinas from P10-P13 mice with OGB-1 AM (Blankenship et al., 2009, Stosiek et al., 2003).

Data Analysis. CEPSC cluster frequency in whole cell recordings was quantified as previously described (Blankenship et al., 2009), using current clamp recordings, voltage clamp recordings or both. In glutamate receptor antagonist experiments (Figures 3, 4), we occasionally observed currents resembling very small cEPSCs in the presence of DNQX and DAP5. We recorded these currents only very rarely, and they were not counted because they were barely visible above the recording noise. Drugs were considered "rinsed" when waves began occurring at a regular interval. This criterion was typically met 8-15 minutes after control ACSF was reapplied. In order to accurately appraise frequency once activity had begun again, the time period examined to quantify the frequency of waves was midway between the 1st and 2nd waves after activity had become regular to the end of the recording. Because of this, rinse recordings in which the retina generated few waves but then went silent again were not counted as having rinsed.

Immunofluorescence. Retinas were fixed in 4% paraformaldehyde for 10 minutes. Retinas were then washed in 0.01M PBS for 30 minutes, and blocked for non-specific binding in blocking solution of 10% normal donkey serum, 5% bovine serum albumin, and 1% Triton-x in 0.01M PBS for 2 hours at room temperature. Next, retinas were cryoprotected in 30% sucrose for one hour. Retinas were then placed into a cryomold biopsy chamber (27181; Ted Pella, Inc) and sliced into 16µm sections on a cryostat.

The primary antibodies used were Mouse anti-GFP 1:1000 (Chemicon #MAB3580; panel B), Rabbit anti-GFP 1:1000 (Molecular Probes #A11122; panel C), Rabbit anti-GABA 1:2500 (Sigma # A2052; panels A and B), Goat anti-ChAT 1:200

(Chemicon #AB144P; panel C). The secondary antibodies usedwere Alexa 488-conjugated goat anti-mouse 1:500 (Molecular Probes #A-11001; panel B), Alexa 488-conjugated donkey anti-rabbit 1:200 (Molecular Probes #A21206, panel C), Alexa 568-conjugated goat anti-rabbit 1:500 (Molecular Probes A-11036, panels A and B), Cy3-conjugated donkey anti-goat 1:200 (Jackson Immunoresearch #705-165-147.

Acknowledgement

This chapter is original work in preparation as: Blankenship, AG; Maxeiner, S; Willecke, K; Feller, MB. Neuronal connexin 45 does not contribute to retinal wave function and is included with permission from all the manuscript's authors. The dissertation author was the primary author of this paper.

References

Arumugam H, Liu X, Colombo PJ, Corriveau RA, Belousov AB (2005) NMDA receptors regulate developmental gap junction uncoupling via CREB signaling. Nat Neurosci 8:1720-6.

Bansal A, Singer JH, Hwang BJ, Xu W, Beaudet A, Feller MB (2000) Mice lacking specific nicotinic acetylcholine receptor subunits exhibit dramatically altered spontaneous activity patterns and reveal a limited role for retinal waves in forming ON and OFF circuits in the inner retina. J Neurosci 20:7672-7681.

Blankenship AG, Feller MB (submitted) Mechanisms underlying spontaneous patterned activity in developing neural circuits. Nat Rev Neurosci .

Blankenship AG, Ford KJ, Johnson J, Seal RP, Edwards RH, Copenhagen DR, Feller MB (2009) Synaptic and extrasynaptic factors governing glutamatergic retinal waves. Neuron 62:230-41.

Brandon C (1985) Retinal GABA neurons: Localization in vertebrate species using an antiserum to rabbit brain glutamate decarboxylase. Brain Res 344:286-295.

Catsicas M, Bonness V, Becker D, Mobbs P (1998) Spontaneous Ca2+ transients and their transmission in the developing chick retina. Curr Biol 8:283-6.

Connors BW, Long MA (2004) Electrical synapses in the mammalian brain. Annu Rev Neurosci 27:393-418.

Cruikshank SJ, Hopperstad M, Younger M, Connors BW, Spray DC, Srinivas M (2004) Potent block of Cx36 and Cx50 gap junction channels by mefloquine. Proc Natl Acad Sci U S A 101:12364-12369.

Deans MR, Paul DL (2001) Mouse horizontal cells do not express connexin26 or connexin36. Cell Commun Adhes 8:361-6.

Deans MR, Volgyi B, Goodenough DA, Bloomfield SA, Paul DL (2002) Connexin36 is essential for transmission of rod-mediated visual signals in the mammalian retina. Neuron 36:703-12.

Dvoriantchikova G, Ivanov D, Panchin Y, Shestopalov VI (2006) Expression of pannexin family of proteins in the retina. FEBS Lett 580:2178-2182.

Feller MB, Wellis DP, Stellwagen D, Werblin FS, Shatz CJ (1996) Requirement for cholinergic synaptic transmission in the propagation of spontaneous retinal waves. Science 272:1182-1187.

Firth SI, Wang CT, Feller MB (2005) Retinal waves: Mechanisms and function in visual system development. Cell Calcium 37:425-432.

Guldenagel M, Sohl G, Plum A, Traub O, Teubner B, Weiler R, Willecke K (2000) Expression patterns of connexin genes in mouse retina. J Comp Neurol 425:193-201.

Hansen KA, Torborg CL, Elstrott J, Feller MB (2005) Expression and function of the neuronal gap junction protein connexin 36 in developing mammalian retina. J Comp Neurol 493:309-20.

Harks EG, de Roos AD, Peters PH, de Haan LH, Brouwer A, Ypey DL, van Zoelen EJ, Theuvenet AP (2001) Fenamates: A novel class of reversible gap junction blockers. J Pharmacol Exp Ther 298:1033-1041.

Hombach S, Janssen-Bienhold U, Sohl G, Schubert T, Bussow H, Ott T, Weiler R, Willecke K (2004) Functional expression of connexin57 in horizontal cells of the mouse retina. Eur J Neurosci 19:2633-40.

Huang H, Li H, He SG (2005) Identification of connexin 50 and 57 mRNA in A-type horizontal cells of the rabbit retina. Cell Res 15:207-11.

Kerschensteiner D, Wong RO (2008) A precisely timed asynchronous pattern of ON and OFF retinal ganglion cell activity during propagation of retinal waves. Neuron 58:851-8.

Kruger O, Plum A, Kim JS, Winterhager E, Maxeiner S, Hallas G, Kirchhoff S, Traub O, Lamers WH, Willecke K (2000) Defective vascular development in connexin 45-deficient mice. Development 127:4179-4193.

Kumai M, Nishii K, Nakamura K, Takeda N, Suzuki M, Shibata Y (2000) Loss of connexin45 causes a cushion defect in early cardiogenesis. Development 127:3501-3512.

Maxeiner S, Dedek K, Janssen-Bienhold U, Ammermuller J, Brune H, Kirsch T, Pieper M, Degen J, Kruger O, Willecke K, Weiler R (2005) Deletion of connexin45 in mouse retinal neurons disrupts the rod/cone signaling pathway between AII amacrine and ON cone bipolar cells and leads to impaired visual transmission. J Neurosci 25:566-76.

Pan F, Mills SL, Massey SC (2007) Screening of gap junction antagonists on dye coupling in the rabbit retina. Vis Neurosci 24:609-618.

Penn AA, Wong RO, Shatz CJ (1994) Neuronal coupling in the developing mammalian retina. J Neurosci 14:3805-15.

Ray A, Zoidl G, Weickert S, Wahle P, Dermietzel R (2005) Site-specific and developmental expression of pannexin1 in the mouse nervous system. Eur J Neurosci 21:3277-3290.

Roerig B, Feller MB (2000) Neurotransmitters and gap junctions in developing neural circuits. Brain Res Brain Res Rev 32:86-114.

Scemes E, Suadicani SO, Dahl G, Spray DC (2007) Connexin and pannexin mediated cell-cell communication. Neuron Glia Biol 3:199-208.

Sheu SJ, Bee YS, Chen CH (2008) Resveratrol and large-conductance calcium-activated potassium channels in the protection of human retinal pigment epithelial cells. J Ocul Pharmacol Ther 24:551-555.

Singer JH, Mirotznik RR, Feller MB (2001) Potentiation of L-type calcium channels reveals nonsynaptic mechanisms that correlate spontaneous activity in the developing mammalian retina. J Neurosci 21:8514-22.

Sohl G, Maxeiner S, Willecke K (2005) Expression and functions of neuronal gap junctions. Nat Rev Neurosci 6:191-200.

Sohl G, Guldenagel M, Traub O, Willecke K (2000) Connexin expression in the retina. Brain Res Brain Res Rev 32:138-45.

Stacy RC, Demas J, Burgess RW, Sanes JR, Wong RO (2005) Disruption and recovery of patterned retinal activity in the absence of acetylcholine. J Neurosci 25:9347-9357.

Stosiek C, Garaschuk O, Holthoff K, Konnerth A (2003) In vivo two-photon calcium imaging of neuronal networks. Proc Natl Acad Sci U S A 100:7319-7324.

Syed MM, Lee S, Zheng J, Zhou ZJ (2004) Stage-dependent dynamics and modulation of spontaneous waves in the developing rabbit retina. J Physiol 560:533-49.

Takeda Y, Ward SM, Sanders KM, Koh SD (2005) Effects of the gap junction blocker glycyrrhetinic acid on gastrointestinal smooth muscle cells. Am J Physiol Gastrointest Liver Physiol 288:G832-41.

Torborg CL, Hansen KA, Feller MB (2005) High frequency, synchronized bursting drives eye-specific segregation of retinogeniculate projections. Nat Neurosci 8:72-8.

Tovar KR, Maher BJ, Westbrook GL (2009) Direct actions of carbenoxolone on synaptic transmission and neuronal membrane properties. J Neurophysiol 102:974-978.

Tronche F, Kellendonk C, Kretz O, Gass P, Anlag K, Orban PC, Bock R, Klein R, Schutz G (1999) Disruption of the glucocorticoid receptor gene in the nervous system results in reduced anxiety. Nat Genet 23:99-103.

Veruki ML, Hartveit E (2009) Meclofenamic acid blocks electrical synapses of retinal AII amacrine and on-cone bipolar cells. J Neurophysiol 101:2339-2347.

Vessey JP, Lalonde MR, Mizan HA, Welch NC, Kelly ME, Barnes S (2004) Carbenoxolone inhibition of voltage-gated ca channels and synaptic transmission in the retina. J Neurophysiol 92:1252-6.

Wong RO, Chernjavsky A, Smith SJ, Shatz CJ (1995) Early functional neural networks in the developing retina. Nature 374:716-718.

Wong WT, Sanes JR, Wong ROL (1998) Developmentally regulated spontaneous activity in the embryonic chick retina. Journal of Neuroscience 18:8839-8852.

Wu SN, Jan CR, Chiang HT (2001) Fenamates stimulate BKCa channel osteoblast-like MG-63 cells activity in the human. J Investig Med 49:522-533.

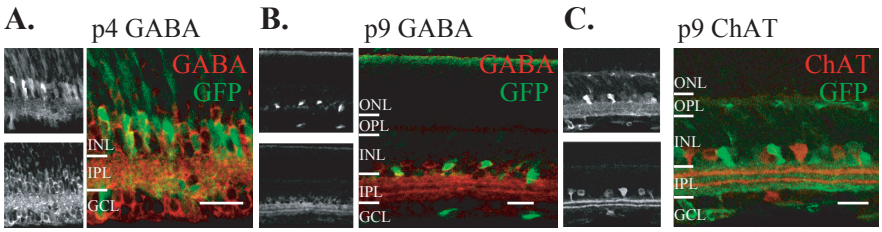

Figure III-1: Cx45 is expressed in a subset of developing RGCs and GABAergic amacrine cells.

A. GFP (green) expressed under the Cx45 promoter colocalized with GABA (red) in the first postnatal week (p4) and in the second postnatal week (p9, B). C. GFP did not colocalize with choline acetyl transferase (ChAT, red) in the second week (p9). Scale bar = 25 micron.

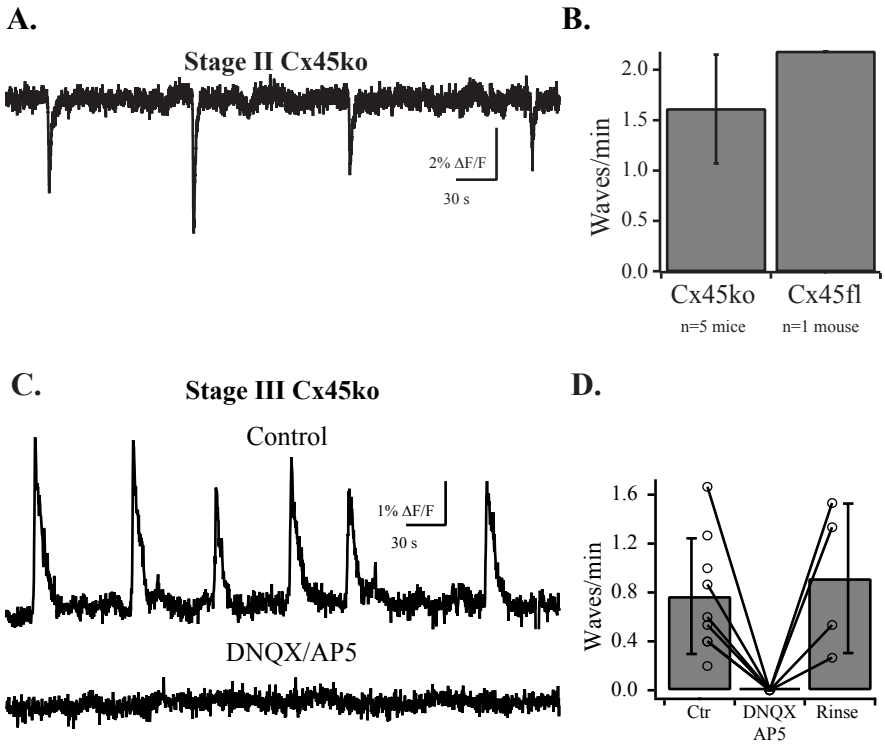

Figure III-2: Cx45ko mice exhibit normal retinal waves.

A. Time course of ΔF/F in a 7 min long recording from a P2 Cx45ko retina.
B. Graph showing average wave frequency in Cx45ko and Cx45fl retinas. N=5 mice for Cx45ko, n=1 mouse for Cx45fl.
C. Top, Time course of ΔF/F in a 7 min long control recording from a Cx45ko. Bottom, same retina in the presence of 10μM DNQX and 50 μM ap5.
D. Summary graph of recordings from P10 – P13 Cx45ko retinas. Bars are average ± SD, circles are individual retinas. Control, n = 9 retinas from 3 mice; DNQX, n = 6 retinas from 3 mice; Rinse, n = 4 retinas from 3 mice. Rinse not observed in other 2 retinas.

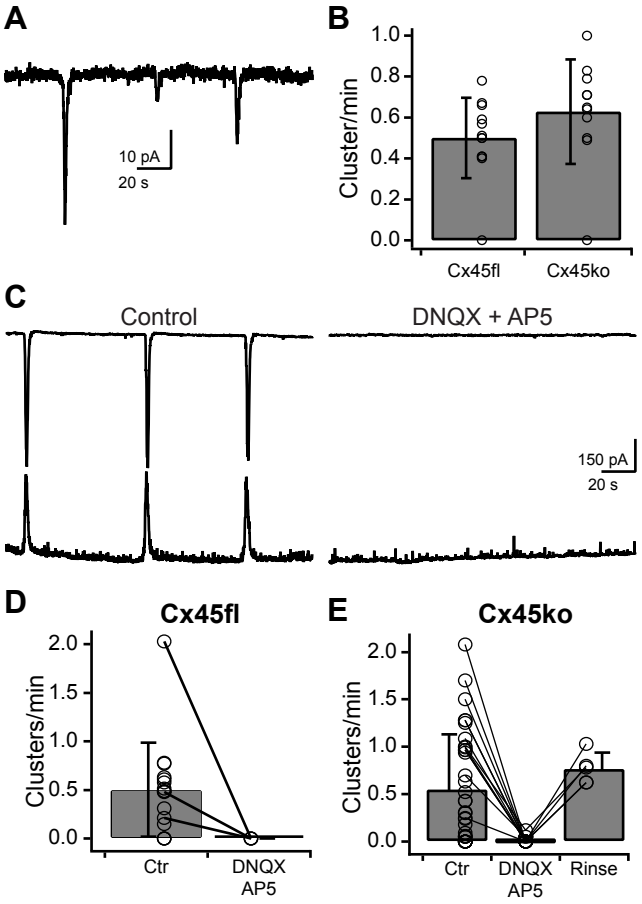

Figure III-3: Cx45ko mice have normal wave-associated synaptic inputs.

A. Whole cell voltage clamp recording of cEPSCs in a P3 Cx45ko mouse.
B. Average cEPSC cluster frequency in stage II Cx45fl and Cx45 ko retinas. Bars are average ± SD, circles are individual cells. Cx45fl, n = 12 cells in 6 mice; Cx45ko, n = 11 cells in 6 mice.
C. Dual, simultaneous whole-cell voltage-clamp recordings from a P10 Cx45ko mouse showing cEPSCs in top traces and cIPSCs in bottom traces. Left, control ACSF; Right, 20µM DNQX + 50 µM AP5.
D. Average cEPSC cluster frequency during stage III waves in Cx45fl mice. Bars are average ± SD, circles are individual cells. Control, n = 16 cells in 6 mice; DNQX/AP5, n = 3 cells in 2 mice.
E. Average cEPSC cluster frequency during stage III waves in Cx45ko mice. Bars are average ± SD, circles are individual cells. Control, n = 35 cells in 13 mice; DNQX/AP5, n = 12 cells in 4 mice.

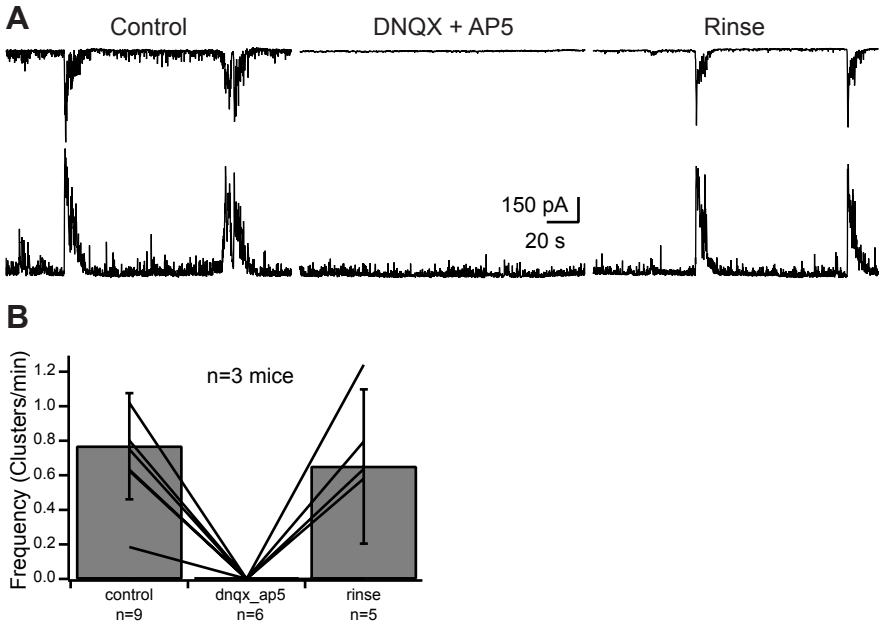

Figure III-4: Cx36/45dko mice have normal wave-associated synaptic inputs.

A. Dual whole-cell voltage-clamp recordings from a P10 Cx36/45dko retina. Left, control; middle, 20 µM DNQX, 50µm D-AP5; right, rinse. Recordings in each condition are three minutes long.
B. Average cEPSC cluster frequency in P10 – P12 Cx36/45dko retinas. n=3 Cx36/45dko mice; n=9 cells in control, n=6 cells in DNQX/AP5, n=5 cells in rinse. Error bars = standard deviation.